Mechanics of bio-based thermosetting polymers and water-induced rejuvenation

Raphaëlle Kulis

PSL UNIVERSITÉ PARIS

THÈSE DE DOCTORAT
DE L'UNIVERSITÉ PSL

Préparée à ESPCI Paris

Mécanique de polymères thermodurcissables bio-sourcés et rajeunissement hydrique

Soutenue par

Raphaëlle KULIS

Le 8 mars 2019

École doctorale n°397

Physique et Chimie des Matériaux

Spécialité

Physico-chimie

Composition du jury :

Laurence ROZES	Professeur, Sorbonne Université/UPMC	*Présidente du jury*
Laurent HEUX	Directeur de recherche, CNRS-CERMAV	*Rapporteur*
John Christopher PLUMMER	Professeur, EPFL	*Rapporteur*
Sylvie CASTAGNET	Directeur de recherche, ENSMA	*Examinateur*
Christian GAUTHIER	Directeur de recherche, Institut Charles Sadron	*Examinateur*
Etienne BARTHEL	Directeur de recherche, ESPCI Paris	*Directeur de thèse*
Keyvan PIROIRD	Ingénieur, Saint-Gobain Recherche	*Invité*

ESPCI PARIS | PSL

Mechanics of bio-based thermosetting polymers and their water-induced rejuvenation

Raphaëlle KULIS

Étienne BARTHEL, Alessandro BENEDETTO and Pierre SALOMON

Remerciements

Ce manuscrit clôture trois années de travail dont l'accomplissement est en très grande partie dû à l'aide d'un grand nombre de personnes que je souhaiterais remercier ici.

Ce travail n'aurait pas été possible sans le soutien et la confiance infaillible de mon encadrant académique, Etienne Barthel, et de mes encadrants industriels, Alessandro Benedetto, Pierre Salomon et initialement, Keyvan Piroird. Merci à vous pour votre enthousiasme pour le sujet, la liberté que vous m'avez accordée durant ces trois années et votre disponibilité (et ce, malgré un agenda des plus chargés).

Etienne, merci pour ton exemplarité scientifique et professionnelle, ta bonne humeur continue et ton effervescence d'idées lors de nos discussions. Je me souviendrai pour toujours de tes envolées lyriques qui m'ont souvent fait sourire pendant la correction du manuscrit.

Alessandro, merci pour ton accompagnement tout au long de cette thèse et pour ton regard critique sur les résultats. Merci également d'avoir toujours prêté une oreille attentive lors de mes passages à Saint-Gobain et de m'avoir familiarisée avec le fonctionnement interne et les outils administratifs de SGR.

Pierre, merci pour la touche de chimie que tu as su apporter et vulgariser dans ce monde de mécaniciens, pour tes intuitions toujours justes et pour ton franc-parler.

Keyvan, merci pour ta curiosité scientifique et tes précieux conseils tout au long de mon stage de master et au début de ma thèse. Ces quelques mois ensemble auront été très formateurs pour moi. Enfin, merci d'avoir accepté de prendre part au jury de soutenance.

Je tiens ensuite à remercier les membres de jury qui ont évalué ce travail : John Christopher Plummer et Laurent Heux pour avoir pris le temps de relire et commenter ce document, Christian Gauthier et Sylvie Castagnet pour avoir accepté de prendre part à mon jury de thèse et enfin, Laurence Rozes pour avoir présidé ce jury. Les discussions très enrichissantes que nous avons eues lors de la soutenance me font regretter que ces trois années touchent à leur fin mais elles ouvriront, j'en suis sûre, des perspectives intéressantes pour la suite.

J'adresse mes plus sincères remerciements à l'entreprise Saint-Gobain qui a lancé et financé ce très beau sujet de thèse.

Je voudrais en particulier remercier tous ceux à Saint-Gobain qui ont suivi de près cette thèse et m'ont aidée dans la compréhension des phénomènes observés, en particulier : Aurélie Legrand, Bernadette Charleux, Boris Jaffrennou, Edouard Obert, François Creuzet, Jean-Baptiste Denis, Jean-Marc Flesselles, Jocelyn Clenet, Marion Chenal, René Gy et Xavier Brajer. Merci à vous pour l'intérêt que vous avez porté à ce sujet, pour votre suivi assidu tout au long du projet et pour vos apports très pertinents lors de nos discussions.

Je souhaite également remercier l'ensemble des deux départements que j'ai intégrés à Saint-Gobain Recherche, TMM et PCRS, pour leur accueil à chacune de mes visites à Aubervilliers. Je tiens en particulier à remercier Emmanuel Garre, Guillaume Durieu, Jaona Girard, Joel Azevedo, Joel Robineau, Marc Yonger, Marie Lamblet, Nathalie Dideron et Nathalie Rohault, qui ont toujours pris le temps de discuter de sciences et d'autres sujets plus philosophiques, notamment autour d'un morceau de galette.

Ce travail n'aurait pas été possible sans la contribution de plusieurs personnes envers lesquelles je suis très reconnaissante. Merci à Justine Laurent pour m'avoir initiée à Labview. Merci à Guillaume Laffite, Olivier Lesage et Nawel Cherkaoui pour m'avoir formée aux différents équipements du plateau technique de l'IPGG. Merci à Aurélie Bernard et Claire Troufflard pour les nombreuses analyses RMN. Enfin, merci à Mathilde Reyssat et Kamel Khelloufi pour leur aide précieuse sur l'utilisation d'un réacteur à plasma.

Je tiens également à remercier les deux stagiaires que j'ai eu la chance d'encadrer et qui ont contribué à cette thèse : Marion Gallo et Louis Henrard.

L'essentiel de cette thèse ayant été réalisée au sein du laboratoire SIMM, je souhaiterais remercier très chaleureusement l'ensemble de ses membres, présents et passés.

Merci à Christian Frétigny et Guylaine Ducouret pour leur accueil au laboratoire. Merci également à l'ensemble des permanents du laboratoire pour le regard neuf qu'ils ont apporté sur ce projet lors de nos discussions. En particulier, merci à Ludovic Olanier, Alexandre Lantheaume et David Martina pour m'avoir aidée à concevoir mes dispositifs expérimentaux. Merci à Antoine Chateauminois et Emilie Verneuil pour leurs multiples formations (spin-coating, plasma, DVS). Merci à Mohamed Hanafi pour m'avoir formée aux secrets de l'ATG et de la DSC. Merci à Hélène Montes pour ses conseils sur la DSC et sa bonne humeur quotidienne. Merci à Armand Hakopian pour ses précieuses compétences informatiques et les nombreuses discussions que nous avons eues. Merci également à Fabienne Decuq, Freddy Martin, Gilles Garnaud, Marie Theresa Mendy, Mayu Hirano-Courcot, Pierre Christine et Pierre Landais pour les

coups de pouce du quotidien.

Lors de ces trois années au SIMM, j'ai eu la chance de partager des moments très agréables avec les personnes du troisième étage du bâtiment H. Merci notamment à Artem Kovalenko, Juliette Slootman, Giorgia Scetta, Matteo Ciccotti, Mehdi Vahdati et Miléna Lama pour les découvertes culinaires lors de nos nombreux et désormais incontournables repas du 3ème ainsi que pour la bonne ambiance à laquelle vous avez grandement contribué.

Je tiens plus particulièrement à remercier Bruno Bresson pour sa bonne humeur, son humour, ses conseils toujours pertinents en sciences et en dehors ainsi que pour nos innombrables discussions.

J'adresse également mes plus sincères remerciements à Alba Marcellan pour m'avoir donné le goût des polymères il y a quelques années de cela mais également pour m'avoir permis de rencontrer fortuitement Etienne et d'obtenir cette thèse malgré ma réticence initiale à revenir sur Paris. Merci également à toi pour tes conseils avisés tout au long de cette thèse.

Je n'ai pas de mots pour remercier mes co-bureaux sans qui la vie en H301 n'aurait pas eu la même saveur durant ces trois années : Clotilde Richard, Julien Chopin, Mélanie Arangalage et Xavier Morelle. Je garderai pour toujours nos (longues) discussions, nos fous-rires, nos *investigations* et tous les bons moments que nous avons partagés ensemble au travail et en dehors.

Enfin, le SIMM ne serait pas le SIMM sans l'ensemble de ses non-permanents (docteurs, post-docs et stagiaires) avec qui j'ai eu la chance de partager une grande partie de mon temps au laboratoire. Je n'oublierai pas les moments passés autour d'une paillasse, d'une table de restaurant, d'un buffet ou encore d'un plateau de jeu de société, en particulier avec Antoine Fleury, Charles Barrand, Cyprien Poirier, Francisco Cedano, Franz de Soete, Gabriel Sanoja, Guillaume Votte, Helen Minsky, Julien Dupré de Baubigny, Ludovic Feige, Nassim Pujol, Paul Fourton et Tom Saint-Martin. Enfin, un immense merci à Claire Schune, Gaëlle Rondepierre, Jennifer Fusier, Julie Godefroid, Mélanie Arangalage et Valentine Hervio pour votre amitié.

J'en profite pour remercier l'ensemble de mes amis qui, sans le savoir, m'ont permis de trouver un équilibre entre ma vie professionnelle et ma vie sociale. Parmi ces amis, je remercie notamment tous ceux que j'ai eu la chance de rencontrer au Touch, sport qui a occupé une part significative de mon temps-libre ces dernières années. Merci notamment aux clubs CdR Hurricanes, Free Touch et TR91 ainsi qu'à l'équipe France Women's Open pour toutes ces rencontres et ces moments inoubliables que nous avons partagés aux quatre coins de la France, de l'Europe et bientôt du monde.

Je voudrais également remercier les enseignants qui ont grandement contribué à mon parcours actuel, plus spécifiquement Franck et Patricia Gauthier ainsi que

Natacha Raufast.

Enfin, mes derniers et plus sincères remerciements vont à toute ma famille et à Jules, qui ont fait le déplacement de loin pour pouvoir assister à la fin de mon doctorat. Merci à vous pour votre soutien inconditionnel durant ces (interminables) années d'étude et pour avoir toujours été à mes côtés dans les meilleurs moments comme dans les pires.

Résumé en Français

Dans un contexte de transition énergétique induite par la raréfaction des ressources énergétiques fossiles et le changement climatique, les polymères traditionnels dérivés de ressources pétrochimiques tendent à être remplacés par des chimies biosourcées. Dans le but de réduire l'impact environnemental de ses matériaux, Saint-Gobain a récemment développé de nouvelles résines thermodurcissables biosourcées de type polyester. L'optimisation de ces formulations nécessite néanmoins une meilleure connaissance de leur comportement mécanique en vue de leur application dans un contexte industriel. En effet, pour chaque application, il est primordial de maintenir des performances mécaniques dans des conditions environnementales représentatives du cycle de vie du produit. En raison de la forte hydrophilie des nouvelles résines polyesters d'intérêt, l'influence de l'humidité sur leurs propriétés mécaniques est un paramètre majeur à prendre en compte.

Dans ce cadre, cette thèse a pour objet une résine thermodurcissable modèle de type polyester élaborée à partir de matières premières renouvelables. Nous avons pour objectif de caractériser le comportement mécanique de ce polymère en fonction de l'humidité et d'identifier les mécanismes moléculaires d'action de l'eau sur le polymère.

Dans la littérature, nous avons identifié deux mécanismes principaux d'action de l'eau sur les résines polyester : 1/ la plastification, c'est-à-dire l'augmentation locale de la mobilité des chaines polymères par lubrification et/ou rupture des interactions physiques entre chaines suite à l'absorption d'eau. Ce phénomène est en théorie réversible puisqu'il n'altère pas la structure chimique du polymère. 2/ L'hydrolyse, c'est-à-dire une rupture irréversible des liaisons covalentes lors de la réaction entre les fonctions esters et l'eau. Ces deux mécanismes sont schématisés sur la Figure 1.

En raison de la complexité de la structure chimique de la résine polyester considérée, ces deux processus ne peuvent être différenciés par une caractérisation chimique de la structure macromoléculaire. Une approche indirecte est donc privilégiée. Pour cela, nous nous intéressons à la capacité du polymère à recouvrir ses propriétés mécaniques initiales suite à la désorption d'eau. En effet, la plastification par l'eau est théoriquement réversible, c'est-à-dire que le polymère recouvre entièrement ses propriétés initiales après séchage. A l'inverse, l'hydrolyse induit une dégradation irréversible du

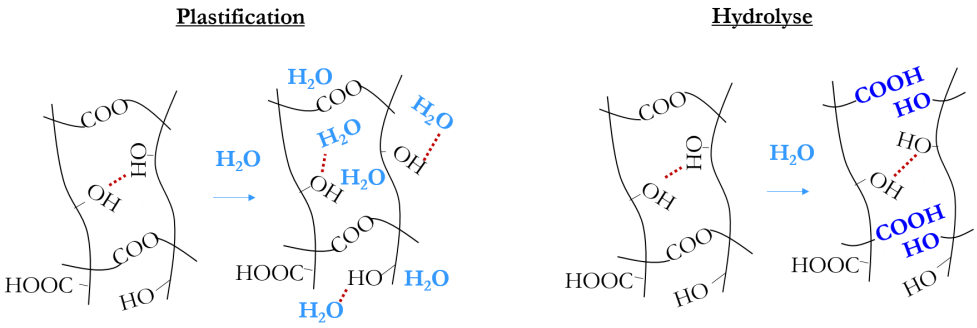

Figure 1 – Représentation schématique de deux mécanismes d'action de l'eau sur une résine polyester : la plastification et l'hydrolyse.

matériau qui s'accompagne d'une détérioration de ses propriétés mécaniques et ce, même après séchage.

La caractérisation mécanique du polymère considéré est cependant limitée par l'impossibilité de réaliser des échantillons massifs dans des conditions représentatives des procédés industriels. L'évaporation du solvant et l'émission d'espèces volatiles produites au cours de la réaction entrainent un moussage important du matériau. Pour surmonter ces difficultés, nous développons un procédé de micro fabrication combinant une cuisson sous pression et un moule perméable aux espèces volatiles (cf. Figure 3). Ce procédé nous permet de préparer des échantillons sans porosité d'une taille caractéristique de l'ordre d'une dizaine de microns et de géométrie variée : films minces déposés sur un substrat, micro piliers et micro éprouvettes de traction.

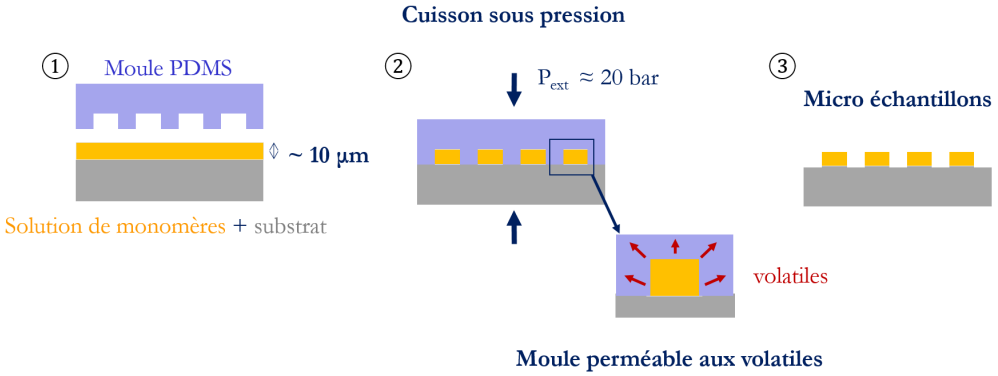

Figure 2 – Procédé de fabrication de micro échantillons de polymère. (1) Après un pré-séchage de la solution de monomères, (2) le matériau est cuit sous pression dans un moule perméable aux espèces volatiles. (3) Après démoulage, des échantillons sans porosité et de géométrie contrôlée sont obtenus.

Nous étudions ensuite expérimentalement le comportement mécanique de ces échantillons. Pour cela, nous développons des outils de caractérisation micro-mécanique adaptés. Les propriétés élastiques et à rupture du matériau sont déterminées grâce à

un test de traction sur micro fibres de polymère. Le comportement à grandes déformations, notamment les propriétés plastiques, est quant à lui étudié par compression de micro piliers. Enfin, des mesures de courbure de substrat permettent de remonter aux contraintes internes dans des films polymères déposés sur des substrats rigides. L'ensemble de ces tests est réalisé dans des conditions d'humidité contrôlée afin de caractériser la sensibilité à l'humidité du polymère.

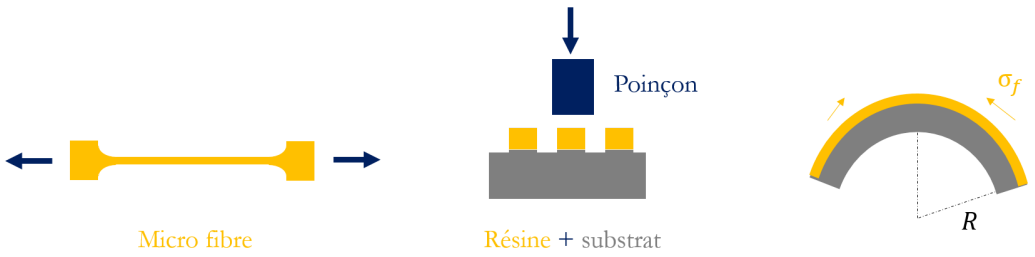

Figure 3 – Caractérisation micro-mécanique de la résine polyester modèle. De gauche à droite : traction de micro fibres de polymère, compression de micro piliers de polymère, mesure de courbure d'un film mince de polymère déposé sur un substrat élastique rigide.

La caractérisation mécanique de la résine polyester se divise en deux grands axes d'étude.

Dans un premier temps, nous nous intéressons à l'influence de l'humidité sur un polyester non vieilli, c'est-à-dire sur des échantillons maintenus dans des dessicateurs et testés rapidement après préparation. A humidité ambiante ($\simeq$ 40 %RH), le polymère présente un comportement vitreux similaire à celui des résines thermodurcissables standards. Néanmoins, en raison de son hydrophilie élevée (jusqu'à 30 %wt d'eau absorbée à 90 %RH), son comportement mécanique se révèle fortement dépendant à l'humidité. En combinant des essais de micro traction et de micro compression, nous mettons en évidence trois régimes mécaniques illustrés sur la Figure 4 :

- **Régime I :** pour des humidités inférieures à 30 %RH, le polymère est dans un état vitreux caractérisé par une rupture fragile ($\sigma_{break-eq} < \sigma_{yield}$) qui est pilotée par la présence de défauts critiques satisfaisant le critère de Griffith. Dans ce régime, nous pensons que l'eau absorbée augmente la mobilité locale des chaines polymères et active leur réarrangement à proximité de ces défauts critiques. La guérison de ces défauts expliquerait l'augmentation de la contrainte à la rupture dans cette gamme d'humidité alors que le module élastique et le seuil de plasticité demeurent constants.
- **Régime II :** pour des humidités comprises entre 30%RH et 80 %RH, le polymère est dans un état vitreux plastifié. L'eau absorbée plastifie le polymère en augmentant localement la mobilité des chaines, notamment via la rupture des liaisons hydrogènes qui existent entre les groupements polaires résiduels. Cette plastification se traduit par une diminution du seuil de plasticité et de la contrainte à

rupture. Dans ce régime, la rupture du matériau est localement pilotée par la plasticité ($\sigma_{break-eq} \simeq \sigma_{yield}$).

- **Régime III :** au delà d'une humidité seuil RH_g de 80 %RH, le polymère transite vers un état gel comme suggéré par la chute du module de deux ordres de grandeur et la transition vers un comportement viscoélastique. Ce phénomène est une conséquence de la plastification du polyester par l'eau qui induit une transition vitreuse du polymère.

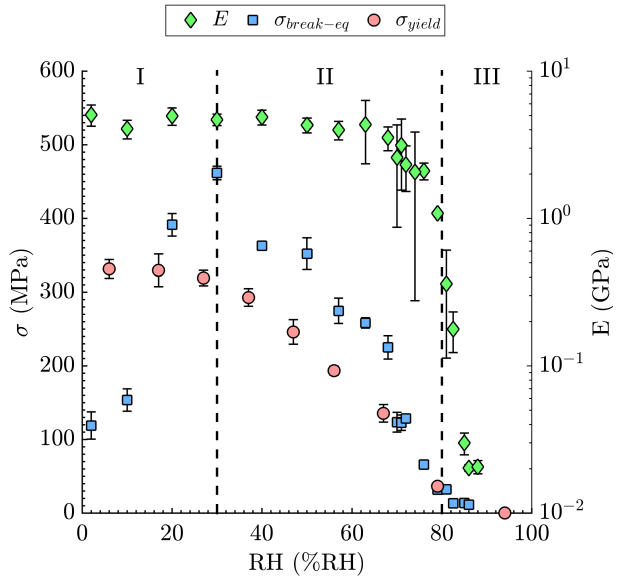

Figure 4 – Influence de l'humidité sur le module élastique E, le seuil de plasticité σ_{yield} et la contrainte à rupture équivalente $\sigma_{break-eq}$ d'une résine polyester modèle non vieillie. E et $\sigma_{break-eq}$ sont estimés par traction de micro fibres entaillées tandis que σ_{yield} est mesuré par compression de micro piliers. Trois domaines peuvent être identifiés : régime I : guérison des défauts majeurs induite par l'eau ($\sigma_{yield} > \sigma_{break-eq}$) - régime II : plastification par l'eau ($\sigma_{yield} \simeq \sigma_{break-eq}$) - régime III : état gel.

Le comportement phénoménologique mis en évidence dans cette étude est schématisé sur la Figure 5. Ces résultats apportent également une meilleure compréhension de la structure macromoléculaire de la résine polyester. En particulier, la chute importante du module élastique lors de la transition vers l'état gel suggère que la densité de réticulation chimique n'est pas aussi grande que celle des résines thermodurcissables standards. A l'inverse, la réticulation physique résultant des interactions hydrogènes entre les groupements polaires résiduels pilote le comportement du matériau dans l'état vitreux et explique sa forte dépendance à l'humidité. Cette hypothèse est étayée par la comparaison à une résine thermodurcissable de type phenol-formaldéhyde pour laquelle l'exposition à des humidités élevées n'induit pas de transition vitreuse du matériau malgré une hydrophilie similaire à celle de la résine polyester.

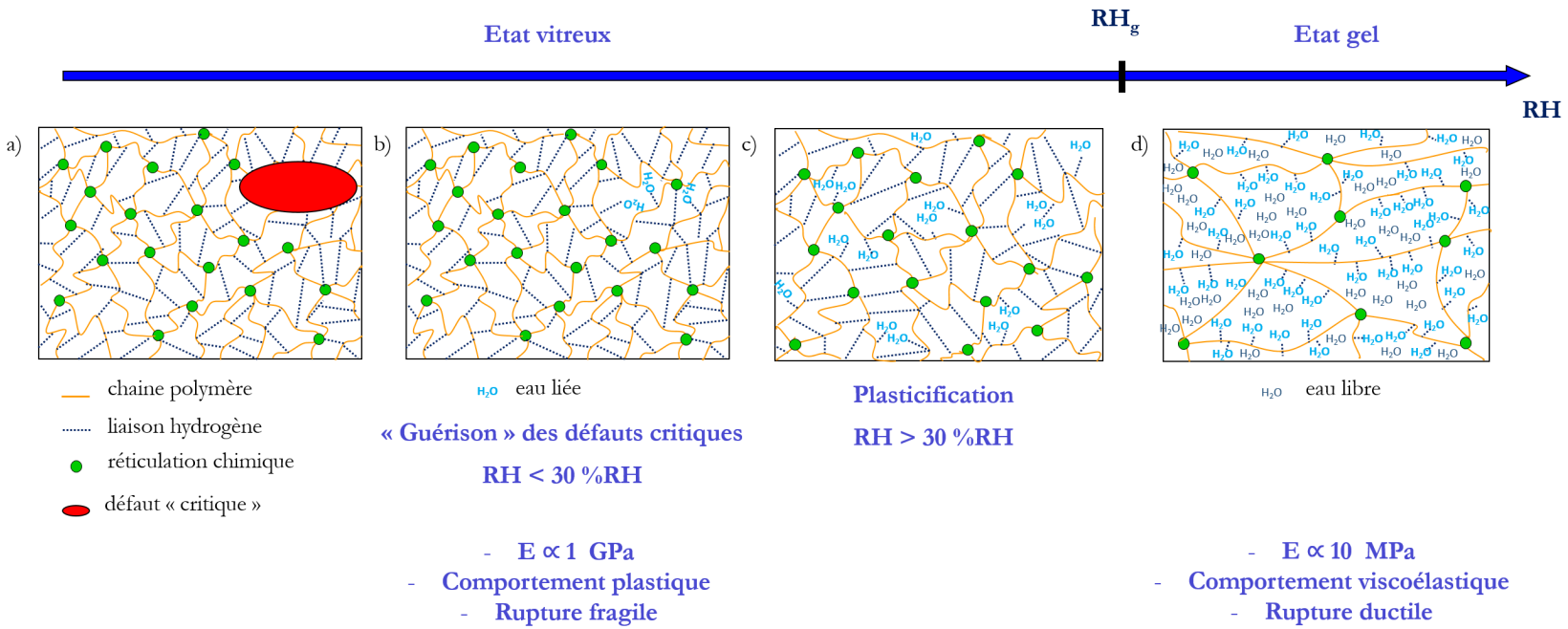

Figure 5 – Mécanismes d'hydratation d'une résine polyester modèle.

Pour le second axe de cette étude, nous nous intéressons à l'influence de l'histoire hydrique sur le comportement de la résine polyester exposée à des conditions d'humidité prolongées (typiquement de quelques jours à quelques semaines). Le suivi des cinétiques d'absorption de l'eau dans le polymère couplé à des mesures de contraintes internes dans des films minces de polymère nous permettent de mettre indirectement en évidence des phénomènes de réorganisation microstructurale dans la résine polyester lorsque celle-ci est soumise à plusieurs cycles successifs d'humidité croissante.

En effet, en raison de son caractère vitreux à des humidités inférieures à RH_g, la structure du polyester évolue lentement via des processus de relaxation structurale et ce, sans impliquer nécessairement une interaction avec l'environnement. Ce vieillissement dit physique est observé sur des échantillons conditionnés à des humidités inférieures à RH_g après préparation.

Par analogie avec les polymères vitreux standards, il est possible de rajeunir ce polyester vieilli physiquement avant sa caractérisation mécanique. Pour cela, un nouvel état de référence est obtenu en exposant le matériau à une humidité supérieure à RH_g puis en le séchant rapidement en dessous de RH_g. Le passage par l'état gel à haute humidité permet de relaxer les contraintes qui se sont développées lors des phases de fabrication et de stockage. Lors du séchage, la transition vers l'état vitreux entraine une diminution importante de la mobilité des chaines de polymère. Le matériau est figé dans un un état rajeuni caractérisé par un plus grand volume libre et un degré de relaxation structurale plus faible que l'état initial. Les tests sont ensuite effectués sur ce nouvel état de référence. Cette méthodologie permet donc de comparer des échantillons indépendamment de leur histoire hydrique et de leur degré de relaxation initial.

Considéré dans leur ensemble, nos résultats montrent que l'histoire hydrique agit sur les propriétés mécaniques, diffusives et microstructurales de la résine polyester de manière similaire à l'impact de l'histoire thermomécanique sur les polymères vitreux. Cette dépendance des propriétés du matériau vis-à-vis de l'histoire hydrique est résumée sur la Figure 6.

Alors que les phénomènes observés précédemment sont réversibles et n'affectent pas la structure chimique du polymère, le vieillissement thermohydrique prolongé du polyester (1 mois - 35 °C - 85 %RH) entraine une dégradation irréversible de ses propriétés mécaniques, notamment une diminution de l'humidité seuil, RH_g et une augmentation du seuil de plasticité dans le régime vitreux comme illustré sur la Figure 7. Bien que la nature exacte de cette variation n'ait pas été identifiée, ces résultats sont néanmoins cohérents avec une réduction de la longueur des chaines polymère via un mécanisme d'hydrolyse.

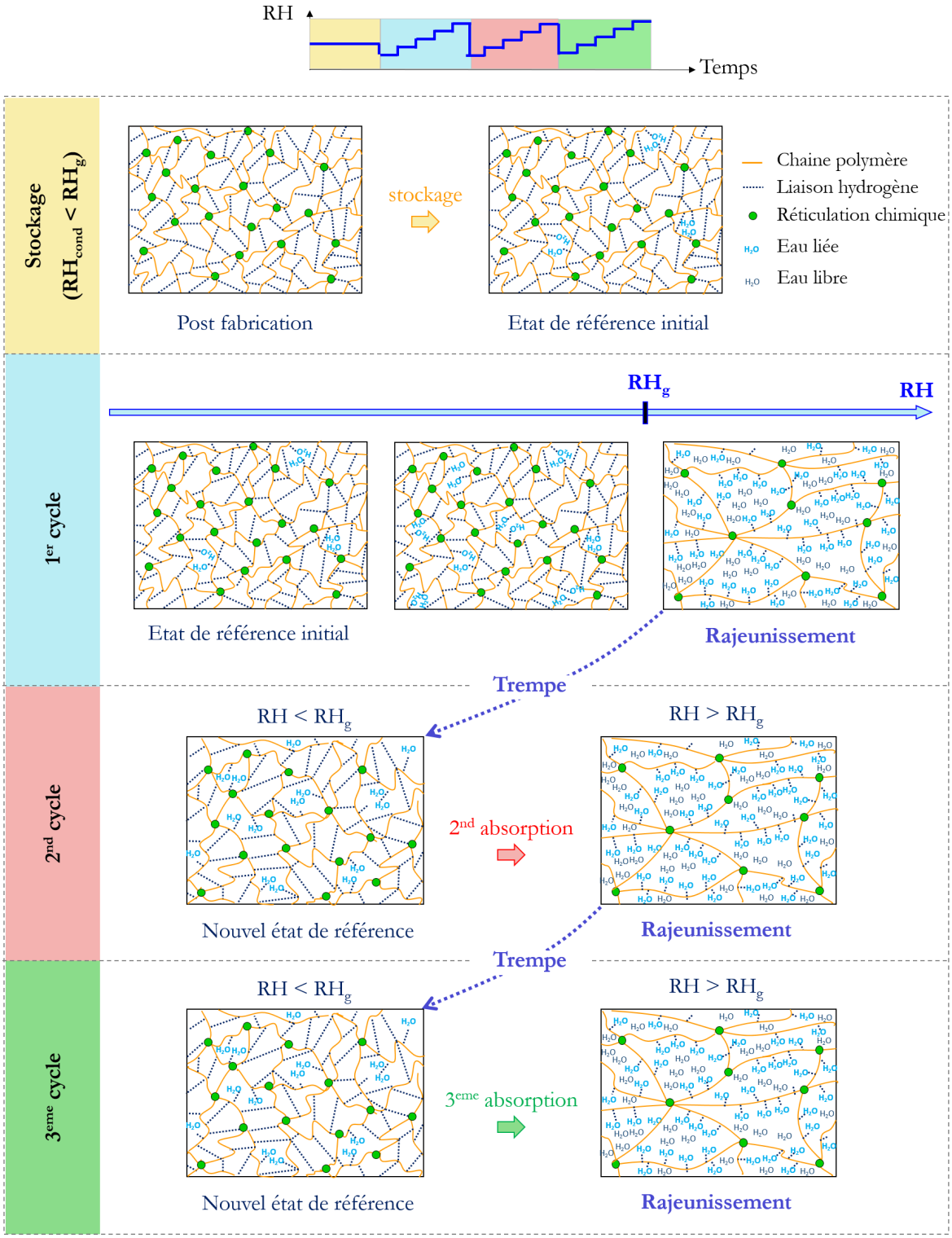

Figure 6 – Influence de l'histoire hydrique sur la microstructure d'une résine polyester non-vieillie, initialement conditionnée à une humidité inférieure à RH_g puis successivement exposée à trois cycles d'absorption.

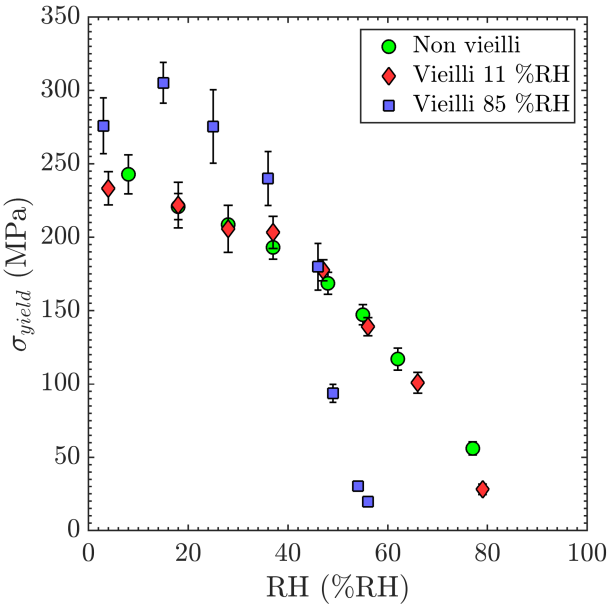

Figure 7 – Evolution du seuil de plasticité en fonction de l'humidité pour une résine polyester modèle soumise à différents taux de vieillissement thermohydrique. Trois conditions sont comparées : un échantillon non vieilli, un échantillon vieilli 1 mois à 35 °C et 11 %RH et un échantillon vieilli 1 mois à 35 °C et 85 %RH.

En conclusion, notre étude apporte un aperçu fondamental de la dépendance à l'humidité du comportement mécanique d'un polyester biosourcé modèle et des mécanismes moléculaires en jeu derrière cette dépendance. Par ailleurs, plusieurs résultats trouvent une application pratique pour Saint-Gobain, notamment les méthodes de préparation et de caractérisation mécanique développées dans cette thèse qui ouvrent dorénavant la route à la caractérisation d'une large gamme de nouveaux polymères dans des conditions environnementales représentatives du cycle de vie des produits industriels.

Contents

Résumé en Français **v**

1 Introduction **1**
1.1 Industrial context . . . 1
1.2 Scientific problem . . . 2
1.3 Scope of the manuscript . . . 2

2 State of the art **5**
2.1 Introduction . . . 5
2.2 Generalities about thermosetting resins . . . 5
2.2.1 Definition . . . 5
2.2.2 Mechanical response of polymeric thermosets . . . 6
2.2.2.1 General features . . . 6
2.2.2.2 Influence of the thermo-mechanical history in glassy polymers . . . 10
2.3 Influence of hygrothermal ageing on glassy polymers . . . 11
2.3.1 General aspects . . . 11
2.3.2 Physical ageing of polymers . . . 12
2.3.2.1 Plasticization . . . 12
2.3.2.2 Water-triggered structural reorganization . . . 16
2.3.2.3 Antiplasticization . . . 18
2.3.3 Chemical ageing of polymers . . . 19
2.3.3.1 Hydrolysis - Mechanism and consequences . . . 19
2.3.3.2 Other water-induced degradation mechanisms . . . 21
2.4 Discussion . . . 21
2.5 Conclusion . . . 24

3 Micro mechanical characterization of polymeric resins **25**
3.1 Introduction . . . 25
3.2 Resin chemistry . . . 25
3.3 Preparation of resin micro samples by soft lithography . . . 26
3.3.1 Preparation limitations . . . 26

3.3.2 Micro molding 27
3.3.3 Micro sample characterization 29
3.4 Compression of polymeric micro pillars 30
3.4.1 Experimental setup description 30
3.4.2 Access to the true stress-strain behaviour 31
3.4.3 Compressive behaviour of the polyester resin at ambient humidity 37
3.5 Tensile testing of polymeric micro fibers 40
3.5.1 Tensile testing method 40
3.5.2 Tensile properties of the polyester resin at ambient humidity . . 42
3.6 Conclusion 44

4 Influence of moisture on the mechanical response of the pristine polyester resin 47
4.1 Introduction 47
4.2 Polyester resin hygroscopy 47
4.2.1 Experimental description - Dynamic vapor sorption 47
4.2.2 Polyester resin/water affinity 49
4.3 Influence of moisture on polyester resin mechanics 49
4.3.1 Controlling relative humidity upon mechanical testing 50
4.3.2 Moisture-dependent compressive properties 51
4.3.3 Moisture-dependent tensile properties 52
4.4 Discussion 57
4.4.1 A water-induced plasticization 57
4.4.2 Antiplasticization of the polyester resin? 59
4.4.3 Existence of a water-triggered glass transition 61
4.4.4 A material model for the polyester resin 63
4.5 Influence of resin chemistry - Comparison to a phenol formaldehyde resin 65
4.6 Conclusion 69

5 Influence of hygric history on polyester resin mechanics 73
5.1 Introduction 73
5.2 Some preliminary evidence of the influence of hygric history - the polyester sorption properties 74
5.3 Internal stresses in polyester layers - a signature of the resin microstructural reorganization 76
5.3.1 Origin of internal stresses 76
5.3.2 Description of the curvature measurement setup 78
5.3.3 Measurement of internal stress isotherms 81
5.4 Influence of hygric history on microstructural reorganization processes in the polyester resin 84

5.4.1 Evolution of internal stresses upon exposure to multiple humidity cycles . . . 85
5.4.2 A water-induced microstructural reorganization . . . 86
5.4.3 A methodology to compare polyester samples independently of hygric history . . . 90
5.5 A first insight into the effect of hygrothermal ageing on polyester mechanics 91
5.6 Conclusion . . . 94

6 Conclusion and perspectives **97**

A Estimation of the water content in polymers **101**
A.1 DVS protocol . . . 101
A.2 Sorption/desorption isotherms - Protocol A . . . 101
A.3 Water sorption/desorption kinetics in pristine polyester resin . . . 102
A.4 Sorption/desorption isotherms - Protocol B . . . 102

B Humidity control setup description **105**

Bibliography **107**

Chapter 1

Introduction

1.1 Industrial context

Polymers are one of the most commonly used materials and can be found almost everywhere in daily life. However, challenges remain regarding their impact on the environment and human health. In order to meet growing environmental concerns, there has been a considerable interest in generating bio-based polymers, namely polymers derived from renewable feedstock, with a goal of replacing the traditional fossil fuel-based chemistry. In addition to their environmental impact, some conventional polymers are also known to be important sources of volatile organic compounds (VOCs) such as formaldehyde and ammonia which are in turn responsible for adverse health effects. In the case of building and furnishing applications, evidence exists about the detrimental impact of these VOCs emissions on the indoor air quality and on the health of building occupants [1, 2, 3].

In order to reduce the ecological footprint of its building materials while minimizing the sources of indoor air pollution, Saint-Gobain has recently developed new bio-based polyester thermosetting resins with reduced VOCs emissions. Product optimization is however currently impeded by the limited knowledge about the mechanical properties of these new polymers. For each application, this knowledge is essential in order to predict the behaviour, performance and durability of the polyester component over the product's lifecycle in natural ageing conditions.

Saint-Gobain is thus interested in a better characterization of the mechanical behaviour of these new bio-based polyester resins, especially under ageing conditions which are representative of the product lifecycle. Among the various types of ageing, hygric ageing is of high interest since a) water is one of the omnipresent substances in our environment, whether in the form of humidity, rain or dew and b) water adsorption is known to be a major cause of mechanical degradation in polyester polymers [4, 5, 6, 7].

1.2 Scientific problem

In this context, we are interested in a model bio-based polyester thermoset provided by Saint-Gobain, a hydrophilic, hard and brittle material which at first sight appears to be a highly chemically crosslinked resin when prepared under industrial curing conditions. The aim of this thesis is to characterize its mechanical behaviour upon hydric ageing and to identify the water-triggered mechanisms which contribute to the variation in its properties. To do so, the following aspects must be considered.

Preparation of polyester samples When cured under technologically relevant conditions, the large foamability of this polyester resin coupled to its fast polymerization prevents the preparation of void-free macroscopic samples. To overcome this processing limitation, we will develop a method to prepare void-free samples with micrometric sizes (typically in the 10 µm range) and controlled geometries.

Micro mechanical characterization of polyester micro samples Because of their micrometric sizes, the polyester samples cannot be characterized using standard mechanical apparati. As a consequence, a micro mechanical approach will be considered. Various micro mechanical testing methods are reported in the literature such as indentation, micro tensile testing and bulge testing [8, 9, 10]. These techniques have been extensively applied on metals, silica glasses and to a much lower extent, on polymers [11]. The second challenge of this study will be to identify the relevant micro mechanical techniques suitable for the study of our material and to develop the corresponding setups in the laboratory.

Influence of humidity and hygrothermal history on polyester mechanics The influence of humidity on the mechanical behaviour of the polyester resin will be investigated using the micro mechanical characterization methods developed. By exposing pristine specimens to various humidities and ageing conditions, we will show that the mechanical properties of the polyester material are largely dependent on the humidity level and hydric history. In the literature, various molecular processes have been reported to account for the reversible and irreversible change in the polymers properties upon water sorption [12]. We will try to identify the dominant mechanisms responsible for this change in properties and propose a material model taking into consideration the micro and macromolecular structure of the polymer.

1.3 Scope of the manuscript

We will first introduce the fundamental concepts of thermosetting resins, their typical mechanical behaviour and the potential impact of hygrothermal ageing on their behaviour in Chapter 1. In Chapter 2, we will present the model bio-based resin of

interest and describe the two complementary micro mechanical characterization techniques used to investigate its mechanical properties: micro tensile testing and micro pillar compression. Chapter 3 will be dedicated to the influence of relative humidity on the tensile an compressive properties of pristine resin specimens, namely samples never exposed to humidity before testing. Finally, Chapter 4 will be devoted to the impact of hydric history on the mechanical and microstructural properties of the model polymer.

Chapter 2

State of the art

2.1 Introduction

The aim of this chapter is to define the specific vocabulary and set the common framework of this study. To do so, we provide a panorama of the literature on two main aspects. The first one concerns the mechanical behaviour of thermosetting resins. After a brief definition of the material structure, we recall the basic principles of the mechanical behaviour of thermosets below and above their glass transition. The second aspect focuses on the effect of hygrothermal ageing, namely ageing under specified conditions of humidity and temperature, on the mechanical properties of polymers. In a third part, we discuss how difficult it is to relate the water-induced change in mechanical behaviour to molecular processes and to extrapolate the results from the literature to the material of interest in this study.

2.2 Generalities about thermosetting resins

2.2.1 Definition

Based on their response to temperature, polymeric materials can be classified into two main categories as shown in Figure 2.1: thermoplastics and thermosets. While a thermoplastic polymer enters a fluid state above its melting temperature, heating a thermoset polymer results in its degradation without the transition to a fluid state. The thermosetting nature of a polymer is due to the presence of a chemically-crosslinked polymeric network which keeps the material solid even at high temperature. Depending on the molecular weight between chemical crosslinks, thermoset polymers can be grouped into thermosetting resins (low molecular weight) and elastomers (high molecular weight) as illustrated in Figure 2.1. The avatars of a material which looks like a thermosetting resin, at first sight, are the subject of this study.

Because of their three-dimensional crosslinked network, thermosetting resins are by definition, infusible and insoluble materials which cannot be reprocessed once cured.

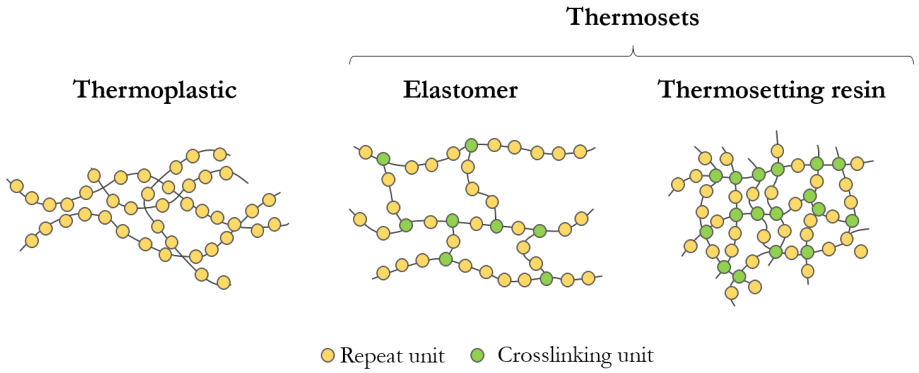

Figure 2.1 – Schematized illustration of the macromolecular structure of a thermoplastic, an elastomer and a thermosetting resin.

However, their high crosslinking characteristics also impart a number of desirable properties to thermosetting resins such as high strength, high modulus, high creep resistance as well as enhanced thermal and chemical resistance [13, 14, 15]. This makes them good candidates for applications in aerospace, automotive, coatings and microelectronics industries that require reliable performance, especially under harsh conditions such high temperature or mechanical load. Thermosetting resins are also widely used as structural materials where they are generally associated with various reinforcements in order to produce composite structures with enhanced mechanical properties.

2.2.2 Mechanical response of polymeric thermosets

One of the most important characteristics of a thermosetting polymer is its glass transition. Most thermosetting polymers are formulated so that their glass transition temperature, T_g is higher than their operating temperature. In this section, we will mainly focus on the basic principles of their mechanical response in the glassy regime, namely for temperatures lower than T_g.

2.2.2.1 General features

The glassy region In the glassy state, the physical behavior of thermosets is essentially controlled by the cohesion and local mobility of the polymer chains, both properties being insensitive to the large-scale structure. As a consequence, only second-order differences exist between linear and crosslinked polymers in the glassy region and most of the results about the physics of linear polymers can be used to predict the properties of thermosets [13, 16, 17].

Because of the presence of large size network defects in the material, whose influence is more pronounced in tension, glassy thermosets usually exhibit a brittle behaviour in tension characterized by a fracture of the specimen without plastic deformation

[13, 18]. In order to investigate their mechanical properties at larger deformation stages, compression tests are carried out. Figure 2.2 shows a comparison between the compressive and tensile strain-stress curves of a standard glassy thermoset.

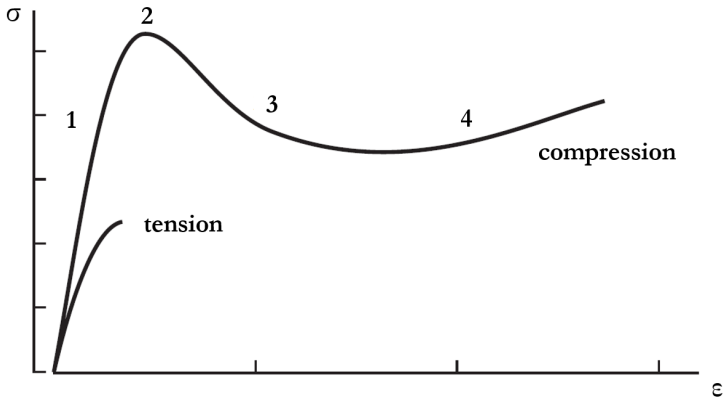

Figure 2.2 – Typical intrinsic stress-strain behaviour of a glassy thermosetting polymer during a uniaxial tensile test and a uniaxial compression test. Adapted from [19].

The compression curve exhibits the following stages [16, 17, 20]:

- **Zone 1 - an elasto-viscoelastic region:** at low deformation level, a linear stress-strain regime is observed where the deformation is fully and instantaneously recovered upon unloading. This so-called elastic region is characterized by the slope of the stress-strain curve defined as the uniaxial Young's modulus, E. Most glassy polymers have similar values of Young's modulus which is typically between 1 GPa and 5 GPa [21]. These properties are determined largely by the intermolecular interactions such as the van der Waals interactions [16]. Beyond a deformation of a few percents, the linear region is followed by a non-linear elastic response where the slope of the stress-strain progressively decreases and where a moderate hysteresis appears upon unloading. Strain is still fully recoverable in times of the order of magnitude of the test time but a delay is observed because of the retarded molecular movement of polymer chains. This behaviour can be referred to as viscoelastic or anelastic reponse.
- **Zone 2 - a yield peak:** the elastic regime is followed by a local maximum in stress which is often defined as the yield stress, σ_{yield} in the literature [22, 23]. The yield peak can be considered as the boundary between the domain of reversible (elastic) and permanent (plastic) deformation. For stress exceeding σ_{yield}, the specimen exhibits a long-term permanent deformation that cannot be completely recovered without increasing the temperature above T_g [16]. Although the fundamental nature of yielding in polymer glasses is still subjected to debate, it is accepted that yielding of polymer glasses involves the cooperative motions of molecular segments of the polymer chains under the action of stress which result

in an irreversible change of configuration. Being directly related to the local mobility of polymer chains, the yield stress is influenced by several parameters including the strain rate [23, 24] and the distance from the polymer glass transition [22, 25]. The oldest theory describing this dependence is attributed to Eyring [26]. Eyring's model postulates that yielding occurs as a result of stress and temperature-activated jumps of molecular segments. Strain energy will be released by these jumps so that applying shear stress lowers the activation energy necessary for these jumps. This effect is controlled by the so-called activation volume $V*$, which is an adjustable parameter with no clear physical meaning. Molecularly-based theories of yield in polymer glasses were later proposed by Roberston [27] and Argon [28] for instance.

- **Zone 3 - a strain softening region:** beyond the yield peak, the stress decreases to reach a minimum value and (nearly) constant plastic plateau as the polymer undergoes plastic flow. This drop in true stress after yielding is referred to as intrinsic strain softening. Although the origin of this phenomenon is not yet completely understood, intrinsic strain softening is closely related to yield stress and will be affected by the same parameters.
- **Zone 4 - a strain hardening region:** as deformation continues, either the material fails or the stress strongly increases again in the case of entangled or crosslinked polymers. This strain-hardening behaviour has been associated with the entropic resistance to the progressive chain alignement between crosslinks at large strains [29, 30, 31]. As a consequence, the strain hardening modulus is significantly affected by the network crosslinking density. This fact has been confirmed by Melick who observed a more pronounced strain hardening for increasing network densities irrespectively of the nature of the network, i.e. physical entanglements or chemical crosslinks [29]. However, the exact role of entropic effects is not clear and thermally-assisted local rearrangements must also be taken into consideration to fully understand the large strain behaviour of crosslinked glassy polymers [32].

In the tensile configuration, a glassy thermoset exhibits a brittle behaviour as shown by the premature rupture of the material in the elastic regime in Figure 2.2. Because of this brittleness, the intrinsic fracture properties of thermosets are often difficult to measure. When tested under uniaxial tensile testing, the fracture behaviour can be characterized using the stress and strain at break which will be denoted as σ_{break} and ε_{break}, respectively. However, these parameters have been found to depend on the sample dimensions [16, 33]. Higher stresses at break are measured as sample dimensions decrease due to the lower probability of having large defects in the material. As a consequence, σ_{break} and ε_{break} cannot be considered as intrinsic values of the material fracture properties.

The rubbery region For temperatures exceeding the glass transition temperature T_g, thermosetting resins shift to a rubbery regime where their mechanical properties are governed by the crosslinking density of the molecular network. This transition is highlighted by the temperature dependence of the elastic modulus of the material, which is schematized in Figure 2.3 for two different crosslinking densities.

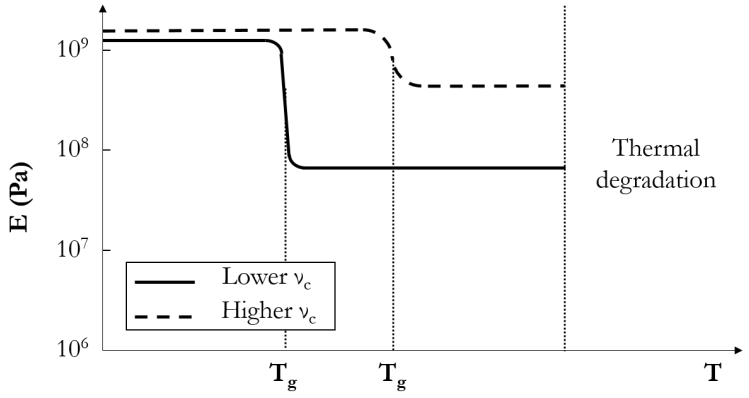

Figure 2.3 – Schematized temperature dependence of the elastic modulus, E of two thermosetting polymers with the same chemical structure but different crosslinking densities ν_c. Adapted from [34].

Below T_g, the polymer is in the glassy region where it is characterized by an elastic modulus of the order of 1 GPa. As temperature increases above T_g, the polymer chains gain sufficient thermal energy to overcome the van der Waals interactions. The elastic modulus decreases moderately, by one order or magnitude or less, to reach a rubbery plateau. Because of the covalent links between polymer chains, the rubber integrity is maintained until thermal degradation occurs.

While the two thermosetting polymers shown in Figure 2.3 cannot be distinguished in the glassy regime, an increase in the crosslinking density results in a larger T_g and a larger modulus on the rubbery plateau because of the reduced mobility of chain segments [35, 36].

Note on the determination of the crosslinking density of thermosets The crosslinking density is a key parameter to understand the behaviour of thermosets in the rubbery region and to follow the evolution of the newtork structure upon ageing. The modulus in the rubbery state can be used to estimate the crosslinking density. According to the rubber elasticity theory [37], the shear elastic modulus G is given by Equation 2.1:

$$G = \frac{\rho R T \phi}{M_c} \tag{2.1}$$

where ρ is the polymer density, R the molar gas constant, T the absolute temperature and M_c the average molecular weight of chain segments between crosslink points. ϕ is a parameter which takes into account the non-ideality of the network and the selected

physical approach. Assuming volume conservation (which is often the case for polymers in the elastic regime), the Young's modulus, E can be deduced from the shear modulus using Equation 2.2:

$$G = \frac{E}{3} \tag{2.2}$$

For a Gaussian network namely an "ideal" rubber, ϕ is equal to unity but Equation 2.1 no longer holds as the non-Gaussian character becomes more and more predominant with increasing crosslinking density. Although thermosets are far from being ideal rubbers, the basic rubber elasticity has been applied to some highly-crosslinked networks [13, 38]. However, the parameter ϕ cannot be predicted theoretically from the network structure. As a consequence, this method can only be considered as a rough estimation of the relative crosslinking density in specimens with similar chemistry and structure apart from their crosslinking density.

Another non-empirical method is based on the Flory-Rehner theory which relates the crosslinking density of a polymer network to its equilibrium swelling ratio when swollen in a solvent [37]. However, this method requires knowing the polymer-solvent interaction parameter which is not easy to determine accurately.

2.2.2.2 Influence of the thermo-mechanical history in glassy polymers

When maintained at temperatures lower than their T_g, thermosets, like any glassy material, undergo a microstructural reorganization through a process known as physical ageing [16, 39]. During processing, thermosets are generally quickly cooled from a temperature above to a temperature below their T_g. When passing through the glass transition temperature, the chain mobility dramatically decreases and polymer chains remain frozen in a configuration which is far from being thermally equilibrated. As a consequence, thermodynamic variables such as volume, entropy and enthalpy deviate from their equilibrium values as illustrated in Figure 2.4 (left). Especially, the excess of volume referred to as free volume, arises because of irregular molecular packing in the glassy state.

Although their mobility is reduced, polymer chains still possess a certain degree of segmental mobility which gives polymer glasses the opportunity to slowly evolve toward equilibrium. This mobility is responsible for the existence of sub-T_g relaxation processes (β relaxation, γ relaxation...) which lead to the local reconfiguration of chain segments and the reduction of the excess in thermodynamic quantities (see Figure 2.4) (left).

This drive for an energetically more favourable state is accompanied by a change in the polymer physical properties. More precisely, this reorganization leads to the formation of a more compact molecular structure with a global strengthening of the intermolecular interactions. The reduction in polymer free volume results in a densification of the material over time. Mechanical properties are also affected by physical

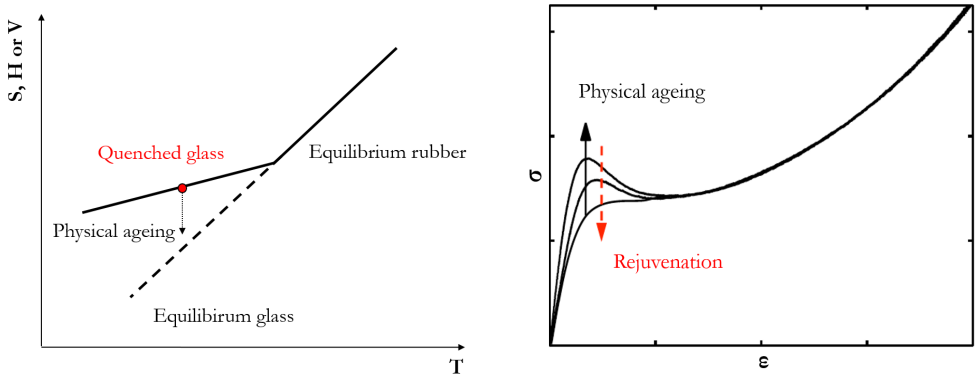

Figure 2.4 – Left: schematized illustration of physical ageing: thermodynamic variable (entropy S, volume V or enthalpy H) as a function of temperature T. Right: schematized representation of the influence of physical ageing on the stress-strain behaviour of a glassy polymer. Physical ageing is accompanied by an increase in elastic modulus, yield stress and strain softening amplitude. Adapted from [17].

ageing as shown in Figure 2.4 (right). Upon ageing, the elastic modulus, yield stress and strain softening amplitude slowly increase over time while the large strain behaviour remains unaffected [40, 41, 42].

Physical ageing is a reversible process and contrasts with chemical ageing which induces irreversible modifications of the polymer chemical structure. To erase the effect of physical ageing and return the polymer to its non-equilibrium state, the material can be rejuvenated. Thermal rejuvenation consists in reheating a polymer specimen above its T_g for a sufficiently long time to increase its amount of free volume. The specimen is then rapidly cooled down below its T_g in order to quench this excess free volume (quenching) [40]. Rejuvenation can be also achieved by applying plastic deformation to the material as explained by Melick who reported a reduction in yield stress and strain softening amplitude by pre-deforming glassy polystyrene [42].

As a conclusion, because of their non equilibrium nature, the microstructure and physical properties of thermoset glasses are strongly influenced by the processing conditions and the whole sample history (thermal and mechanical) below their glass transition temperature.

2.3 Influence of hygrothermal ageing on glassy polymers

2.3.1 General aspects

Water is one of the omnipresent substances in our environment, either in the gazeous (ambient humidity) or liquid (rain, dew) form, and all materials are exposed to its influence. The change in the polymer physical and chemical properties upon hygrothermal ageing is a critical issue which impacts the long-term performance of the material.

Moisture absorption can indeed lead to a wide range of effects which can be divided into two main categories:

- Reversible effect or physical ageing which results from a reorganization of the polymer microstructure without any alteration of the network chemical structure. The suppression of the ageing source leads to a progressive return to the initial material properties.
- Irreversible effect or chemical ageing which leads to an irreversible degradation of the macromolecular structure. The material properties are only partially recovered after the suppression of the ageing source.

We attempt here to provide a global overview of the main physical and chemical ageing events taking place in polymers upon hygrothermal ageing, with a closer attention to their effect on the mechanical behaviour of glassy polymers and chemically-crosslinked resins.

2.3.2 Physical ageing of polymers

2.3.2.1 Plasticization

Definition The notion of plasticizer is not restricted to water and more generally designates a small molecular weight compound incorporated into polymers in order to improve their processability and modify the properties of the final product [43]. Plasticization refers to the phenomenological behavior associated to the reversible depression of glass transition temperature T_g as a result of plasticizer incorporation. In the case of water, sorbed water partially disrupts the cohesion of the material without any alteration of the network chemical structure which leads to a sharp increase in the mobility of the macromolecular chains. Enhanced chain mobility in turn affects the polymer T_g and other physical properties. The extent of the T_g depression depends on the concentration of the plasticizer and its interaction with the polymeric material. For instance, the T_g of most epoxy resins is reduced by about 10 °C per percent of sorbed moisture [44, 45, 46].

Plasticization is considered as reversible since initial properties can be recovered upon water desorption. However, this reversibility may be seemingly affected because of the internal stress relaxation and structural reorganization induced by plasticization [46] or because of the presence of residual water which cannot be desorbed under moderate drying conditions [47]. The notion of water-induced structural relaxation will be discussed in more detail in Section 2.3.2.2.

Molecular theories It is widely accepted that low-molecular weight plasticizers reduce the secondary interactions (such as van der Waals and hydrogen interactions) between the polymer chains and thus, reduce the resistance to molecular motion. These

changes take place via different mechanisms depending on the level of interaction between the plasticizer and the polymer matrix. Three main theories have been proposed to explain the mechanism and action of plasticizers on polymers [43, 48, 49]:

- **The lubricity theory:** this theory assumes that the rigidity of polymers originates from intermolecular friction. By diffusing into the polymer and inserting in between polymer chains, the plasticizer acts as a lubricant by reducing the resistance to sliding and thus, facilitates polymer chain mobility. According to this theory, a plasticized polymer can be represented by plasticizing molecules lubricating layers of polymer as illustrated in Figure 2.5.a.
- **The gel theory:** this theory assumes that the rigidity of polymers comes from three-dimensional polymeric structures formed by weak polymer-polymer interactions along the chains such as hydrogen bonds, van der Waals forces or ionic forces. By interacting with the attachment sites, the plasticizer molecules hinder the forces holding the polymer chains together and prevent the reformation of the intermolecular interactions. As a consequence, the "gel" rigidity is reduced.
- **The free volume theory:** in a polymeric material, the free volume can be defined as the internal space unoccupied by the polymer molecules and available for chain motion. An increase in free volume is thus accompanied by an increase in chain mobility. A large increase in free volume is for instance observed during the transition from a glassy to a rubbery state. The free volume theory suggests that a plasticizer molecule increases the free volume between polymer chains, resulting in enhanced chain mobility.

These theories are summarized in Figure 2.5. Because of their conceptual overlap, plasticization can be often explained by the combination of the three theories.

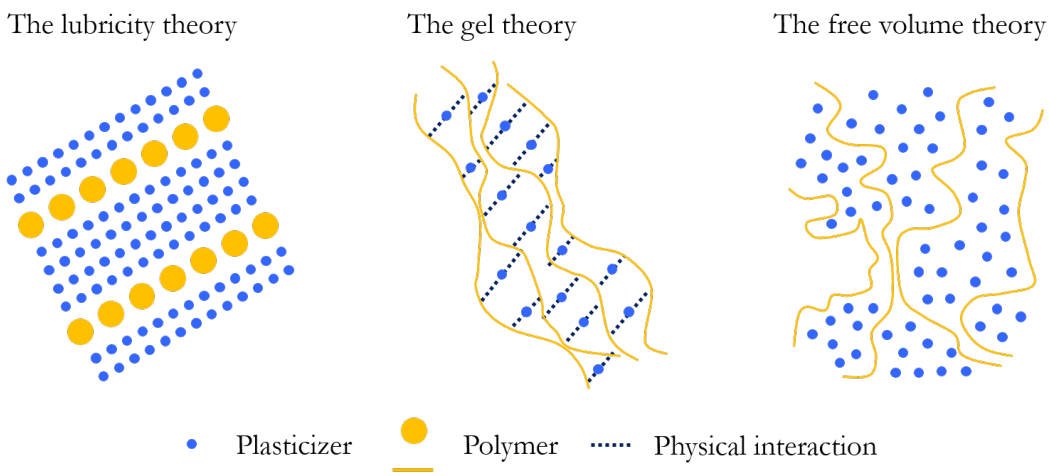

Figure 2.5 – Illustration of the molecular theories of plasticization. Adapted from [48].

For the specific case of water-induced plasticization, most papers deal with hydrophilic polymers such as epoxy resins [44, 45, 46], polyamide (PA) [25, 50, 51] and polyvinylalcohol (PVA) [52, 53]. It has been demonstrated experimentally that water plasticizes polymers not only by disrupting intermolecular interactions (lubrication/gel theory) [47, 52, 54] but also by creating free volume in the polymer (free volume theory) [50, 52].

Numerous studies have also suggested that various states of water exist in polymers and that these states may have different influence on the T_g variation. Briefly, the water absorbed in polymers is generally classified into two main different classes [55, 56, 57]:

- Free water, i.e., water molecules which do not interact with polymer chains and behave as bulk water. Free water forms clusters and resides in the microvoids as described in epoxy resins by Apicella [55] for instance.
- Bound water, i.e., water molecules which interact with the hydrophilic groups along the polymer chains through hydrogen bonding.

By considering only the amount of bound water in the prediction of the T_g of a water-plasticized PVA, Hodge showed that bound water is responsible for the majority of plasticization while free water has a limited influence on the polymer T_g [52]. Moreover, bound water can be classified into different sub-categories depending on the degree of interactions with the polymer chains [47, 57, 58] and leads to non-trivial plasticization effects in polymers. According to Zhou [47, 54], single-hydrogen-bonded water acts as a classical plasticizer by disrupting the intermolecular physical interactions and increasing chain mobility. Inversely, water forming multiple hydrogen bonds with polymer chains is believed to produce a crosslinking effect which leads to a reduction of molecular mobility and an increase in the polymer T_g. This phenomenon referred to as antiplasticization will be discussed in more detail in Section 4.4.2.

Effect on glassy polymer mechanics By depressing the polymer T_g, plasticization has a considerable influence on the mechanical behaviour of glassy polymers. By enhancing chain mobility and softening the material, plasticization plays a role similar to an increase in temperature on the mechanical properties. More precisely, water sorption generally results in a reduction of the polymer elastic modulus [25, 59, 60, 61], yield stress [25, 51, 59] and tensile strength [6, 53, 59] and in an increase in the elongation at break [6, 53, 59].

These tendencies and the amplitude of the variations however differ from one polymeric system to another. For instance, polyamide specimens displayed a non-negligible reduction in the elastic modulus for a water uptake of 5 %wt [25] while no significant variation of the elastic modulus was observed for an epoxy resin containing 5 %wt of water [62] although the increase in water content was accompanied by a depression of the polymer T_g in both cases.

More interestingly, plasticization can significantly lower the glass transition temperature so that the polymer T_g becomes lower than the testing temperature. This causes a transition from a glassy to a rubbery state. Water-induced glass transition has been reported in various polymers such as in PVA upon moist exposure [53, 63] or inversely, in polymeric hydrogels upon dehydration [64, 65]. By analogy to the glass transition induced by a temperature change, the relative humidity at which this transition occurs is sometimes referred to as the glass transition relative humidity, RH_g. As for the classical thermally-activated glass transition, the water-triggered transition is accompanied by a marked change in the polymer mechanical properties as illustrated in Figure 2.6 for a non-crosslinked PVA polymer exposed to various relative humidities [53]. When increasing humidity from 42 %RH to 65 %RH (equivalent to water contents varying from 8 %wt to 14%wt, respectively), the polymer exhibits a large drop in its elastic modulus and undergoes a transition from a brittle to a ductile behaviour. The curve at 65 %RH is characteristic of a rubbery state.

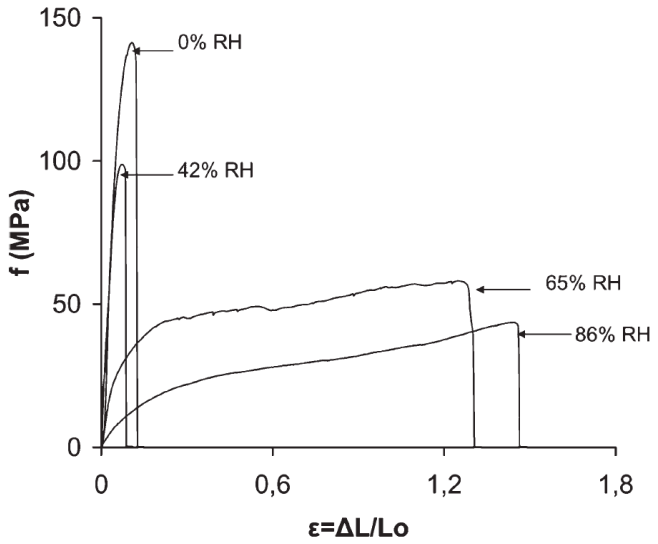

Figure 2.6 – Representative tensile engineering stress (f) - strain (ε) curves obtained on PVA samples tested at ambient temperature (23 °C) and different relative humidities. Adapted from [53].

Based on the results of Annaka and Ilyas [64, 65], this transition can be associated to a change in the state of water molecules in the polymer matrix. Both authors studied the gel-to-glass transition of hydrogels upon dehydration by measuring the evolution of their elastic properties while studying the change in water structure which was divided in the two classes: non-freezable water (i.e., bound water restricted by its strong interactions with polymer) and freezable water (i.e., free water or weakly interacting water). The amount of freezable water in the polymers was estimated from the water melting peak measured by differential scanning calorimetry while the bound water content was deduced knowing the total water uptake, determined gravimetri-

cally. Those results showed that the transition to a gel state was correlated to the large increase in free water content whereas most water existed as bound water in the glassy state. This change in interactions was confirmed by Sekine [57] who studied the local structures of water molecules during the dehydration of polydimethylacrylamide (PDMAA) hydrogel using Raman spectroscopy. Unfortunately, those results were not correlated to variation in the mechanical properties of PDMMA gel.

Although the existence of a water-triggered glass transition is considered as detrimental in fields such as food and pharmaceutical products [66, 67], moisture can be used as a stimulus in shape-memory polymers [68, 69] where the shape recovery is induced by the transition of the polymer from its glassy to its rubbery state upon moist exposure as displayed in Figure 2.7.

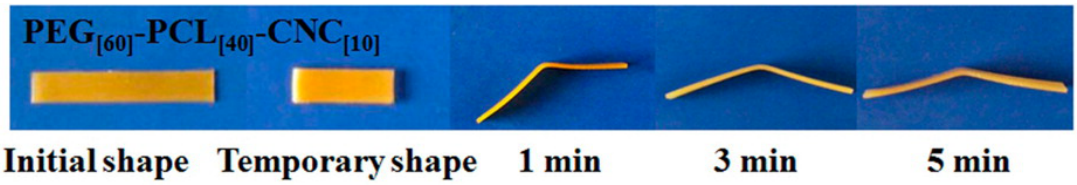

Figure 2.7 – Shape-memory process of a folded film made of a water-responsive polymer nanocomposite. Shape recovery is achieved by immersing the sample in water. Adapted from [68].

2.3.2.2 Water-triggered structural reorganization

By locally increasing the mobility of the polymer chains, plasticization contributes to structural rearrangements within glassy polymers without altering their chemical structure. The effect of this structural reorganization has been evidenced on the diffusion and sorption properties of glassy polymers [46, 70, 71]. A deviation from the classical Fickian diffusion is often reported in glassy polymers because of the existence of water-induced relaxation processes [12, 72, 73]. An example of the sorption behaviour of a glassy polymer is displayed in Figure 2.8 (top). When water molecules penetrate into the glassy matrix, the mobility of polymer chains locally increases as a result of plasticization. The associated increase in free volume allows the material to incorporate more water as structural relaxation proceeds [46].

Another consequence of this water-induced microstructural reconfiguration is that the physical properties of glassy polymers are also affected by their hydric history. This history-dependence has been evidenced in glassy resins subjected to multiple sorption-desorption cycles [46, 70]. For instance, enhanced water uptake level and faster diffusivity were observed in a bismaleide resin between successive cycles [70] as shown in Figure 2.8 (bottom). During the first sorption, sorbed water plasticizes and rearranges the polymer in a more open structure because of swelling. Upon desorption,

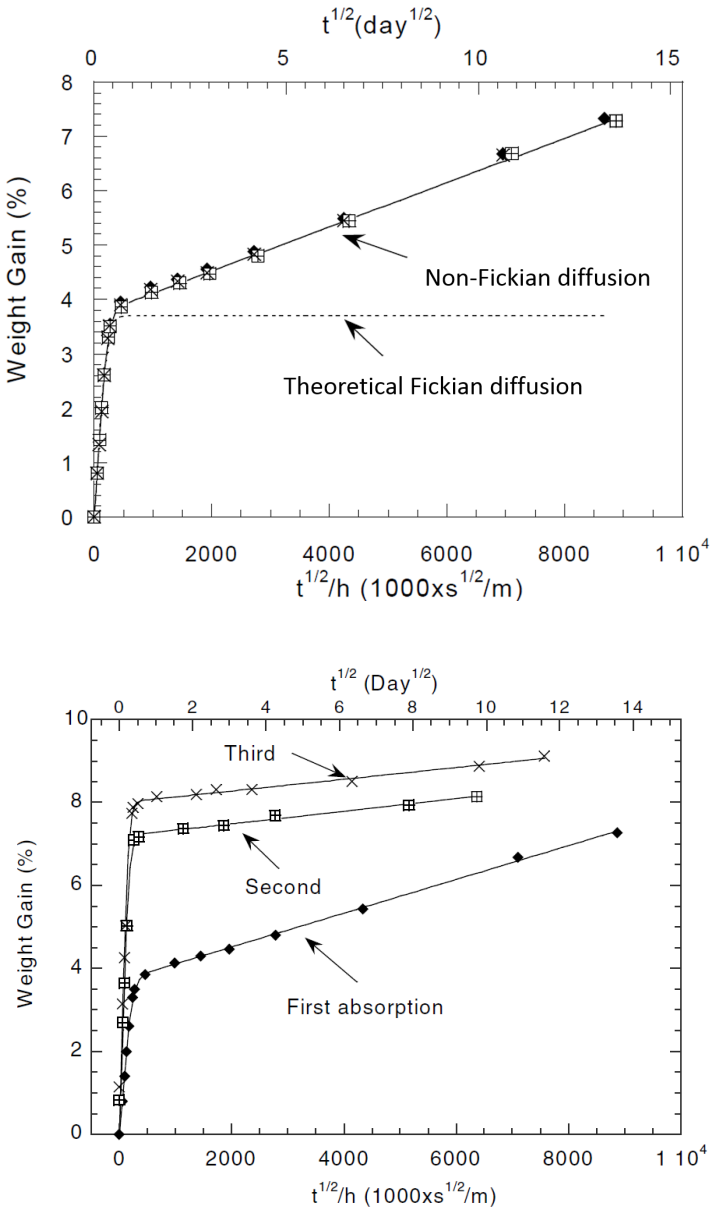

Figure 2.8 – Sorption behaviour of a glassy bismaleide resin immersed in water. Top: illustration of the deviation from the classical Fickian diffusion theory (dotted line). Bottom: evolution of the sorption properties upon exposure to successive sorption/desorption cycles. Adapted from [70].

the reduction in chain mobility freezes the structure which cannot relaxe to its initial dry state configuration. As a consequence, the enhanced free volume at the beginning of the second sorption cycle results in enhanced sorption properties.

It it is well known that microstructure of polymer glasses has a significant impact on their mechanical properties as previously discussed in the case of thermally-activated physical ageing in Section 2.2.2.2. The water-induced microstructural reorganization coupled to the variation in water content is thus likely to impact the mechanical behaviour of glassy polymers.

2.3.2.3 Antiplasticization

While most papers have suggested that water absorption induces a loss in the polymer mechanical properties as a result of plasticization, several studies have also reported some abnormal properties increase with hygrothermal exposure in various polymers containing low to intermediate water contents, such as epoxy resins [45, 74] and starch [60, 75]. With increasing hydration, a maximum of certain mechanical properties including the tensile strength, elastic modulus or yield stress have been observed in glassy polymer-plasticizer systems, even though a T_g depression may be evident [60, 75, 76, 77]. The conventional plasticization effects are then observed again for water content exceeding a "plasticization threshold" [76]. A broader literature is available about antiplasticization by plasticizers other than water, such as phthalates [6, 78] and polyols [75, 79, 80].

Antiplasticization is a complex phenomenon whose effects on the physical properties of glassy polymers cannot be generalized. Opposite trends have been indeed reported in the literature depending on the polymer-plasticizer system considered. For instance, Chang [75] studied the effect of two plasticizers (water and glycerol) on the mechanical properties of starch using tensile testing. Both plasticizers led to a reduction of the polymer T_g but when studied as a function of water content, the starch films exhibited a maximum in tensile strength while the elastic modulus was gradually reduced. Inversely, a maximum in elastic modulus but a gradual reduction in tensile strength were measured for increasing glycerol content.

To describe antiplasticization, various mechanisms and explanations have been suggested: free volume reduction through "hole filling" by plasticizer molecules [50, 81, 82], crosslinking effect of water molecules leading to a reduction of the segmental cooperative motions in polymer chains [47, 81], improved reorganization of the material which promotes molecule packing, post-curing reactions or crystallization [80, 83, 84]. However, experimental evidence is missing to support current assumptions and antiplasticization remains to date a complex phenomenon which is strongly dependent upon compositional and structural details, and in which several causes seem to be interrelated.

2.3.3 Chemical ageing of polymers

When exposed to humidity or immersed in water, polymers can undergo irreversible (or chemical) damage which superimposes with the reversible (or physical) effects of water described in the last section. Hydrolysis is a very common damage mechanism observed in polymers. After a description of the hydrolysis process, we provide a brief overview of the alternative water-induced degradation mechanisms reported in polymers.

2.3.3.1 Hydrolysis - Mechanism and consequences

Definition and mechanism Hydrolysis involves a chemical reaction between polymer chains and water molecules which results in bond scissions along the polymer backbone or along the polymer lateral groups. As a consequence, hydrolysis leads to a reduction of the polymers molecular mass or crosslinking density. Water-induced chain cleavage is observed in polymers possessing groups which chemically react with water, such as ester [85], amide [86] and epoxyde functions [87]. The generalized chemical reaction can be written as follows:

$$X - Y + H_2O \longrightarrow X - OH + H - Y$$

Hydrolysis is generally a slow process at ambient temperature but reaction kinetics can be accelerated by elevating temperature [88, 89]. This principle is applied in thermally-accelerated ageing procedures where specimens are aged at higher temperature in order to overcome the temporal limitation of natural ageing under ambient conditions. Indeed, long exposure times (varying from weeks, to months and even years depending on the system) are usually necessary to observe significant variation in the material properties due to chemical ageing. However, the question of whether accelerated ageing produces the same effect as natural ageing remains controversial since the accelerated procedure may activate other chemical reactions and degradation mechanisms that do not occur under natural ageing conditions.

Consequences of hydrolysis As a result of chain scissions, hydrolysis decreases the molecular mass or crosslinking density, which usually degrades the functional, structural and mechanical properties of the polymer matrix. As a consequence, various methods can be used to track hydrolytic degradation depending on the type of polymer and available characterization techniques.

Mass variation is probably the most reported techniques to study polymers degradation upon hygrothermal ageing [5, 86, 90]. A schematized evolution of the water content of polymer subjected to hygrothermal ageing is sketched in Figure 2.9. After an initial water uptake, the water content reaches a steady-state value dictated by

the polymer free volume and the polymer/water affinity [12, 61]. In the presence of chemical ageing, water content starts increasing again, which can be attributed to an increase in polymer free volume resulting from chain cleavage or to the development of osmotic/swelling cracks. The change in chemical structure can also induce a change in the polymer hydrophilicity. In polyesters, the substitution of moderately polar groups (ester) by strongly polar groups (hydroxyl and carboxyl acid) enhances the polymer hydrophilicity which in turn enhances water uptake as hydrolytic degradation progresses. In the case of specimens aged by immersion in water, mass loss is finally observed for large extent of degradation due to the leaching of degradation products. Despite its ease of implementation, this method is however very restrictive and does not allow differentiating the mechanisms responsible for the mass variation. Water-induced structural reorganization may also contribute to an increase in water content while a significant extent of degradation is necessary to observed mass variation.

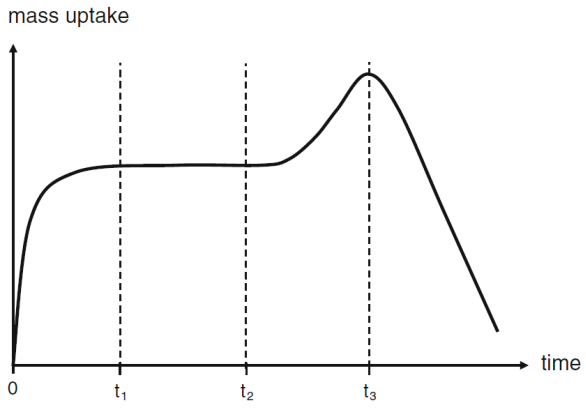

Figure 2.9 – Typical evolution of the mass uptake as a function of time for an immersed specimen subjected to hydrolytic degradation. After an initial diffusion of water ($t < t_1$), the water uptake reaches a steady-state ($t_1 > t > t_2$) until the activation of hydrolysis ($t > t_2$) and the mass loss induced by leaching of degradation products ($t > t_3$). Adapted from [12].

Chemical characterization techniques such as Fourier transform infrared (FTIR) spectroscopy [85, 87, 91] and X-ray photoelectron spectroscopy (XPS) [91] are also used to investigate the impact of hydrolysis at the molecular and macromolecular scales, for instance by measuring the apparition/disparition of water-sensitive functions as a result of chain cleavage in the polymeric matrix.

Hydrolysis has been also evidenced from its impact on the polymer mechanics [12]. More precisely, for chemically crosslinked polymers, the reduction in crosslinking density is accompanied by a decrease in the glass transition temperature, T_g and elastic modulus in the rubbery state while little effect is usually reported on the modulus in the glassy state [12, 92]. Other mechanical properties may be affected upon hydrolytic ageing such as the tensile fracture strength and elongation at break which were found to decrease over time in polyamide [86]. It is however difficult to extract general ten-

dencies as opposite effects are observed from one material to another [5]. Moreover, in the peculiar case of thermosetting resins, polymers are often studied as composite structure [5, 84, 86, 92] in which the presence of fillers makes it difficult to decorrelate the effect of hydrolysis from the effects of other degradation mechanisms such as fiber/matrix debonding.

Note finally that the influence of hydrolysis on polymer mechanical properties bears close similarities with plasticization (see Section 2.3.2.1). Both phenomena are usually decorrelated by evaluating the ability of the material to recover its initial property upon drying [87, 93, 94]. While plasticization is supposed to be reversible, hydrolysis leads to an irreversible loss of mechanical properties even after water removal.

2.3.3.2 Other water-induced degradation mechanisms

Other water-induced degradation mechanisms can lead to an irreversible loss of the mechanical properties in polymers. These phenomena usually superimpose with the chemical degradation resulting from hydrolysis. Among these mechanisms, the effects of differential swelling [90] and osmotic cracking [95, 96] are presented here.

During the product's life cycle, polymers are generally subjected to multiple humidity cycles when exposed to natural weather conditions. During the transient stage of water sorption, the heterogeneous in-thickness moisture concentration induces a differential hygroscopic swelling [90, 97]. The resulting internal stresses may eventually cause irreversible damage such as the development of cracks within the material. Note that differential swelling is often problematic in polymeric composites in which the presence of rigid fillers hinders the volume change of the thermosetting matrix, leading to a degradation of the matrix/filler interface [92].

Osmotic cracking has also been described in literature as a damage mechanism in polymers aged by immersion in water [95, 96]. This phenomenon originates from the segregation in micro voids of pre-existing small organic impurities or small degradation products generated by hydrolysis. Some of these inclusions, especially water-soluble, interact with dissolved water through the polymer matrix which acts as a semi permeable membrane between the inclusions and surrounding water. This leads to the build-up of an osmotic pressure which eventually results in the propagation of micro cracks when the internal pressure in the micro voids overcomes the polymer strength.

2.4 Discussion

The aim of this review was to introduce the notion of thermosetting resins, their typical mechanical behaviour and its potential evolution upon hygrothermal ageing.

The high chemical crosslinking density imparts to thermosets enhanced mechanical properties and resistance. Because of the reduced mobility of the polymeric network,

these materials behave as glassy polymers under ambient conditions. Since polymer glasses are a non equilibrium state by nature, their microstructure undergoes local reconfiguration over time through a reversible process known as physical ageing. As a consequence, even in the absence of water, the mechanical response of thermoset glasses are strongly influenced by the processing conditions and the whole sample history (thermal and mechanical) below the glass transition. This aspect must be taken into consideration when characterizing this class of materials.

In addition to the effect of physical ageing, the mechanical behaviour of thermosets and polymers in general is known to be affected by the environmental conditions, especially by moisture. An extended literature exists about the reversible (physical) and irreversible (chemical) effects of hygrothermal ageing on the mechanical properties of polymers. However, several limitations remain to extend these notions to the material of interest in this study.

The degradation kinetics and consequences of moist ageing strongly differ depending on the polymer nature, sample geometry [98] and ageing conditions considered. In addition, in the peculiar case of thermosets, a handful of papers about the effect of hygrothermal ageing deals with composite structures in which it is rarely possible to decorrelate the influence of the polymeric matrix degradation from the polymer/filler coupling [5, 92]. As a consequence, the results from the literature cannot be directly extrapolated to our system.

Identifying the dominant mechanisms responsible for properties degradation is of high importance in order to optimize the material formulation. The loss of properties generally results from several molecular processes which simultaneously take place in the material. However, papers reporting at the same time the variation in polymers mechanical behaviour upon hygrothermal ageing and relevant chemical investigation of the change in macromolecular structure are scarce.

In the absence of chemical investigation, highlighting the relevant degradation processes is complex as different mechanisms can lead to similar change in material properties. For instance, plasticization and hydrolysis both reduce the glass transition temperature of polymers although the fundamental reasons differ between the two mechanisms (monomer friction vs. network structure). Inversely, phenomena such as antiplasticization may counteract the effect of moist ageing and surprisingly improve the material properties. Plasticization and irreversible degradation may however be decorrelated by measuring the temporal evolution of a given property as explained by Verdu [90]. The principle is illustrated in Figure 2.10. In the case of plasticization, after an initial reduction, the property finally reaches a steady state value as no further damage occurs in the material (case I). Inversely, if chemical ageing superimposes to plasticization, a continuing loss of properties is observed over time as the material is gradually degraded (case II).

In addition, several authors have proposed to evaluate the extent of reversible

and irreversible damage by measuring the ability of the material to recover its initial properties after water removal [87, 93, 94]. However, care must be taken to ensure that no residual water remains in the sample. Moreover, water-induced microstructural rearrangements may in appearance affect properties recovery although no network damage has occurred. Both methods will be consider in this study to investigate the molecular processes responsible for the change in mechanics upon hygrothermal ageing.

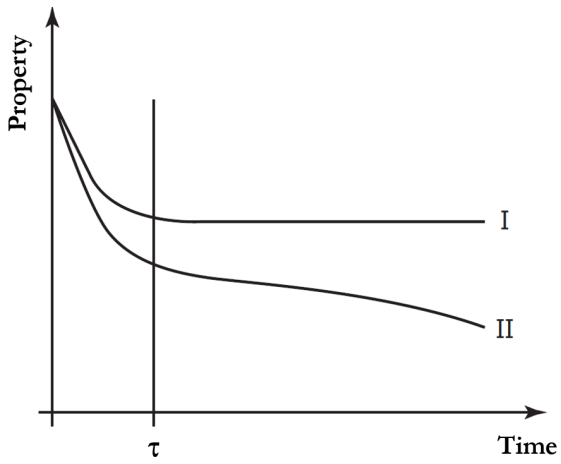

Figure 2.10 – Temporal evolution of a property (for instance, elastic modulus) of an hydrophilic polymer exposed to moisture. Case I : solely plasticization - Case II: plasticization + degradation (such as hydrolysis). Adapted from [90].

2.5 Conclusion

The aim of this work is to characterize the mechanical behaviour of model hydrophilic bio-based resins exposed to environmental conditions, especially to moisture, with a view to optimizing their formulation for future industrial applications at Saint-Gobain. The current state of the art showed that multiple molecular processes occur when a polymer is exposed to humidity and that water sorption is generally accompanied by a change in its mechanical response. However, there is a large variability reported in the literature depending on the polymer nature and ageing conditions coupled to the complexity of the molecular processes so that it is not possible to predict the influence of hydric ageing on the mechanical properties of our model material. As a consequence, we will consider an experimental approach to investigate the evolution of the mechanical behaviour of a model bio-based resin as a function of humidity.

Chapter 3

Micro mechanical characterization of polymeric resins

3.1 Introduction

The aim of this chapter is to introduce the bio-based polymeric resin of interest and to provide an overview of the mechanical characterization techniques. Because of processing limitations, macroscopic polymer samples cannot be fabricated and characterized under technologically relevant curing conditions. To overcome this limitation, polymeric samples with micrometric sizes (in the 10 µm range) have been be prepared and relevant micromechanical strategies have been developed. The mechanical properties of the polymeric micro samples will be then investigated using two complementary micro mechanical tests: tensile testing of micro fibers and micro compression of micro pillars. A few results about the mechanical properties of the bio-based resin at ambient conditions will be given as illustration.

3.2 Resin chemistry

Bio-based polyester resin As a model material, a bio-based polyester is prepared by reacting two monomers: a polyol and a polyacid. A catalyst is also incorporated to speed up the reaction. Both monomers and catalyzer are provided by Saint-Gobain.

The polyol, polyacid and catalyzer are first diluted in deionized water. The molar ratio of the two monomers is fixed so that approximatively two hydroxyl groups are introduced for one carboxilic acid group. The dry content, namely the mass of dry reactants divided by the total mass of the solution, is fixed at 70 %wt.

Due to the vitreous character of the material, common wisdom was that a highly crosslinked polymeric network is formed upon curing. A schematic description of the network is shown in Figure 3.1. From a simplified point of view, the two monomers react through an esterification reaction between the hydroxyl group of the polyol and

the carboxilic acid group of the polyacid to form a polyester network. Water is also released as a by-product of the esterification reaction. In addition to these chemical crosslinks, the presence of unreacted polar groups leads to the formation of physical crosslinks through hydrogen bondings.

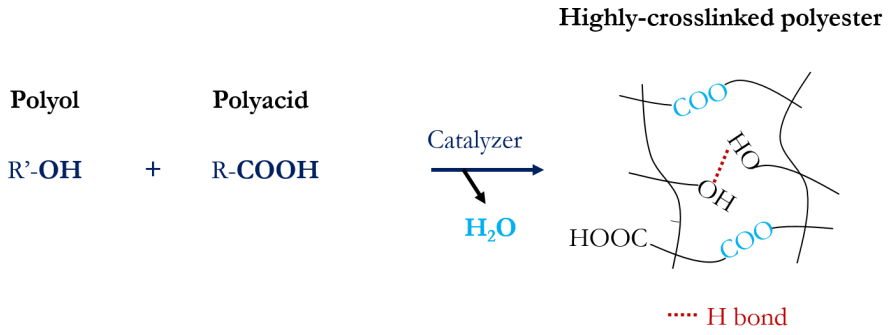

Figure 3.1 – Model esterification in polyester resin.

In this study, the model bio-based resin will be referred to as the polyester resin. However, we would like to draw the reader's attention that the chemical reactions taking place during the curing process are much more complex than solely esterification. Little is known about the macromolecular structure of the polyester resin because of the complexity of the reaction pathways. The polyester resin is believed to be a highly chemically-crosslinked thermosetting resin but a deeper investigation would be required to confirm this assumption. Further work is under way at Saint-Gobain.

3.3 Preparation of resin micro samples by soft lithography

3.3.1 Preparation limitations

As most thermosets, the resin chemistry considered in this study suffers from the release of volatiles upon curing [99, 100, 101]. Two main causes have been identified: a) the evaporation of the solvent (water) used to dissolve the initial reactants and b) the volatilization of by-products generated by the polymerization/crosslinking reactions. In the case of the polyester resin, the origins of these volatiles include the water produced by the esterification reaction and the volatile by-products coming from side reactions.

While the initial dilution solvent can be evaporated before curing, the inherent emission of volatile by-products remains a major issue for the preparation of void-free samples. Previous studies at Saint-Gobain Recherche (Aubervilliers) showed that these emissions represent up to 25 %wt of the initial monomers content for the polyester resin [102]. Volatile emissions coupled to the fast polymerization kinetics prevent the fabrication of standard macroscopic specimens because of intense foaming as illustrated

in Figure 3.2. In this study, an original micro molding process is developed to prepare void-free micro samples of controlled geometries.

Figure 3.2 – Illustration of the volatile -induced porosity in the polyester resin. Left : initial monomer solution (dry content of 70 %wt). Right: resin obtained after curing. A huge foaming is observed due to the release of volatiles upon curing.

3.3.2 Micro molding

In order to eliminate the volatile-induced porosity in resins, the preparation route developed in this study combines:

- A pre-evaporation of the monomers solution before curing in order to eliminate solvent volatization upon curing.
- Curing at high pressure to prevent bubble nucleation. If the pressure in the resin exceeds a critical value, nucleation is suppressed and volatile species remain as solutes in the resin [99, 100, 101].
- The use of a mold permeable to volatiles which allows the diffusion and extraction of these volatiles upon curing [103] and prevent the formation of bubbles when the pressure is released at the end of curing.
- The preparation of micrometric samples. At such scales, diffusion times are small enough to allow solubilized volatiles to diffuse out of the polymeric matrix by the end of the curing.

The polymeric micro samples are prepared by a soft lithography process [104, 105] using a mold made of poly(dimethyl siloxane) (PDMS), a material known for its permeability to many gazeous species [106]. The preparation process is sketched in Figure 3.3.

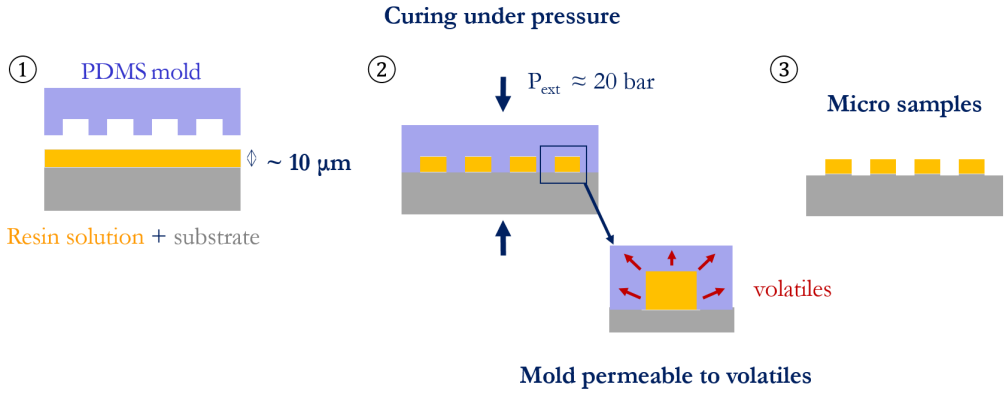

Figure 3.3 – Preparation route of polymeric micro samples in order to eliminate volatile-induced porosity. (1) After a pre-evaporation of the monomer solution, (2) curing is performed under high pressure in a mold permeable to volatiles. (3) After demolding, void-free polymeric micro samples are obtained.

To prepare a PDMS mold, a master pattern is first fabricated on a silicon wafer by a photolithography process. Briefly, photolithography allows preparing micro-patterned surfaces by selectively illuminating a photo-sensitive resin through a mask. Further details about the preparation can be found elsewhere [107]. Two master pattern geometries are fabricated: micro pillars and micro fibers. A Sylgard 184 PDMS (from Neyco) solution is then cast on the micro-patterned master. After a 3 h-curing at 70 °C, a PDMS mold containing cavities is obtained by carefully peeling off the master. This mold is then silanized in order to prevent resin/PDMS adhesion upon curing. Silanization is done by wiping a solution of 2 %wt perfluorooctyltriethoxysilane (from Sigma-Aldrich) on a plasma-activated PDMS part. More details about the silanization procedure can be found in Elzière's doctoral dissertation [108].

To prepare the micro pillars and thin films, the aqueous monomer solution is first spin coated on cleaned glass slides. For micro fibers, the solution is directly deposited on a silanized PDMS part. In both cases, the solution is then dried at 80 °C overnight to remove the excess of solvent from the monomer film. The silanized PDMS mold is then applied on the dried monomer layer. The mold-film assembly is first preheated for 1 min at 190 °C to soften the monomer film. A pressure of 20 bar is then applied for 6 min at 190 °C to cure the resin. Finally, the pressure is released and polymeric micro samples are separated from the PDMS mold.

As depicted in Figure 3.4, various sample geometries can be prepared by adapting the mold configuration: a polymeric film on a silicon substrate, a micro-patterned polymeric film on a glass substrate and a free-standing micro fiber. Note that the application of pressure is also needed in the case of flat films to prevent foaming.

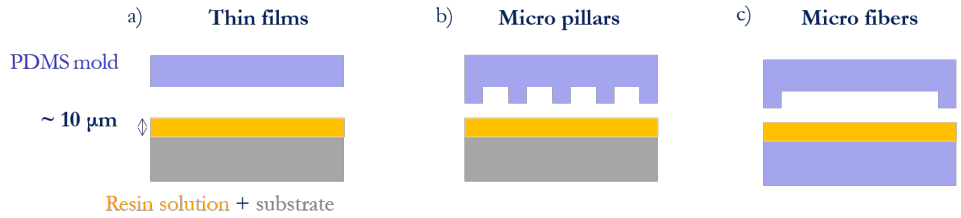

Figure 3.4 – Micro samples geometries obtained by micro molding. Different geometries are obtained: a) a polymeric film on a silicon substrate, b) polymeric micro pillars on a glass substrate, c) a free-standing micro fiber.

The micro samples obtained are observed by optical microscopy (Leica DM2500) and scanning electron microscopy (MEB FEG FEI Magellan from Thermo Fischer Scientific) which confirms the successful preparation of void-free micro samples. As an illustration, micro pillars and micro fibers are shown in Figure 3.5.

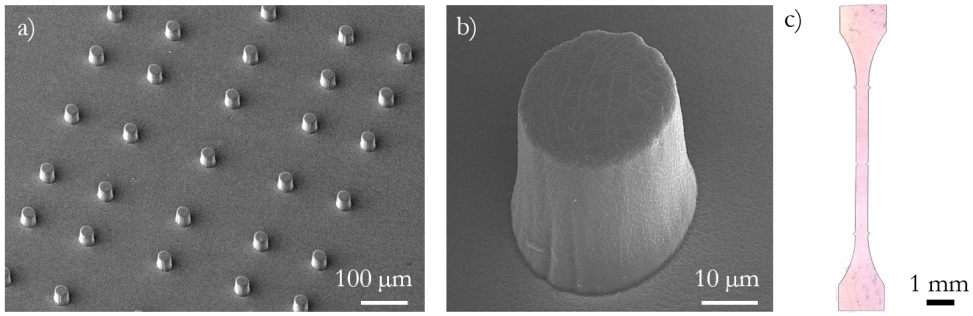

Figure 3.5 – Polyester micro samples: a) and b) SEM micrographs of micro pillars on a glass substrate and c) a free-standing micro fiber under microscope.

3.3.3 Micro sample characterization

Before mechanical testing, the dimensions of each micro sample are measured using either an optical microscope (Leica DM2500) or an optical profilometer (Fogale Nanotech). The variability in dimensions between different specimen batches comes from the deformation of the PDMS mold at high pressure.

For the resin thin films, the thickness of the resin layer is measured by profilometry while the silicon substrate thickness is measured by optical microscopy. The film and substrate thickness are about 7 µm ± 0.5 µm and 270 µm ± 10 µm, respectively.

The thickness and width of polymeric micro fibers are measured by optical microscopy. The average thickness and width of micro fibers are about 25 µm ± 5 µm and 450 µm ± 20 µm, respectively.

For polymeric micro pillars, the final pillar height and upper section are measured by profilometry and by optical microscopy, respectively. The upper section is almost circular with a diameter of 27 ± 2 µm. The height is 27 µm ± 2 µm. The pillars have

an aspect ratio of about 1:1. The distance between individual pillar is 150 µm. Note that they are not isolated micro pillars on a bare glass substrate. A 4 µm-thick residual layer exists in between pillars because of the polymer affinity for glass combined to the difficulty to bring in close contact the PDMS mold and the substrate [109].

3.4 Compression of polymeric micro pillars

The mechanical response of individual polymeric micro pillars is characterized using micro compression. This method has been extensively applied to metals [110, 111] and glasses [112, 113] but solely a handful of papers exits about polymers [114, 115, 116].

3.4.1 Experimental setup description

A home-made micro compression setup is developed in this study, in collaboration with *Ludovic Olanier*,*Alexandre Lantheaume* and *David Martina*. A schematic of the setup is displayed in Figure 3.6.

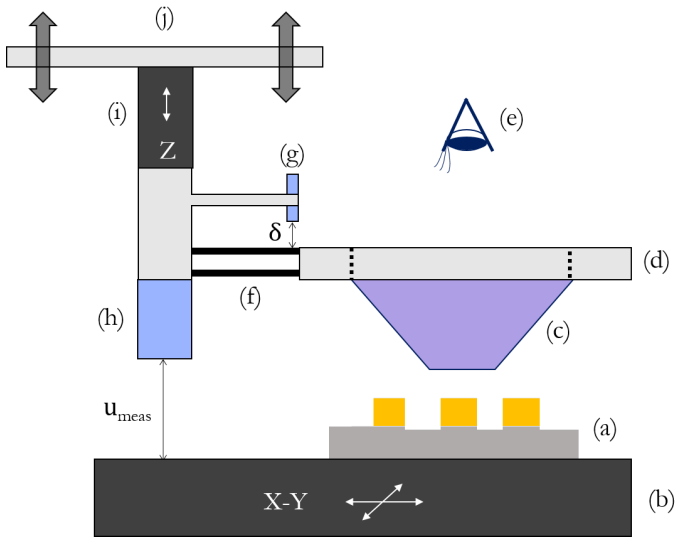

Figure 3.6 – Schematic of the micro compression setup. The setup consists of (a) a micro-patterned sample, (b) a X-Y translational stage, (c) a transparent flat punch, (d) a punch holder, (e) a microscope, (f) a double cantilever whose deflection is measured with (g) a displacement sensor, (h) a second displacement sensor to measure the relative displacement between the punch holder and the sample holder, (i) a piezo actuator and (j) 3-axis alignment motors.

Micro compression testing is carried out by compressing individual pillars with a diamond tip terminated by a 100 µm-diameter flat extremity (from Synthon MDP). This tip is subsequently referred to as "the punch" in this thesis. The punch displacement is controlled with a piezo actuator. The selection of individual pillars is made

using precise translational stages. Punch/pillar alignment is adjusted with a 3-axis aligner. The setup control and data readings are performed with a LabView code.

The force F applied on a given pillar is measured from the deflection δ of a double cantilever characterized by a stiffness k (force resolution of 10 mN) which is calibrated with certified test weights. The change in deflection, $\Delta\delta$ is measured with a capacitive displacement sensor from which the force F is deduced using Equation 3.1:

$$F = k.\Delta\delta \tag{3.1}$$

The relative displacement between punch holder and sample is measured with a second capacitive displacement sensor (displacement resolution of 0.2 µm). In this study, the compression tests are conducted under displacement-controlled conditions using the piezo actuator. Individual pillars are compressed up to a maximal setpoint displacement before being unloaded. The initiation of contact between the pillar upper section and the punch is detected using phase sensitive detection with a lock-in amplifier. If not mentionned otherwise, tests are conducted at a strain rate of 3.10^{-2} s^{-1} but it can be varied from 10^{-1} s^{-1} to 10^{-3} s^{-1} to investigate strain rate effects. The lateral distance of 150 µm between individual pillars ensures that only one pillar is compressed at each test. Five or more experiments are conducted under the same conditions to obtain reproducible data. Between each test, the punch extremity is carefully cleaned with ethanol to reduce the friction between the punch and the top surface of the pillar. Tests are carried out in a small chamber in which the local relative humidity can be controlled to study the influence of moisture on resin compressive behaviour. A detailed description of the humidity control can be found in Chapter 4. Tests are performed at room temperature (23 °C ± 2 °C) which is not controlled.

For each test, a load-displacement curve is obtained such as the representative curve shown in Figure 3.7.

3.4.2 Access to the true stress-strain behaviour

Several aspects have to be taken into consideration in order to transform the load-displacement data into a true stress-strain relationship: raw data corrections for thermal drift and setup compliance, punch-to-pillar alignment upon testing and extraction of the true pillar section to estimate the true stress in the pillar. Each aspect is detailed in the subsequent paragraphs.

Data correction Two corrections must be applied on the load-displacement curve to obtain quantitative data.

The first correction aims at reducing the effect of thermal drift on the force signal. This drift is related to several effects including the thermal expansion of the setup and sensor components as well as the effect of thermal drift on the response of the

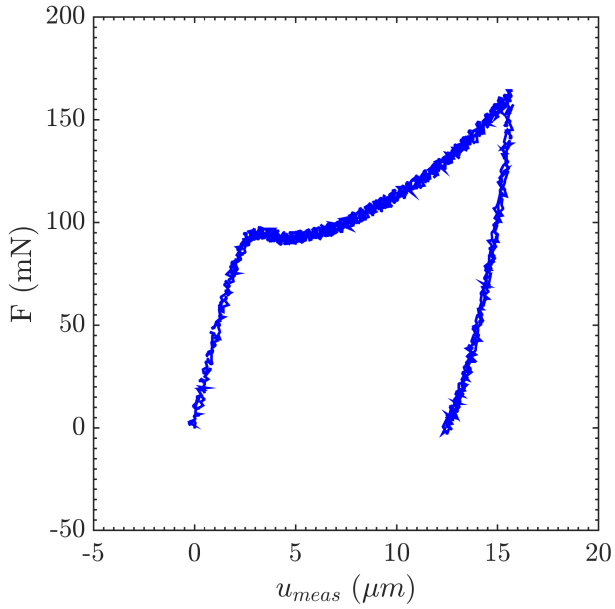

Figure 3.7 – Typical load-displacement curve obtained by compressing a polyester micro pillar until a setpoint displacement of 15 µm.

electronic sensors. These effects lead to a slight deviation of the measurement over time. The force is corrected for thermal drift by subtracting a linear extrapolation of the baseline to the time-force signal. In this study, thermal drift was found to be negligible for experiments shorter than 5 min.

A second correction is applied with a view to estimating the true pillar displacement upon compression. When a load is applied on a pillar, a fraction of the punch displacement is actually related to the displacement of the different setup components. These components also deform upon loading and contribute to the overall displacement. To remove the setup contribution from the measured displacement, we have combined: a) the use of an external displacement sensor which directly measures the displacement of the punch with respect to the sample holder b) the consideration of the setup compliance, k_{setup}, to correct the apparent pillar displacement measured by the displacement sensor, u_{meas}. A setup compliance of about 1.10^5 N.m^{-1} is estimated from a compression test carried out on the residual layer in between micro pillars at a strain rate of 10^{-2} s^{-1}. The true pillar displacement, u_{true} is then deduced by subtracting the setup contribution according to Equation 3.2:

$$u_{true} = u_{meas} - \frac{F}{k_{setup}} \tag{3.2}$$

The effect of these corrections is shown in Figure 3.8 where a raw and corrected load-displacement curves are compared. While thermal drift correction has a negligible effect at this time scale, the correction for setup compliance significantly affects the effective displacement of the pillar.

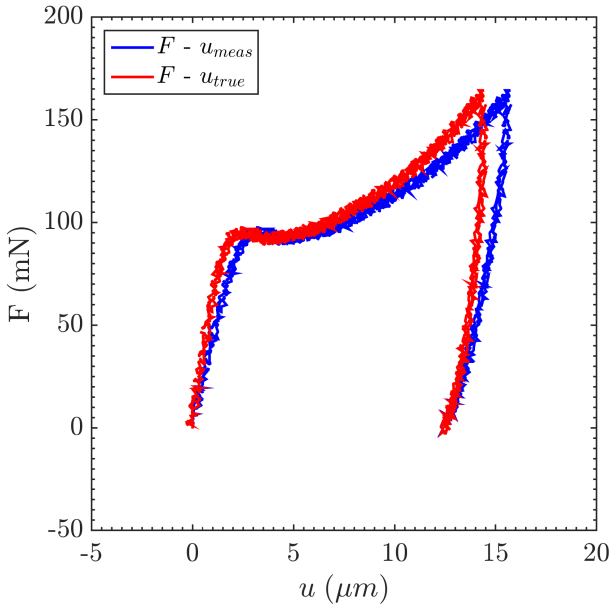

Figure 3.8 – Effect of thermal drift and compliance corrections on a typical load-displacement curve. The F-u_{meas} curve represents raw data whereas the F-u_{true} curve corresponds to corrected data.

From the corrected load, F and corrected pillar displacement, u_{true}, a nominal stress-strain curve is obtained by normalizing the data using the initial pillar upper section, S_0 and the initial pillar length, l_0. The nominal strain ε_N and the nominal stress σ_N are estimated using Equation 3.4 and Equation 3.3, respectively:

$$\varepsilon_N = \frac{u_{true}}{l_0} \tag{3.3}$$

$$\sigma_N = \frac{F}{S_0} \tag{3.4}$$

The typical nominal stress-strain curve displayed in Figure 3.9 exhibits two main stages: an initial linear elastic regime followed by an inflection point and an apparent strain hardening at larger deformations. Upon unloading, a residual deformation is observed suggesting a plastic deformation of the pillar.

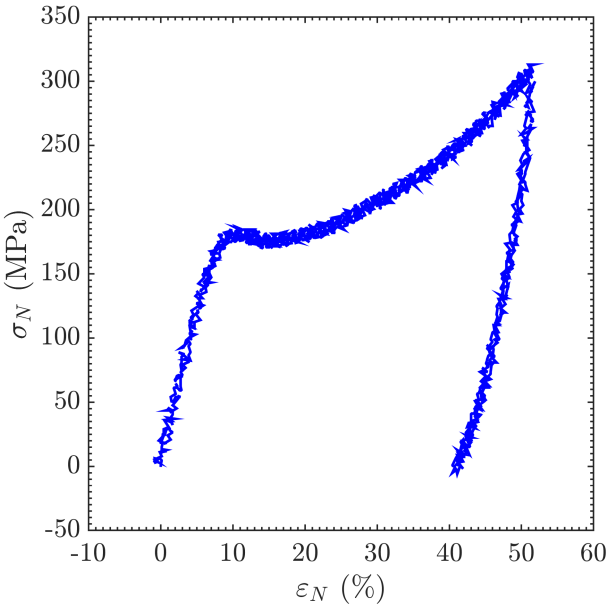

Figure 3.9 – Typical nominal stress-strain curve for a polyester micro pillar tested at ambient atmosphere (T = 23 °C - RH = 40 %RH).

Punch-to-pillar alignment A difficulty in micro compression experiments is the possible misalignment between the punch and the top surface of the micropillar. A perfect alignment is obtained when the flat punch is parallel to the pillar section as sketched in Figure 3.10. Alignment has been found to affect the apparent mechanical behaviour of micro pillars [117].

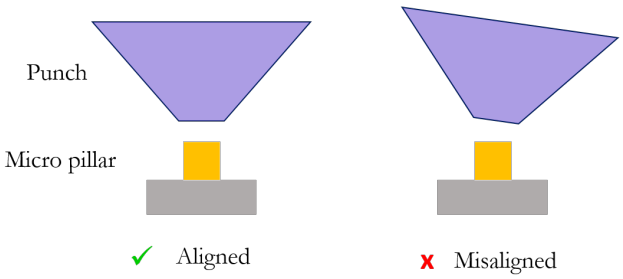

Figure 3.10 – Punch/pillar alignement in micro compression testing.

In this study, we propose an original approach for punch/pillar alignment. An optical microscope is positioned above the transparent punch to visualize the contact between the punch extremity and the pillar. Upon testing, the contact is simultaneously recorded with a camera. By visual inspection of the contact between the punch and the top surface of the pillar, we can evaluate the pillar/punch misalignment and correct it accordingly with the 3-axis aligner.

A typical image sequence of the contact establishement between the pillar section and the punch extremity is shown in Figure 3.11. Upon approach, interferences start

appearing between the pillar upper section and the punch flat (see Figure 3.11.a). The circular symmetry of these interferences is characteristic of a perfect pillar/punch alignment. The punch then contacts uniformely the pillar upper section. On the contrary, equal thickness fringes are visible in the case of a punch/pillar misalignment and accommodation occurs upon contact establishement.

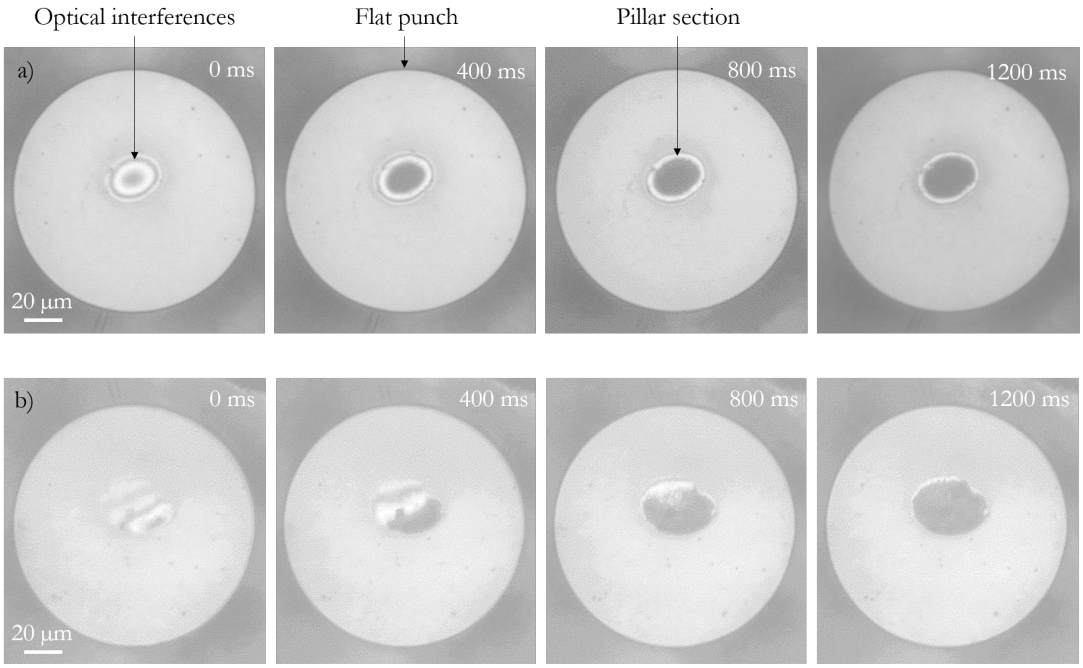

Figure 3.11 – Visual observation of punch/pillar contact establishement a) in the case of a perfect alignment and b) in the case a misalignment.

Access to large strain behaviour Another advantage of using a transparent flat punch is the possibility to estimate the true pillar upper section upon testing. A typical image sequence of the temporal evolution of the pillar section is shown in Figure 3.12. After the initial full contact between the punch and the top surface of the pillar, the pillar section progressively increases upon compression.

The temporal evolution of the pillar upper section is measured and used for true stress estimation. A comparison between the true and nominal stress-strain responses of a polyester micro pillar is shown in Figure 3.13. While the two curves exhibit similar trends in the elastic regime, the expansion of the pillar cross section significantly affects the apparent mechanical behaviour at larger deformations. The apparent strain hardening in nominal stress-strain relationship is an artefact of stress calculation. The substantial increase in pillar area results in a true stress smaller than the nominal stress with minimal strain hardening at deformations larger than 40 %.

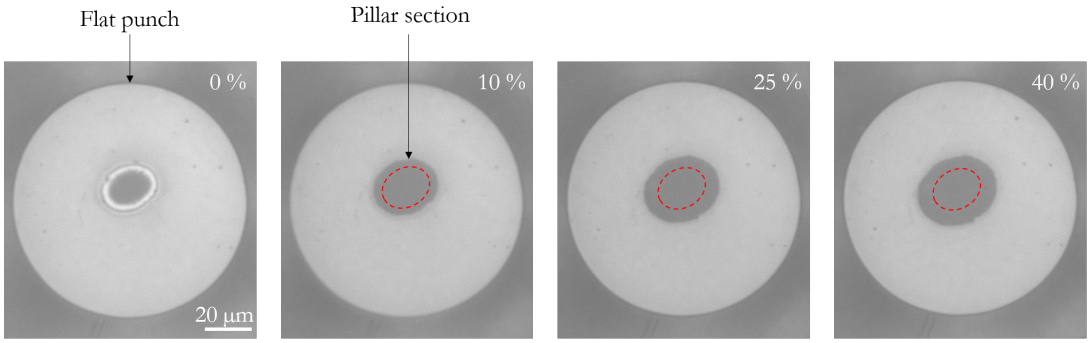

Figure 3.12 – Observation of pillar upper section upon compression testing after pillar/punch contact establishment for pillar deformations ranging from 0 % to 40 %. The initial pillar section is materialized by the dotted line.

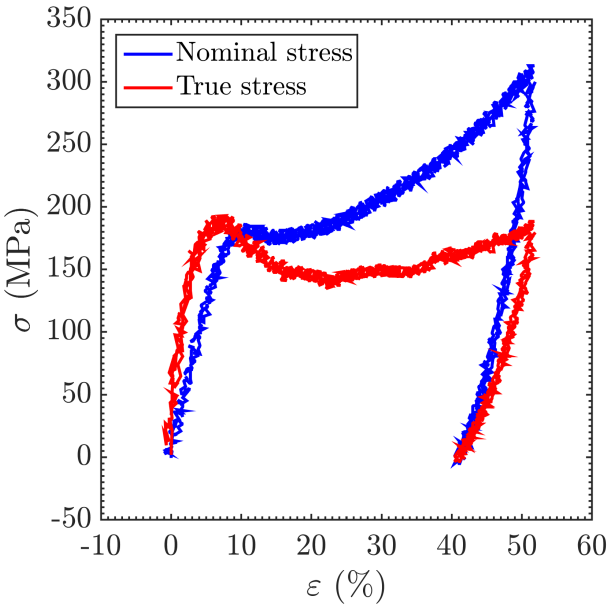

Figure 3.13 – Comparison of the nominal and true stress-strain responses of a polyester micro pillar tested at ambient atmosphere (T = 23 °C - RH = 40 %RH).

3.4.3 Compressive behaviour of the polyester resin at ambient humidity

As an illustration of the possible uses of the micro compression setup, the properties of polyester resin micro pillars are characterized at ambient atmosphere (T = 23 °C and RH = 40 %RH).

Identification of the mechanical regimes In Figure 3.14, individual pillars are compressed at various maximal deformations, ε_{max} in order to identify the different mechanical regimes of the polymer.

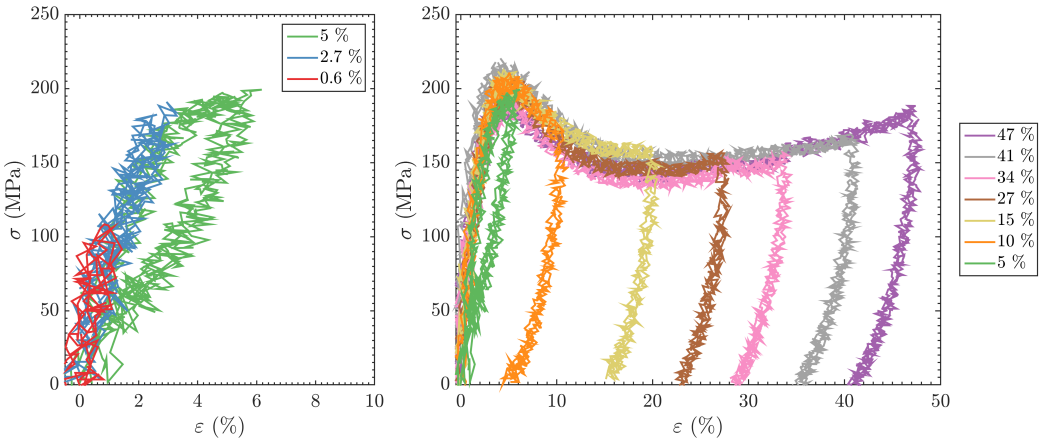

Figure 3.14 – Influence of the maximal deformation, ε_{max} on the compressive response of polyester micro pillars for ε_{max} lower than 5 % (left) and for ε_{max} larger than 5 % (right).

The true-stress response of polyester resin exhibits five main stages at ambient humidity. (1) For deformation smaller than 3 %, the stress increases linearly with the strain. No hysteresis exists between the loading and unloading paths and the pillar deformation is fully recovered upon unloading. This response marks the linear elastic regime expected at low deformation. (2) This regime is followed by a non-linear elastic response where the slope of the stress-strain curve progressively decreases for increasing deformation. Although no residual deformation is observed upon unloading, a moderate dissipative contribution appears as shown by the small hysteresis loop between the loading and unloading paths of the curve recorded at ε_{max} = 5 %. This region is defined as a viscoelastic or anelastic regime. (3) The elastic regime is followed by a local maximum in stress which is often defined as the yield stress, σ_{yield} in literature [22, 23]. The polyester resin exhibits a yield stress of about 200 MPa at ambient humidity. This value agrees with the order of magnitude of published values for glassy polymers and thermosets [17, 22, 23, 24]. For stresses exceeding the yield peak, plastic flow occurs in the pillar. The plastic region is characterized by a large hysteresis and the existence of irreversible flow and a residual plastic deformation upon unloading. Both properties increase for increasing compression level. (4) After the yield peak, strain softening occurs: the stress decreases to reach a minimum value and (nearly)

constant plastic plateau. (5) In the last stage, the stress increases again at larger deformations, which corresponds to the strain hardening regime. This behaviour can be associated with the response of the crosslinked network which starts prevailing through chain orientation [29, 30, 31]. The presence of a rigid substrate may also contribute to this apparent strain hardening behaviour at large deformations.

As a comparison, successive compression tests are also carried out on the same pillar at increasing compression levels, ε_{max}. The test is displacement-controlled and the punch goes back to the initial pillar height position between two subsequent deformation cycles. The results are depicted in Figure 3.15 and compared to a single compression response at $\varepsilon_{max} = 46$ %. While the pillar response is not affected for ε_{max} remaining in the elastic regime, the compression tests exceeding the yield peak lead to an irreversible pillar deformation as seen before. The present experiment also demonstrates that upon reloading, the material behaves elastically until reaching the previous maximal deformation state. The modulus of the elastic region remains constant during the successive reloadings. When the previous maximal deformation is reached, the material response becomes identical to that of single loaded specimen. Interestingly, partial relaxation of the polymeric micro pillar deformation is visible between two successive compression cycles highlighting a viscous contribution in the resin mechanical response. Creep is also visible upon unloading as suggested by the steep slope at the beginning of the unloading steps. This time-dependent behaviour is investigated in a different set of experiments in the next paragraph.

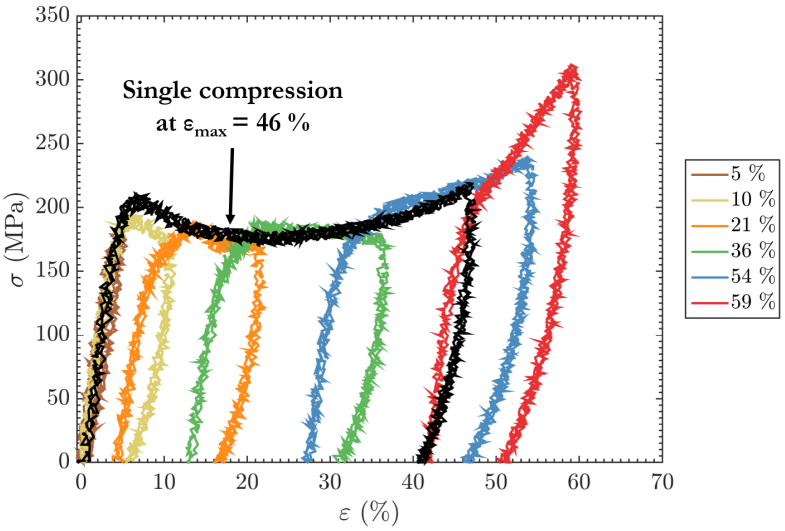

Figure 3.15 – Compressive stress-strain response of a polyester micro pillar subjected to successive compression cycles and comparison to a single compression response (black).

Time-dependent mechanical behaviour The time-dependence of the polyester compressive properties is investigated by varying the strain rate upon compression. Four representative stress-strain curves are compared in Figure 3.16 for strain rates ranging from 10^{-3} s^{-1} to 10^{-1} s^{-1}.

Clearly, the stress-strain relationship is extensively sensitive to the applied strain rate. More precisely, a significant increase in yield stress is observed for increasing strain rate. On the contrary, the elastic modulus as well as the strain softening and strain hardening behaviours exhibit little dependence in this range of strain rates.

As depicted in Figure 3.17, the strain rate-dependence of yield stress is consistent with Eyring's theory [26] which predicts that the yield stress σ_{yield} is thermally activated and therefore logarithmically related to the strain rate $\dot{\varepsilon}$ using Equation 3.5:

$$\sigma_{yield} = \sigma_0 + \frac{k_B T}{V^*} ln\left(\frac{\dot{\varepsilon}}{\dot{\varepsilon_0}}\right) \tag{3.5}$$

where $\dot{\varepsilon_0} = 1$ s^{-1}, k_B is the Boltzmann constant, σ_0 is the yield stress at a strain rate of $\dot{\varepsilon} = \dot{\varepsilon_0}$ and V^* is the so-called activation volume, an adjustable parameter with no clear physical meaning. From the slope, an activation volume of 2 nm^3 is estimated which agrees with the order of magnitude of published values for glassy polymers and thermosets [17, 115, 118].

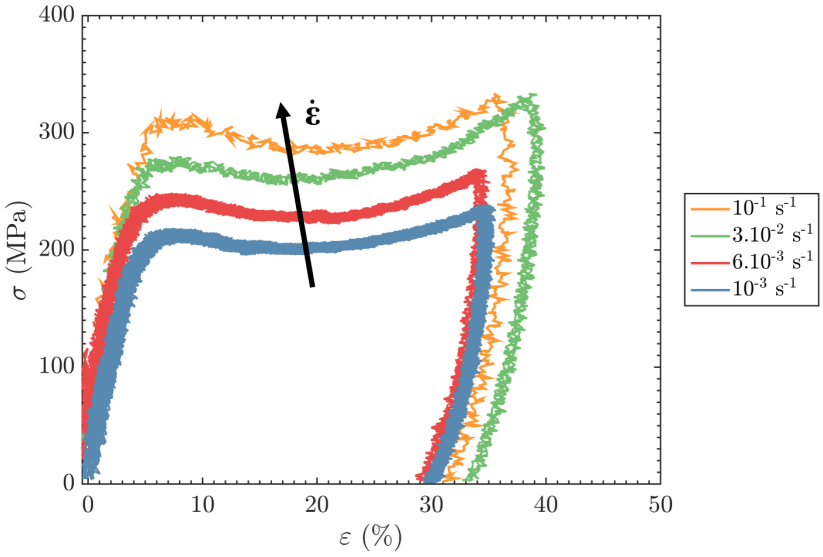

Figure 3.16 – Influence of the strain rate on the true stress-strain response of a polyester pillar at 40 %RH.

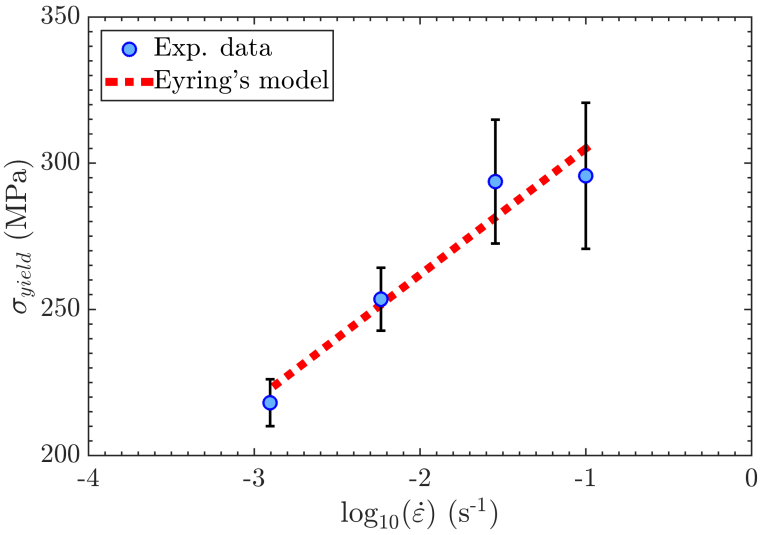

Figure 3.17 – Evolution of the yield stress, σ_{yield} as a function of the logarithm of the strain rate, $\dot{\varepsilon}$ for a polyester micro pillar (RH = 40 %). Experimental data are fitted with Eyring's model using the following fitting parameters: $\sigma_0 = 3.4\ 10^8$ Pa and $\frac{k_B T}{V^*} = 3.5\ 10^7$ J.m^{-3}.

3.5 Tensile testing of polymeric micro fibers

3.5.1 Tensile testing method

In this study, polymeric micro fibers are characterized using a micro tensile testing method. Although tensile testing appears as a straightforward method to get access to the resin elastic and fracture properties, the handling and mounting of micro fibers remain a challenge. The tensile testing method used in this study has been developed in collaboration with *Alba Marcellan* and is inspired from Colomban's [119] and Tan's [120] works about the tensile behaviour of micrometric and nanometric polymeric fibers. The strategy consists in bonding the polymeric fibers on a protective frame to facilitate specimen handling and fixation. The frame is then cut before tensile testing.

Experimental protocole A schematic view of the tensile test working principle is shown in Figure 3.18. Tensile testing specimens consist of dogbone-shaped micro fibers which are fabricated using the micro molding process. The dogbone has a gauge width of 460 µm ± 20 µm, a thickness of 25 µm ± 5 µm and a gauge length of 9 mm ± 1 mm which is deduced from the distance between the clamps after sample mounting on the tensile machine.

Sample gripping contributes to the premature specimen rupture because of stress concentration at the vicinity of the clamped extremities [121]. Improved reproducibility in fracture properties is achieved by introducing a defect of controlled geometry in the micro fibers. Especially, double-notched fibers are obtained by micro molding as shown in Figure 3.18.b. Each notch is 80 µm ± 5 µm-long and has a diameter of

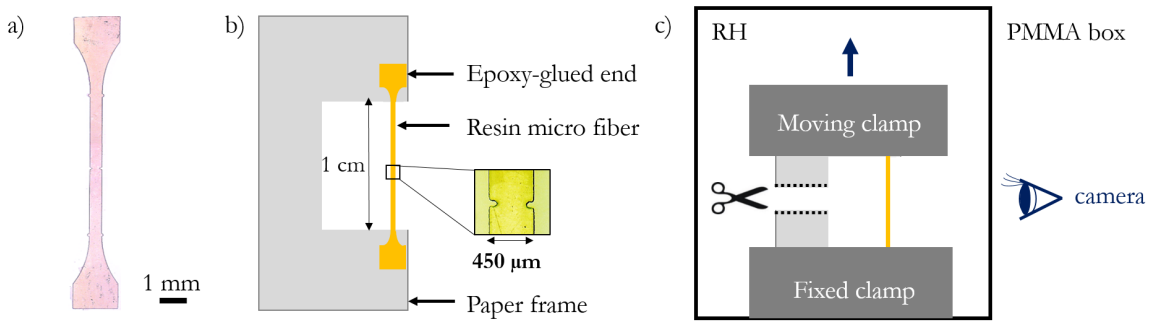

Figure 3.18 – Tensile testing of polymeric micro fibers: a) fiber sample, b) fiber-support assembly and (c) tensile testing method.

65 µm ± 5 µm. The notch was found not to affect the apparent elastic modulus.

The heads of the dogbone are fixed on a paper frame using a 2 h-setting epoxy glue which is allowed to solidify overnight. The tensile testing is then carried out on an Instron tensile machine (Instron 3343) equipped with a 10 N-load cell. After specimen alignment and fixation, the paper frame is cut. The dogbone fiber is then loaded to failure at a constant nominal deformation rate of 0.01 s^{-1} while recording the displacement of the moving clamp and the force. The sample behaviour is simultaneously recorded with a digital camera.

Tensile tests are carried out in a transparent PMMA chamber where the relative humidity can be controlled and varied in order to investigate its effects on resin tensile behaviour. A detailed description of the humidity control setup can be found in Chapter 4. Tests are performed at ambient temperature (T = 23°C ± 2 °C) which is not controlled.

An accurate measurement of the sample extension is critical at such reduced scales. The absence of sample slippage has been confirmed by accurately measuring the fiber extension by extensometry. The strain estimated from the clamp displacement measured by the tensile machine has been found to be in good agreement with the extensometer strain. These results are not displayed here. Consequently, the engineering strain is estimated using Equation 3.7:

$$\varepsilon_N = \frac{l - l_0}{l_0} \tag{3.6}$$

where l_0 is the initial sample length and l is the sample length deduced from the clamp displacement. The engineering stress σ_N is estimated using Equation 3.7:

$$\sigma_N = \frac{F}{w.t} \tag{3.7}$$

where F is the force measured by the load cell, w is the original sample width and t is the original sample thickness.

3.5.2 Tensile properties of the polyester resin at ambient humidity

As an illustration of the tensile testing method, the tensile properties of polyester micro fibers are characterized at ambient atmosphere (RH = 40 %RH). A representative stress-strain curve is shown in Figure 3.19.

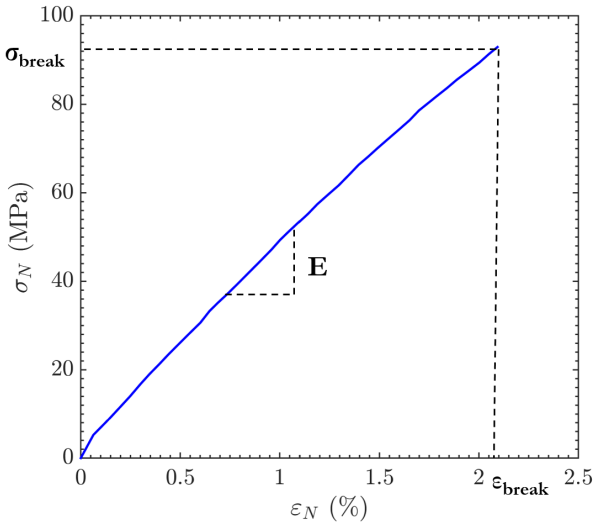

Figure 3.19 – Typical tensile stress-strain curve of a polyester micro fiber (RH = 40 %).

Young's modulus, E is estimated from the slope of the linear part. At ambient atmosphere, a modulus of 4.9 GPa ± 0.5 GPa is obtained, value which agrees with the order of magnitude of published values for glassy polymers and thermosets [13, 21, 34]. Note that this value also correlates with the slope measured using micro pillar compression. The tensile configuration however provides a better estimation of the Young's modulus since base compliance, imperfect sample geometries and smaller sample gauge affect the precision in the case of micro compression [122].

The resin fracture properties are characterized by the stress at break, σ_{break} and the strain at break, ε_{break}. Rupture always occurs at the rounded notch. At ambient humidity, the polyester resin exhibits a stress at break of 95 MPa ± 4 MPa and a strain at break of 2 % ± 0.2 %. Note that these values cannot be considered as intrinsic fracture properties of the material. The reduced fiber stretchability coupled to the absence of a plastic regime are consistent with the brittle fracture behaviour of glassy polymers [13, 18]. This is confirmed by the fracture process of the specimen. A typical image sequence of a brittle fracture of the notched area is shown in Figure 3.20. The sudden crack propagation is too fast to be observed with the frame rate considered (20 images per second).

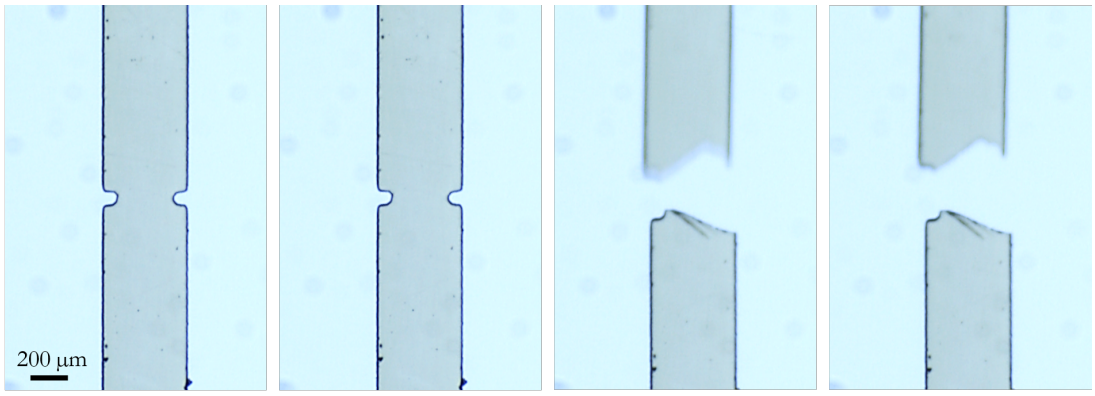

Figure 3.20 – Brittle fracture behaviour of a notched polyester micro fibers at 40 %RH.

3.6 Conclusion

This chapter was dedicated to the preparation of polymeric micro samples and to their subsequent micro mechanical characterization. The bio-based polyester resin considered in this study suffered from the inherent release of volatiles upon curing which prevented the fabrication of standard macroscopic samples. An original micro molding process was developed to prepare void-free micro samples. Resin micro samples of various geometries were fabricated which opened the way to various micro mechanical testing methods.

The mechanical properties of the polymeric micro samples were then investigated using two complementary micro mechanical tests: tensile testing of polymeric micro fibers and micro compression of polymeric micro pillars. These micro tests were natural extensions of their macroscale counterparts. Tensile testing was carried out to characterize the resin elastic and fracture properties while micro pillar compression allowed to investigate the polymer behaviour at larger deformations. A special attention was given to the resin plastic properties and strain rate-dependence of these properties.

As an illustration, the mechanical properties of the polyester resin were determined at ambient atmosphere (23 °C ± 2 °C - 40 %RH). Under these conditions, the polyester resin is characterized by:

- A Young modulus of 4.9 GPa ± 0.5 GPa
- A brittle fracture upon tensile testing with a strain at break of 2 % ± 0.2 % and a stress at break of 95 MPa ± 4 MPa
- A plastic behaviour upon compression, characterized by the presence of a yield peak at 290 MPa ± 20 MPa followed by a plastic plateau. For deformations larger than 40 %, the apparent strain hardening could be a signature of the polymeric network orientation upon compression.
- A viscous response as highlighted by the strain-rate dependence of the yield stress, the partial relaxation of the deformation during cyclic loading and the creep behaviour observed upon unloading

All these properties are consistent with the behaviour of glassy polymers [16]. The influence of relative humidity on this behaviour will be studied in the next chapter using the two micro mechanical tests developed.

Take-home messages

- The volatile-induced porosity can be eliminated by preparing micro samples while combining high-pressure curing to the use of mold permeable to volatiles.
- Characterization of resin mechanical properties:
  - Resin elastic and fracture properties are determined using tensile testing of polymeric micro fibers.
  - Resin large strain behaviour (including its yield stress) is determined using compression testing of polymeric micro pillars.
- The polyester resin exhibits a typical glassy behaviour at ambient atmosphere (23 °C - 40 %RH - no ageing).

Chapter 4

Influence of moisture on the mechanical response of the pristine polyester resin

4.1 Introduction

The aim of this chapter is to investigate the influence of moisture on the mechanical properties of pristine polyester resin. The notion of pristine (or unaged) samples refers to samples never exposed to moisture before testing so that no water-induced irreversible process has occurred yet. As shown in Chapter 3, the polyester resin behaves as a glassy polymer at ambient atmosphere. This non-equilibrium state directly resulting from the heat treatment gradually relaxes toward an equilibrium state via a process designated as physical ageing. Physical ageing is known to induce changes in the polymer structure and mechanical properties [34, 40]. Consequently, a pristine sample must be characterized within a few days after its preparation to limit the extent of physical ageing.

In this chapter, after a characterization of the polyester resin hygroscopy, the influence of humidity on polyester mechanics is measured using the micro compression and micro tensile testing methods. A scenario is then proposed to relate the evolution of the mechanical response upon moist exposure to the molecular processes taking place at the macromolecular scale. The humidity-dependent behaviour of the polyester resin is finally compared to that of a standard phenol formaldehyde resin. As to the impact of humidity on aged samples, it will be studied in Chapter 5.

4.2 Polyester resin hygroscopy

4.2.1 Experimental description - Dynamic vapor sorption

Polymer hygroscopy, namely its ability to sorb water, is characterized using dynamic vapour sorption (DVS). This is a well-established method to gravimetrically follow the mass variation resulting from water uptake upon exposure to water vapour. Measure-

ments are conducted at Saint-Gobain Recherche (Aubervilliers) on a DVS equipment (DVS Intrinsic from Surface Measurement System).

Water sorption/desorption measurements are performed on a small amount of resin (about 20 mg) prepared using the micro molding method previously developed (see Chapter 3). The temperature in the DVS chamber is maintained constant at 23 °C. The standard DVS procedure consists in measuring the resin sorption properties at equilibrium, namely for an homogeneous diffusion of water within the sample. After a 220 min pre-drying at 0 %RH from which the dry mass of the resin m_{dry} is estimated, the humidity level is gradually increased from 0 %RH up to 90 %RH by 10 %RH step (sorption cycle) and then gradually decreased from 90 %RH down to 0 %RH by 10 %RH step (desorption cycle). Each humidity step is maintained until mass stabilization is reached (mass variation smaller than 0.5 mg.min^{-1}) or for step duration of 360 min if the mass stabilization criterion has not been met, in which case equilibrium has not been achieved. At each step, the weight fraction of water in the polymer, w_{water} is deduced from the specimen mass at equilibrium, m, using Equation 4.1:

$$w_{water} = \frac{m - m_{dry}}{m_{dry}} \tag{4.1}$$

Water vapour sorption and desorption isotherms are constructed by plotting the weight fraction of water at equilibrium as a function of relative humidity. Figure 4.1 shows an example of DVS data. In Figure 4.1, the temporal evolution of w_{water} and relative humidity highlights the diffusion kinetics of water vapour in the specimen while the sorption/desorption isotherms provide information about the polyester hygroscopy. A detailed description of these two graphs is given in Chapter 5.

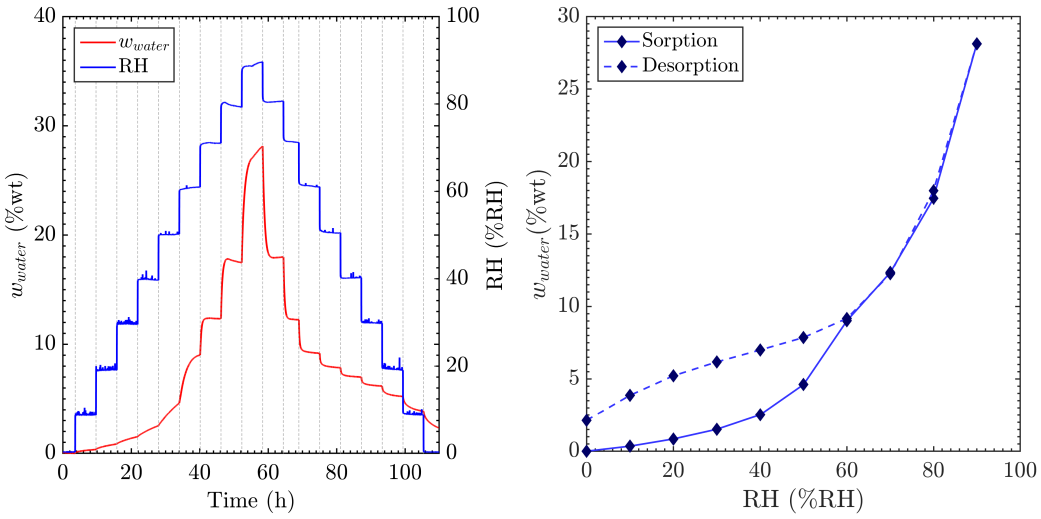

Figure 4.1 – Representative DVS curves showing the temporal evolution of weight fraction of water and relative humidity in the chamber (left) from which the sorption/desorption isotherms (right) are deduced. The sorption values up to 60 %RH are not equilibrium points due to very slow kinetics.

While this procedure is used to provide polyester sorption properties "at equilibrium", shorter procedures are carried out in order to reproduce the humidity conditions under which the micro samples are mechanically characterized. These procedures are detailed in Appendix A.1. The results are used to estimate the water content in the polymer upon mechanical testing. Multiple sorption/desorption cycles will be also conducted in order to investigate the influence of hygrothermal history on resin sorption properties.

4.2.2 Polyester resin/water affinity

The sorption and desorption isotherms of unaged polyester resin are shown in Figure 4.1 (right). The polyester resin is clearly hydrophilic as shown by the large water uptake which reaches up to 30 %wt of water at 90 %RH. Interestingly, we observe that the polymer uptake increases sharply above 60 %RH. Upon desorption, the sample cannot be fully dried and a water content of 2 %wt remains at the end of the drying step. A large hysteresis appears between the sorption and desorption isotherms below the same threshold of 60 %RH.

The high hydrophilicity of the polyester resin can be attributed to the presence of a significant number of unreacted polar groups, especially the hydroxyl groups which are introduced in large excess in the material (almost 2 hydroxyls groups for 1 carboxilic acid group - see Chapter 3 - Section 3.2 for more details). The large water uptake is likely to impact the polyester mechanical behaviour and this will be investigated in the next section.

The asymmetry between the sorption and desorption curves has already been observed in other glassy polymers [71, 123] and could stem from a) the very slow diffusion processes involved during the transition from the wet to the dry states and b) the formation of water-polymer hydrogen bonds which impede the desorption of water molecules. In the first case, water molecules are kinetically trapped in the polymer but may finally desorb if the material is allowed to dry until equilibrium is reached. Inversely, regarding the second assumption, the equilibrium water content differs between adsorption and desorption. This has been already demonstrated in the case of cellulose by Chen [124] who showed that hydrogen-bonded water desorbs at lower humidity than upon adsorption. As a consequence, residual water is 'irreversibly" trapped in the polymer glass, even at 0 %RH, because of the difference between the temperature of the initial heat treatment and the temperature of the DVS measurements.

4.3 Influence of moisture on polyester resin mechanics

After a description of the humidity conditions upon mechanical testing, we study the influence of relative humidity on the polyester compressive and tensile properties.

4.3.1 Controlling relative humidity upon mechanical testing

The two-flow method Each micro mechanical setup is designed with a testing chamber in which relative humidity can be controlled. Relative humidity in the mechanical testing chamber is controlled by mixing dry air (2 %RH) and water saturated air (95 %RH) in desired relative amounts. This method has been chosen over the use of salt solutions because of its higher flexibility regarding humidity selection and because of the potential polymer/salts interactions. A detailed setup description is provided in Appendix B.

Humidity conditions upon testing The procedures for humidity exposure during micro compression and micro tensile testings are specified in Figure 4.2.

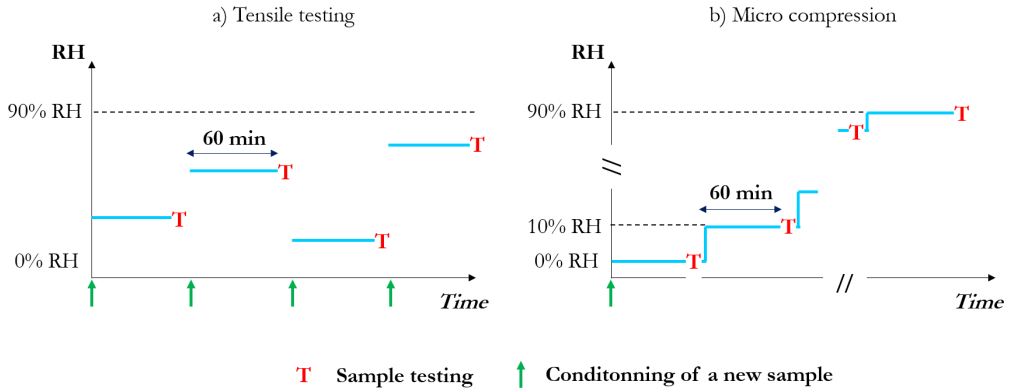

Figure 4.2 – Humidity control procedure for the investigation of moisture effect in a) tensile testing and b) micro compression testing.

For each tensile test, a new specimen is maintained at a given relative humidity for 60 min before being stretched until failure. Although mass stabilization is not systematically reached after 60 min (especially for relative humidities lower than 40 %RH), this duration is considered as a good compromise between the experiment duration and the equilibrium conditions. At least five specimens are tested per humidity condition. For micro compression testing, polyester micro pillars are exposed to a humidity level which is gradually increased over time. A standard humidity cycle consists in gradually increasing humidity from 0 %RH up to 90 %RH by 10 %RH step. After a 60 min-conditioning at the desired relative humidity, at least five pillars are tested before proceeding to the next humidity step. This difference in water exposure protocole, due to the different sample geometries, may have some effect in the slow kinetics regions and must be kept in mind when comparing the results of the different methods.

Note that water sorption can result in polymer swelling and thus, specimen dimensional variations. While being negligible for relative humidities lower than 80 %RH, swelling results in a relative increase in micro fiber length of up to 10 % above 80 %RH.

The moisture-induced change in fiber width, fiber thickness and pillar height are however not taken into consideration in the calculations of stress and strain.

4.3.2 Moisture-dependent compressive properties

Micro compression tests are carried out on unaged polyester micro pillars for relative humidities ranging from 6 %RH to 93 %RH. Representative curves can be found in Figure 4.3. In these tests, the pillar is compressed up to a setpoint displacement of 20 µm at a nominal strain rate of 3.10^{-2} s^{-1} before being unloaded at the same strain rate. The maximal deformation varies with humidity as a result of the compliance correction of the pillar displacement.

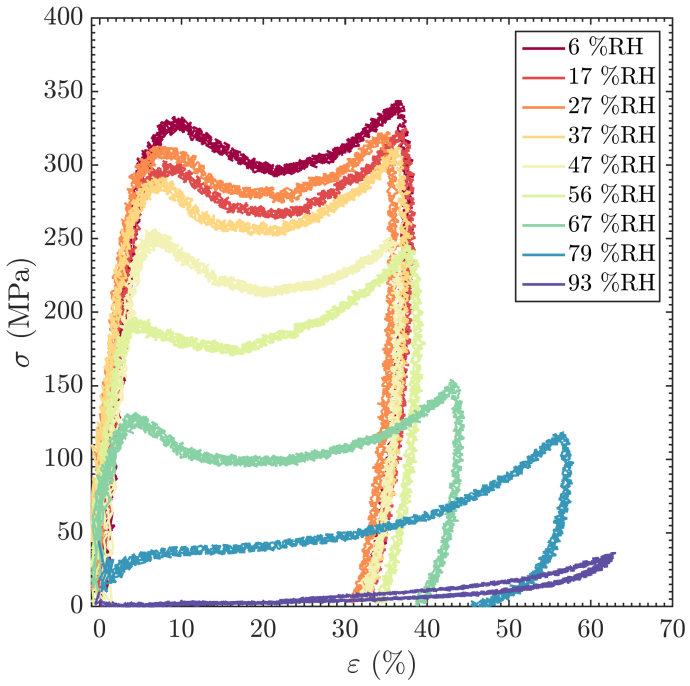

Figure 4.3 – Influence of relative humidity on the true compressive response of unaged polyester micro pillars. Tests are carried out at controlled relative humidity which is gradually increased from 6 %RH to 93 %RH.

Below 80 %RH, the polyester resin exhibits a glassy behaviour similarly to what we previously observed at ambient atmosphere (40 %RH - see Chapter 3). However, the mechanical response is clearly sensitive to humidity. More precisely, the yield stress gradually diminishes for increasing humidity while the elastic modulus and strain hardening behaviour show little moisture-dependence.

At larger humidities, the material undergoes a dramatic softening as highlighted by the stress-strain curve obtained at 93 %RH. An enlargement of this curve is displayed in Figure 4.4. Between 79 %RH and 93 %RH, the material shifts from a plastic to a viscoelastic behaviour. The absence of residual deformation at 93 %RH has been confirmed by performing successive cyclic loadings on a given pillar. All responses

overlap as shown in Figure 4.4. This behavior bears close similarities with the one observed for loosely crosslinked polymers at testing temperature larger than their T_g, namely in the rubbery region [34]. After a initial linear elastic regime, these materials exhibit a strain hardening behaviour at large deformations due to the orientation of their polymeric network. This strain hardening is slightly visible in the polyester sample tested at 93 %RH for deformations larger than 40 %.

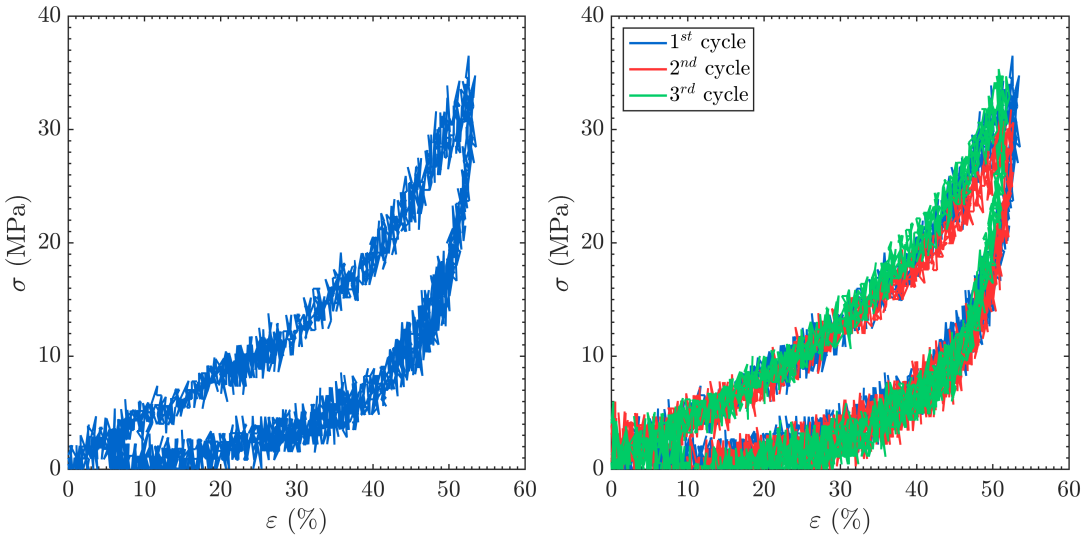

Figure 4.4 – Viscoelastic compressive behaviour of an unaged polyester micro pillar at 93%RH (left) and effect of successive loadings on the mechanical response which confirms the absence of residual deformation (right).

The transition in the polyester mechanical behaviour with humidity is highlighted by the evolution of the yield stress plotted as a function of relative humidity in Figure 4.5. The error bars are defined as the standard deviation measured for 5 specimens. In the plastic region, the yield stress gradually decreases from 330 MPa at 30 %RH down to 40 MPa at 79 %RH whereas by definition, no yielding is observed in the viscoelastic region. The transition between these two regimes occurs at a threshold relative humidity of about 80 %RH.

4.3.3 Moisture-dependent tensile properties

The effect of water on the tensile behaviour of unaged polyester is studied by loading resin micro fibers at a nominal deformation rate of 0.01 s^{-1}, at various relative humidities. Representative curves for humidities ranging from 20 %RH to 88 %RH are shown in Figure 4.6.

Below 70 %RH, the stress-strain relationship is characteristic of a glassy, brittle polymer failing at low elongations [16, 18, 34]. This is similar to the experiments conducted at ambient humidity (40 %RH) in Chapter 3. At higher humidities, the polyester softens and evolves toward a more ductile behaviour.

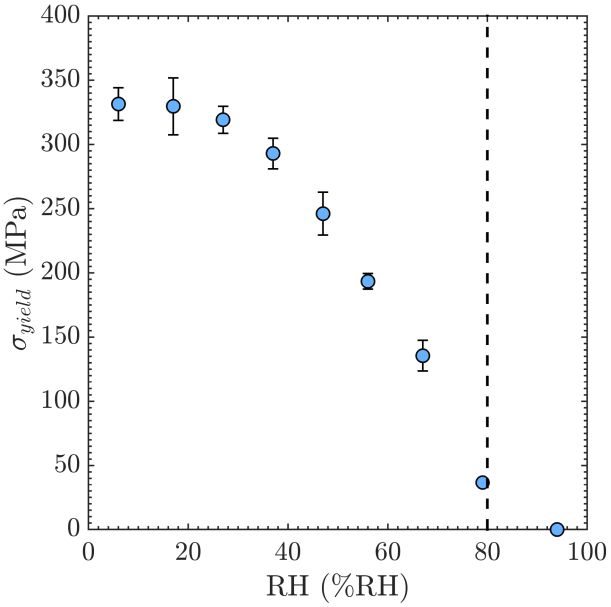

Figure 4.5 – Effect of relative humidity on the yield stress of unaged polyester resin. This graph highlights the existence of a threshold relative humidity at which the polymer undergoes a transition between a plastic (yielding) and a viscoelastic (no yielding) behaviour.

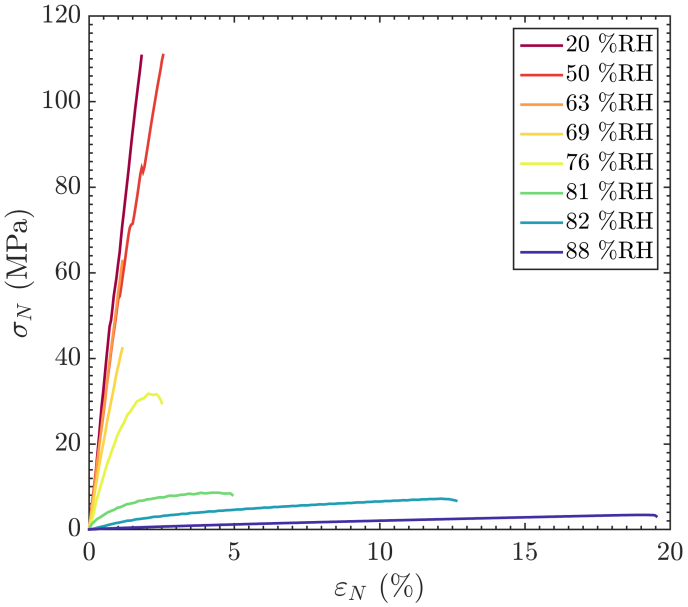

Figure 4.6 – Effect of relative humidity on representative tensile stress-strain curves obtained from unaged polyester fibers. A dramatic softening occurs above 80 %RH.

The evolution of the Young modulus, E and strain at break, ε_{break} are plotted as a function of relative humidity in Figure 4.7 and Figure 4.8, respectively. The error bars are defined as the standard deviation measured for at least 3 specimens. Both quantities highlight the existence of a humidity threshold around 80 %RH at which E suddenly drops from 4.6 GPa down to 20 MPa while a sharp increase from 2 % to 17 % is simultaneously observed for ε_{break}. Interestingly, this is in agreement with the humidity threshold previously observed in compressive testing at which the resin switches between a plastic and a viscoelastic behaviour. The stress at break σ_{break} in Figure 4.9 shows a more complex dependence on moisture. For increasing relative humidity, it first increases, reaches local maximum of 121 MPa $\pm$ 9 MPa at 30 %RH then gradually decreases toward a constant value of 3 MPa above 80 %RH.

Finally, the existence of a humidity threshold also correlates with an abrupt change in the fracture behaviour of the polyester micro fibers around 80 %RH. Typical time sequences of notch fracture are shown in Figure 4.10. The increase in relative humidity brings the system from a brittle (RH $<$ 76 %RH) to a ductile (RH $>$ 80 %RH) crack propagation, via an intermediate fracture behaviour (76 %RH $<$ RH $<$ 80 %RH).

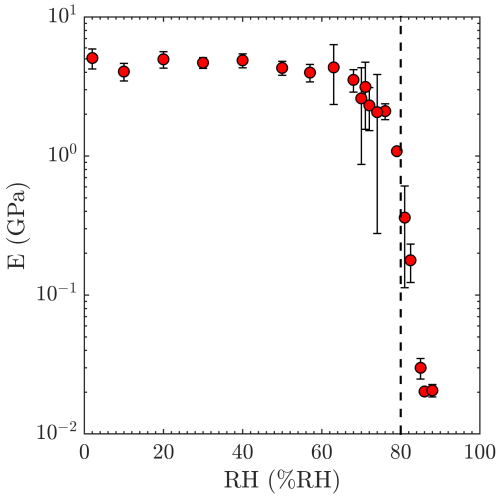

Figure 4.7 – Effect of relative humidity on the Young modulus of unaged polyester fibers.

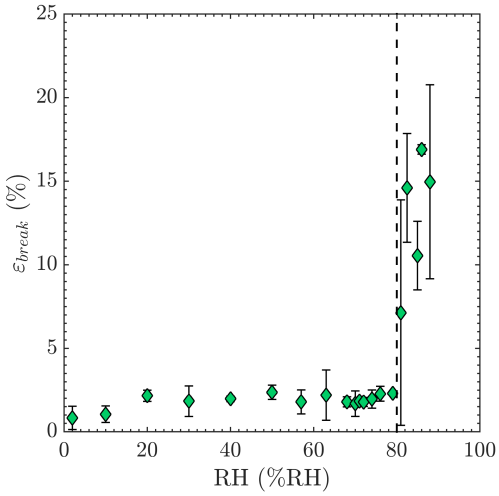

Figure 4.8 – Effect of relative humidity on the strain at break of unaged polyester fibers.

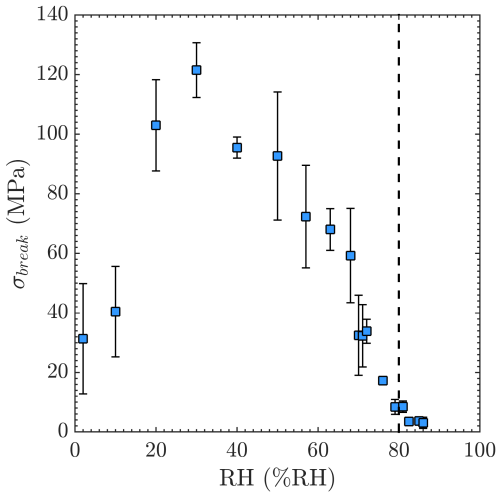

Figure 4.9 – Effect of relative humidity on stress at break of unaged polyester fibers.

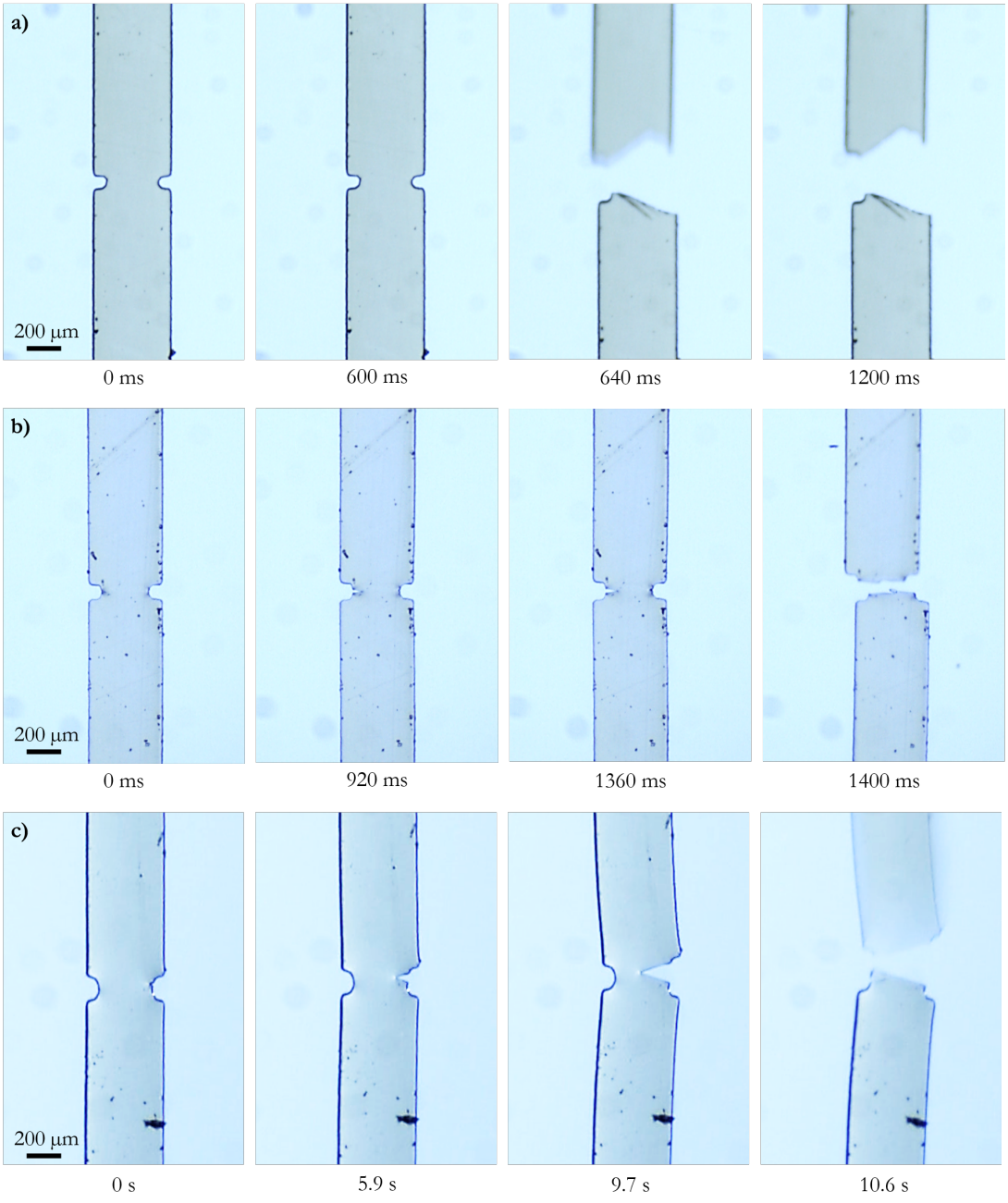

Figure 4.10 – Fracture behaviour of notched micro fibers of unaged polyester resin tested at a relative humidity of a) 22 %RH, b) 76 %RH and c) 88 %RH. Each tensile test is conducted at a nominal strain rate of 10^{-2} s^{-1}. Increasing relative humidity results in a transition from a brittle to a ductile fracture behaviour.

4.4 Discussion

We have shown that the large hydrophilicity of the polyester resin results in a significant change in its mechanical properties upon exposure to humidity. In this section, we aim at understanding the molecular origins of these phenomena. In particular, a special attention will be given to the moisture-dependent properties in the plastic regime and to the existence of a humidity threshold at which the material shifts from a plastic behaviour to a viscoelastic behaviour.

4.4.1 A water-induced plasticization

In this section, we focus on the polyester mechanical behaviour for relative humidities smaller than the humidity threshold, namely in the plastic region. While some mechanical properties, including the elastic modulus, exhibit little moisture-dependence, the yield stress gradually diminishes as humidity increases above 30 %RH.

The decrease in yield stress with humidity correlates with an increase in water uptake as displayed in Figure 4.11. Water content is estimated by DVS measurement as explained in Appendix A.2. This dependence has already been observed in other polymers, including polyamide-6 [25, 51] where it was attributed to a water-induced plasticization. By penetrating in the polymer, water molecules locally enhance the chain mobility which makes polymer deformation easier. However, in the case of the polyester resin, other mechanisms may also affect the mechanical properties such as the partial hydrolysis of the polymer network through the cleavage of ester bonds.

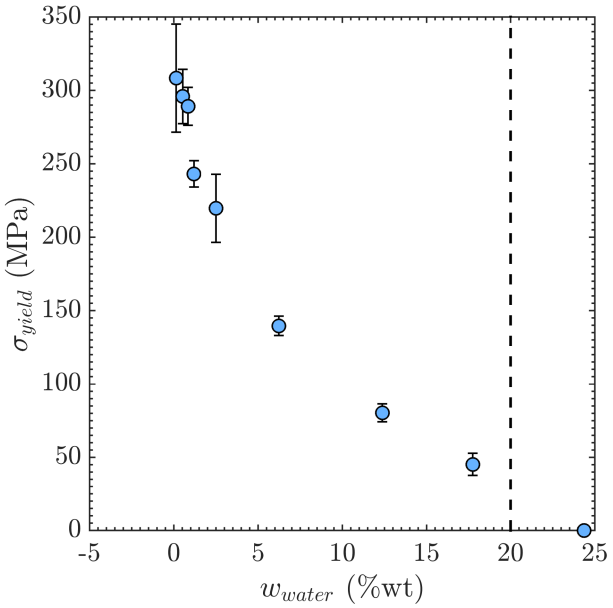

Figure 4.11 – Effect of water content, w_{water} (estimated by DVS) on the yield stress of unaged polyester resin.

To identify the mechanisms responsible for the observed loss in the yield properties, the yield stress is measured for three successive sorption cycles. Each cycle consists in a gradual increase in humidity from 5 %RH up to 90 %RH by 10 %RH step. The extent of reversible and irreversible damage is evaluated on the ability of the material to recover its yield stress at each cycle. While plasticization is regarded as a reversible process with a full recovery of material properties upon drying, significant irreversible damage will lead to a permanent loss of material properties, even after water removal [87, 93, 94]. Results are plotted as a function of relative humidity in Figure 4.12.

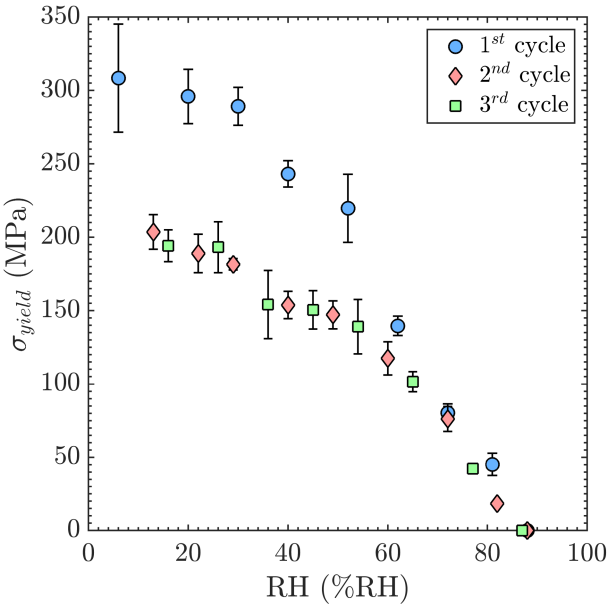

Figure 4.12 – Evolution of the yield stress as a function of relative humidity upon exposure to successive humidity cycles.

When plotted as function of relative humidity, a reduction in yield stress is observed between the first and subsequent humidity cycles. This hysteresis disappears after the second cycle. The curves meet again above 60 %RH. Interestingly, the shape of these curves bears close similarities with the polyester sorption/desorption isotherms measured by DVS in Figure 4.1 (see Section 4.2). All these observations suggest that the material may undergo an initial degradation during the first cycle followed by a stabilization of its properties afterwards.

However, replotting these curves as a function of water content provides a better understanding of this apparent reduction in mechanical properties as shown in Figure 4.13. When plotted as a function of water content, the responses obtained for the three humidity cycles perfectly overlap suggesting that the effect of water is reversible. Despite the reversibility of the molecular process, the curves are shifted to higher water contents after the second humidity cycle. This difference arises from the presence of residual water which cannot be fully removed with the drying conditions

applied between each cycle. At the beginning of the second and third cycles, 2.5 %wt of water remains in the material as shown in the sorption isotherms in Appendix A.2. To remove this excess of water, a more energetic drying would be necessary, for instance by increasing the drying time and temperature or by drying the polymer under vacuum [46, 125]. The excess of water below 60 %RH is responsible for the apparent reduction in yield stress between the first and subsequent humidity cycles when plotted as function of relative humidity as previously observed in Figure 4.12.

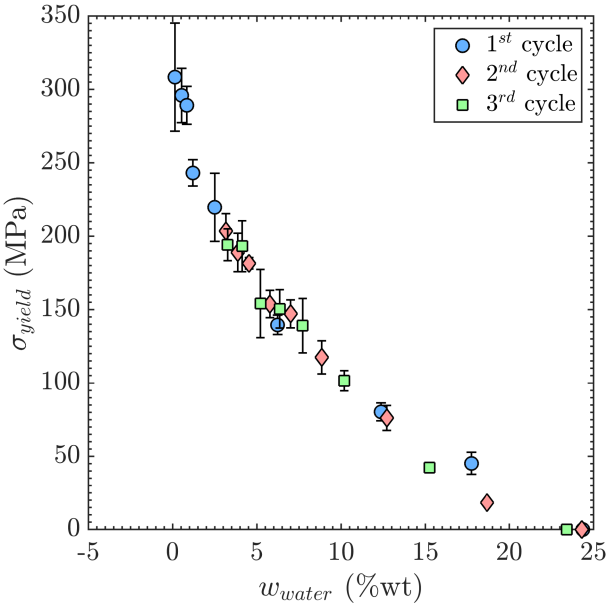

Figure 4.13 – Evolution of the yield stress as a function of rwater content upon exposure to successive humidity cycles.

Plasticization is thus considered as the main mechanism to account for the reduction in yield stress upon water sorption. Especially, we believe that the water molecules are likely to break the initial hydrogen bond network by interacting with the unreacted polar groups. By disrupting the physical crosslinks, water locally enhances the mobility of the chain segments which results in a lower resistance to plastic deformation. This mechanism is illustrated in Figure 4.14. There is no reason to invoke a degradation mechanism such as hydrolysis of the chemical crosslinks.

4.4.2 Antiplasticization of the polyester resin?

In addition to the plasticization effect of water on the polyester yield stress, the presence of a local maximum in the stress at break around 30 %RH in Figure 4.9 may highlight more complex water/polyester interactions. A similar evolution of the stress at break has been reported by Chang in glassy tapioca-starch films and was interpreted as a signature of water antiplasticization [60]. Antiplasticization has been observed in various glassy polymer-plasticizer systems at low plasticizers contents as described in

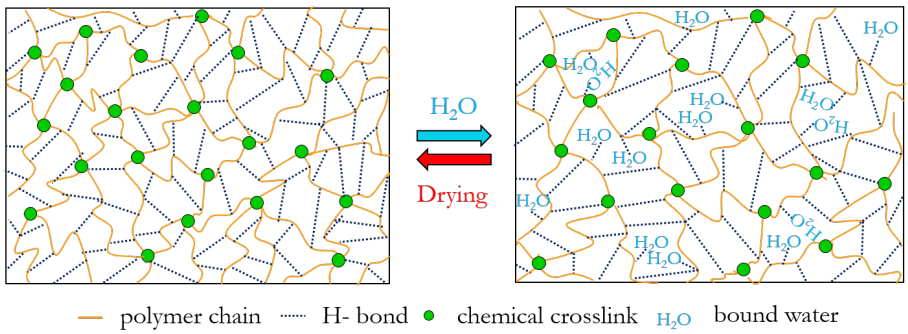

Figure 4.14 – Schematic illustration of the plasticization phenomenon in the polyester resin. Secondary physical crosslinks are thought to reduce mobility.

Section 4.4.2 but this phenomenon remains to date a subject of controversy concerning its molecular origins. Among the theories reported in the literature, a reduction in chain mobility may result from the formation of a secondary physical crosslinking network via strongly interacting water molecules [47, 74, 81]. Upon further water absorption, plasticization will finally compensate this effect after all the available sites of interaction are occupied.

With a view to better understanding this apparent antiplasticization of the polyester resin, the evolution of the elastic modulus (tensile test), yield stress (compressive test) and stress at break (tensile test) are compared as function of relative humidity in Figure 4.15. In this graph, the stress at break is corrected to account for the stress concentration at the notch extremity. For the notch geometry considered (i.e., a notch length of 80 µm ± 5 µm and a notch diameter of 65 µm ± 5), a stress concentration factor of 4.3 is calculated for the tensile stress, which corresponds to a stress concentration factor of 3.8 for the equivalent von Mises stress. This last factor is used to correct the stress at break, σ_{break} and deduce the equivalent von Mises stress at break, $\sigma_{break-eq}$ which will be used as a yielding criterion. Briefly, the Von Mises criterion states that yielding will occur at the notch extremity if the equivalent von Mises stress is larger than the material yield stress. Although the yield stress, σ_{yield} may be somewhat slightly higher in compression because of its hydrostatic pressure dependence [16, 126], we will assume that σ_{yield} measured in compression is equal to that in tension.

In Figure 4.15, for humidities lower than 30 %RH, no effect is evidenced on the polyester elastic modulus and yield stress, although the maximum in σ_{break} interestingly coincides with the end of the yield stress plateau. The constant value of σ_{yield} however challenges the initial assumption to account for the increase in σ_{break}, namely the reduction in molecular mobility due to the formation of a secondary physical crosslinking network and resulting antiplasticization. This comparison allows us to identify three regimes for the polyester resin as a function of relative humidity:

- **Regime I:** a truly brittle regime where no yielding occurs in the glassy polyester resin ($\sigma_{break-eq} < \sigma_{yield}$). In this region, we observe an increase in σ_{break} which may be ascribed to a water-induced healing of network defects. For a brittle material, the fracture strength of the polyester resin is known to be governed by the existence of submicroscopic flaws which satisfy the Griffith criterion for fracture [18]. Sorbed water may promote healing of the major defects in the polyester glass by activating local rearrangements in the vicinity of these defects. Since rupture is controlled by rare large flaws, this mechanism is not expected to affect the yield stress, which is mediated by numerous local rearrangement events. We do not find it necessary to invoke antiplasticization here.
- **Regime II:** the water content exceeds a "plasticization threshold" at 30 %RH (equivalent to a water content of 0.9 %wt) and the classical plasticization effects are observed, namely a reduction in σ_{yield} and σ_{break} of the glassy polyester resin. Note that, in contrast to macroscopic rupture (Section 4.3.3), we find that σ_{break} is such that the von Mises stress in the notch is close to the yield point in compression (though slightly larger) and follows the same trend, suggesting that rupture is mediated by plastic deformation ($\sigma_{break-eq} \simeq \sigma_{yield}$). However, plastic deformation would be confined to a region close to the crack tip, and rupture is still mainly elastic at the macroscopic scale (small scale yielding).
- **Regime III:** above a threshold relative humidity of 80 %RH, the polyester resin undergoes a a dramatic change in its mechanical behaviour characterized by a dramatic softening, the disappearance of yielding and large viscoelastic dissipation which stabilizes the fracture. This is attributed to the transition to a gel state as described in more detail in the next section.

4.4.3 Existence of a water-triggered glass transition

Around 80 %RH, the polyester resin undergoes an abrupt transition between a plastic behaviour and a viscoelastic behaviour with no yielding. This dramatic change in mechanical properties with moisture has been reported in other polymeric systems such as in poly(vinyl alcohol) films upon moist exposure [53] or inversely, during the dehydration of hydrogels [57, 64, 65]. In both cases, it was correlated with the occurrence of a glass transition in polymers, namely a phase transition between a glassy and a rubbery state.

This transition is a direct consequence of the plasticization phenomenon described in Section 4.4.1. By acting as a plasticizing agent, sorbed water enhances polymer chain mobility which also leads to a reduction in the polymer glass transition temperature, T_g. When T_g decreases below the room temperature, the material undergoes a phase transition from a glassy to a rubbery-like material.

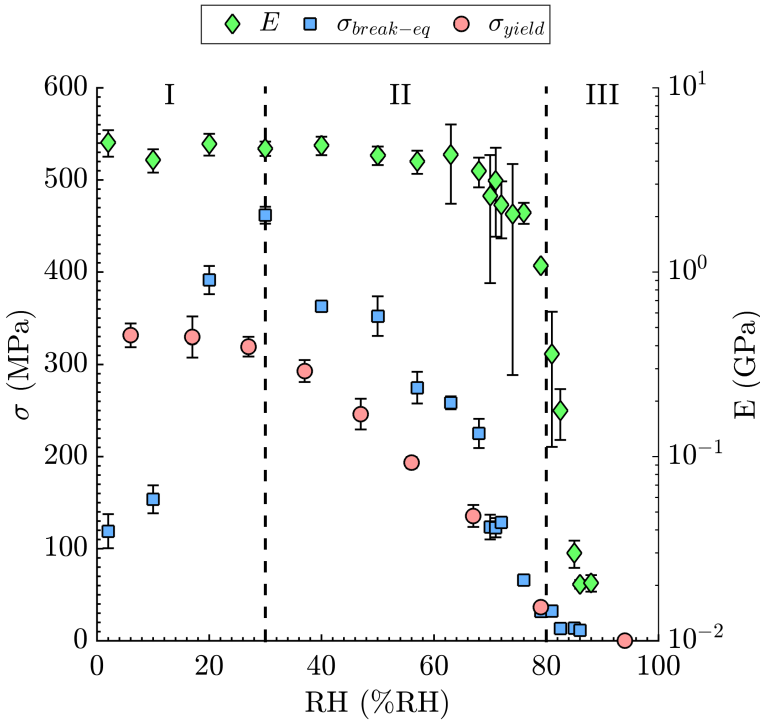

Figure 4.15 – Comparison of the humidity-dependence of the modulus E, yield stress σ_{yield} and equivalent stress at break $\sigma_{break-eq}$ of pristine polyester resin. The stress at break is corrected to account for the stress concentration at the notch extremity. Three regimes can be distinguished: zone I: water-induced healing regime ($\sigma_{yield} > \sigma_{break-eq}$) - zone II : plasticization regime ($\sigma_{yield} < \sigma_{break-eq}$) - zone III : gel regime.

By analogy with the temperature-dependent behaviour of glassy polymers, we define a relative humidity of glass transition, RH_g. From the compressive and tensile results, a humidity RH_g of about 80 %RH is estimated for the polyester resin which corresponds to a water content threshold of about 20 %wt. Assuming that all the carboxilic acid functions react with the hydroxyl functions and that the residual hydroxyl groups do not thermally degrade upon curing, this water content threshold corresponds to a molar composition of hydroxyl:water = 1:0.8 meaning that when one hydroxyl group unit has 0.8 or less hydrated water molecules, the polymer behaves as a glassy polymer. The large water content required to screen all the polymer-polymer interactions suggests that a significant number of physical crosslinks exist in the material.

The most striking example confirming this assumption is the dependence of the elastic modulus, E with relative humidity in Figure 4.7. Around RH_g, the abrupt drop in E of about 2 orders of magnitude bears close similarity to the reduction in modulus observed as a function of temperature in standard glassy polymers [34]. Interestingly, the elastic modulus of the polyester in the gel state is of the same order of magnitude as the modulus of the cornea hydrogels of Annaka [64], suggesting that the resin is not as chemically crosslinked as initially hypothesized. Unfortunately, the density of chemical crosslinks of the polyester resin has not been estimated in this study. Conventional strategies, including the use of the Flory-Rehner equation to deduce the crosslinking density from the sample swelling ratio [127], are difficult to applied on micrometric-scaled samples.

4.4.4 A material model for the polyester resin

From the previous observations, a macromolecular model is proposed to explain the moisture-dependent mechanics of the polyester resin. This model is inspired from [57, 64, 65] who showed that the water-induced glass transition correlates with a change in water molecules mobility. Especially, the transition to the rubbery state is accompanied by the appearance of free water in the polymer, namely water molecules behaving as bulk water. Inversely, mainly bound water, namely water molecules interacting with the polymer chains, exist in the polymer below RH_g. A schematic representation of the model is depicted in Figure 4.16.

When exposed to increasing humidity, pristine polyester resin displays the following characteristics:

a) After curing, a polymer network is formed with two types of crosslinks: a) the physical crosslinks coming from the polar interactions between the unreacted polar groups which also contribute to the polymer hygroscopy and b) to a fewer extent, the chemical crosslinks coming from the esterification reaction. Both

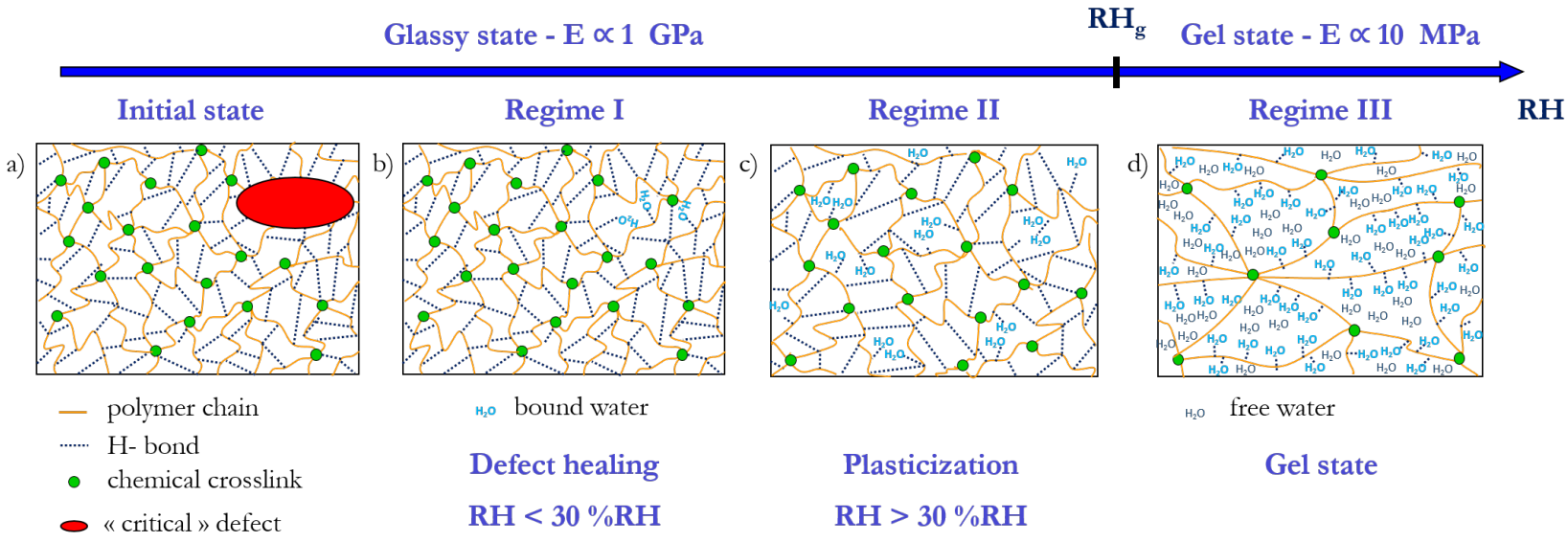

Figure 4.16 – Schematic representation of the molecular hydration process in the polyester resin.

types of crosslinks, but especially the physical crosslinks, impede the polymer chain mobility so that the polymer is in the glassy regime. In this regime, the material exhibits a brittle behaviour with a high yield stress ($E/20$) as most standard glassy polymers [16].

b) As humidity increases, the hydrophilic polymer absorbs water. At low humidity (RH $<$ 30 %RH), water diffusion is slow in the pristine polymer. Water sorption enhances the fracture strength of the material without affecting the other mechanical properties (elastic modulus, yield stress, strain at break). Water molecules are believed to promote healing of the critical defects in the polymer glass by activating local rearrangements in the vicinity of these defects.

c) When the water content exceeds the "plasticization" threshold, water plasticizes the material. Bound water molecules enhance locally the polymer chain mobility by disrupting some of the physical crosslinks. This leads to a reduction in the resistance to plastic deformation, the fracture strength and the polymer glass transition temperature. In this glassy regime, water penetration through the polymer is still limited and slow because overall mobility is still low.

d) When the relative humidity reaches RH_g, the polymer has absorbed enough water molecules so that physical interactions between polymer chains are screened. This also correlates with the humidity at which the glass transition temperature becomes lower than room temperature as a result of plasticization. At that point, the chain mobility suddenly increases and the polymer switches from a glassy to a gel state. This is accompanied by an enhanced sorption capacity. The newly sorbed free water molecules significantly swell the polymer network which behaves as a loosely chemically-crosslinked gel.

4.5 Influence of resin chemistry - Comparison to a phenol formaldehyde resin

As a comparison, the moisture-sensitive mechanical behaviour of the polyester resin is compared to that of a phenol formaldehyde resin, a standard formulation in industry which suffers from well-known hazards due to traces of free formaldehyde. After a characterization of the polymer hygroscopy by DVS, the influence of resin chemistry on the mechanical properties is investigated by micro pillar compression as a function of humidity. All experiments are conducted on pristine samples.

Phenol formaldehyde resin chemistry A schematized illustration of the chemical structure of the phenol formaldehyde resin is displayed in Figure 4.17. An aqueous solution of the phenol formaldehyde resin monomers is provided by Saint-Gobain with

an initial dry content of 50 %wt and cured under the same conditions as the polyester resin in order to form a highly crosslinked network.

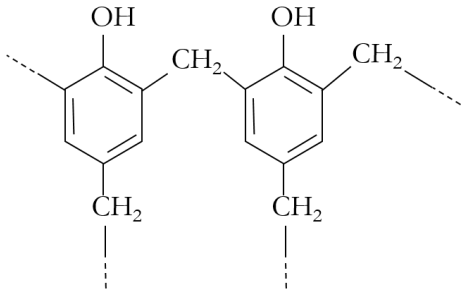

Figure 4.17 – Chemical structure of the phenol formaldehyde resin.

Note that the phenol formaldehyde resin suffers from the release of volatiles upon curing such as water, phenol and formaldehyde. As a consequence, this resin is also prepared with the micro molding process developed in Chapter 3. While all samples geometries can be fabricated for the polyester resin, solely supported thin films and micro pillars are prepared for the phenol formaldehydel resin. Indeed, the low viscosity of the monomer solution coupled to monomer instability upon pre-drying at 80 °C prevents the preparation of phenol formaldehyde micro fibers, which makes tensile testing impossible.

Influence of resin chemistry on hygroscopy The hygroscopy of the phenol formaldehyde resin is characterized by DVS. The sorption isotherms are compared for phenol formaldehyde and polyester resins in Figure 4.18. Both polymers are clearly hydrophilic with a maximal water uptake of 23 %wt at 90 %RH for the phenol formaldehyde resin, which is slightly lower than the maximal sorption capacity of the polyester resin. The threshold for reversible sorption however, is distinctly higher in the case of the phenol formaldehyde resin.

Influence of resin chemistry on moisture-dependent mechanics The influence of resin chemistry on mechanics is investigated using micro pillar compression. Typical stress-strain curves obtained for the phenol formaldehyde resin are shown in Figure 4.19 for relative humidity ranging from 6 %RH to 85 %RH. Similarly to the polyester resin, the material exhibits a glassy behaviour characterized by an elastic modulus in the gigapascal range and a plastic behaviour with a yield stress of the order of 100 MPa. The decrease in yield stress for increasing humidity is attributed to polymer plasticization as confirmed by the reversibility of the phenomenon upon drying.

The humidity dependence of yield stress for the two polymers are compared in Figure 4.20. Both resins present a plasticization phenomenon, namely a reduction in their resistance to yielding for increasing water uptake. However, despite their similar

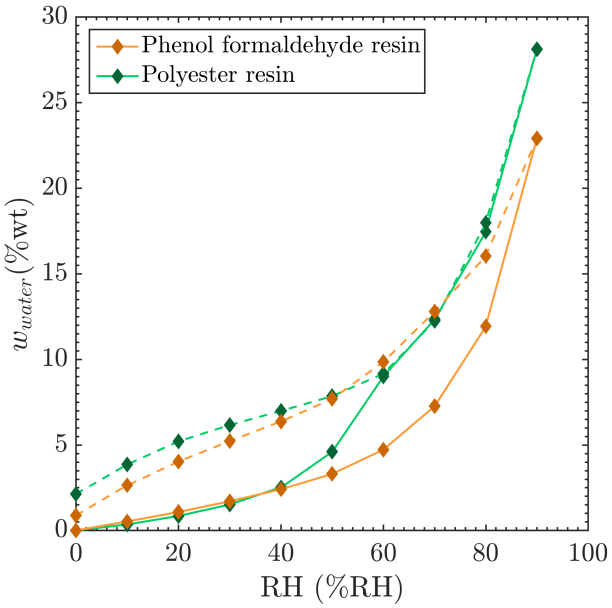

Figure 4.18 – Influence of resin chemistry on the sorption isotherms. Both resins are highly hydrophilic.

hygroscopy, the resins differ in two aspects:

- At a given relative humidity, the phenol formaldehyde resin is always more resistant to yield than the polyester resin.
- More interestingly, the phenol formaldehyde resin does not undergo a water-triggered glass transition despite the large water uptake. Here again, the yield stress correlates directly with the sorption results obtained by DVS.

While the glass transition in polyester resin is driven by the rupture of the polar interchain interactions, these observations suggest a higher cohesion of the phenol formaldehyde network which could be related to a larger density of chemical crosslinks. These assumptions would however require a more in-depth investigation of the macromolecular structure of each resin network.

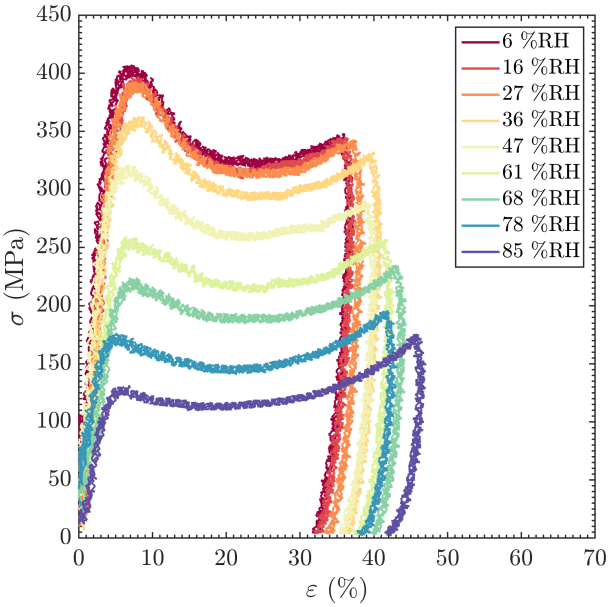

Figure 4.19 – Influence of relative humidity on the compressive response of micro pillars made of unaged phenol formaldehyde resin.

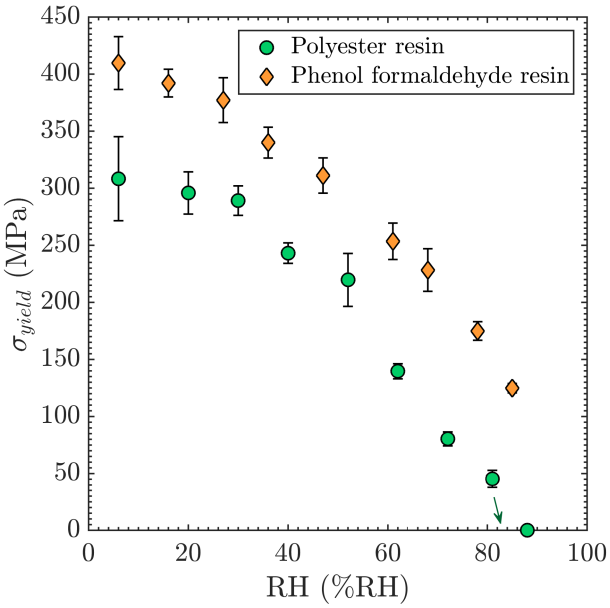

Figure 4.20 – Influence of resin chemistry on the yield stress-relative humidity dependence of unaged resins. Contrary to the polyester resin, the phenol formaldehyde resin exhibits a plastic behaviour on the whole range of humidities and does not undergo a water-triggered glass transition.

4.6 Conclusion

This chapter was dedicated to the characterization of the pristine polyester resin, namely a polymer never exposed to humidity before testing. Dynamic vapor sorption measurements highlighted the large hydrophilicity of the polyester resin which was attributed to the excess of unreacted hydroxyl groups remaining in the polymer network. The mechanical characterization of the polymer using micro tensile testing and micro compression testing showed that this high hydrophilicity results in a large variation in the resin mechanical properties upon exposure to humidity.

At low water content ($w_{water} < 0.9$ %wt), the increase in the polyester fracture strength was first ascribed to the so-called antiplasticization of water. However, the plastic and elastic properties of the material seem unaffected in this range of humidity. We propose instead that increase in water content progressively heals the rare larger defects which result in brittle fracture and that antiplasticization is not an adequate terminology here.

Above a plasticization threshold of 30 %RH (equivalent to a water content of 0.9 %wt), a reversible plasticization phenomenon was evidenced. By interacting with the unreacted polar groups, water molecules reversibly screen the physical interactions between polymer chains and locally increase the mobility of these chains. Water diffusion is still slow in this regime.

At larger humidities, plasticization leads to a water-triggered glass transition which was attributed to the disruption of all physical crosslinks by water molecules. Especially, above a threshold relative humidity RH_g of about 80 %RH, the material undergoes a transition from a glassy to a gel state which is accompanied by:

- An increase in its water sorption capacity with fast water diffusion
- A dramatic drop of the elastic modulus by two orders of magnitude
- A transition from a plastic to a viscoelastic behaviour

These observations provided a better understanding of the macromolecular structure of the polyester resin. The resin hydrophilicity is consistent with a high density of physical crosslinks. By impeding network mobility, these physical interactions maintain the polymer in the glassy state and drive the material properties below RH_g. As a result of their complete disruption at high humidities, the polymer shifts to a gel state whose mechanical response is driven by the chemical crosslinks. The large drop in elastic modulus around RH_g suggested that the polyester is not as highly chemically crosslinked as standard thermosetting resins. On the contrary, the absence of water-triggered glass transition in a phenol formaldehyde resin with similar hygroscopy was attributed to a larger chemical crosslink density and thus, a larger cohesion of the polymeric network.

Finally, the presence of residual water in the polyester samples exposed to multiple

humidity cycles suggested that sample history will have an impact on the apparent mechanical behaviour of the polymer. Moreover, as a disordered state, glassy polymers are known to relax toward equilibrium over time. However, physical ageing was not considered in this chapter since specimens were characterized quickly after preparation. These aspects will be investigated in more detail in the next chapter.

Take-home messages

- As a result of its large hydrophilicity, the mechanical properties of the pristine polyester resin are highly moisture-dependent.
- Water has a gradual healing effect on the larger network defects of the polyester resin below 30 %RH (increase in fracture strength but constant yield strength) and a plasticization effect above 30 %RH (reduction in yield stress, fracture stress and elastic modulus).
- The polyester resin exhibits a water-triggered glass transition at $RH_g = 80$ %RH, humidity which delimits two regimes:
  - A glassy state below RH_g for which the polymer properties are governed by the plasticization of the physical crosslinks
  - A gel state above RH_g whose properties are governed by the chemical crosslinks
- The large drop in elastic modulus above RH_g suggests that the chemical crosslink density of the polyester resin is similar to that of a standard hydrogel. Below RH_g, the glassy behaviour originates from the large number of physical interactions between the unreacted polar groups which impede polymer chain mobility below 80 %RH.

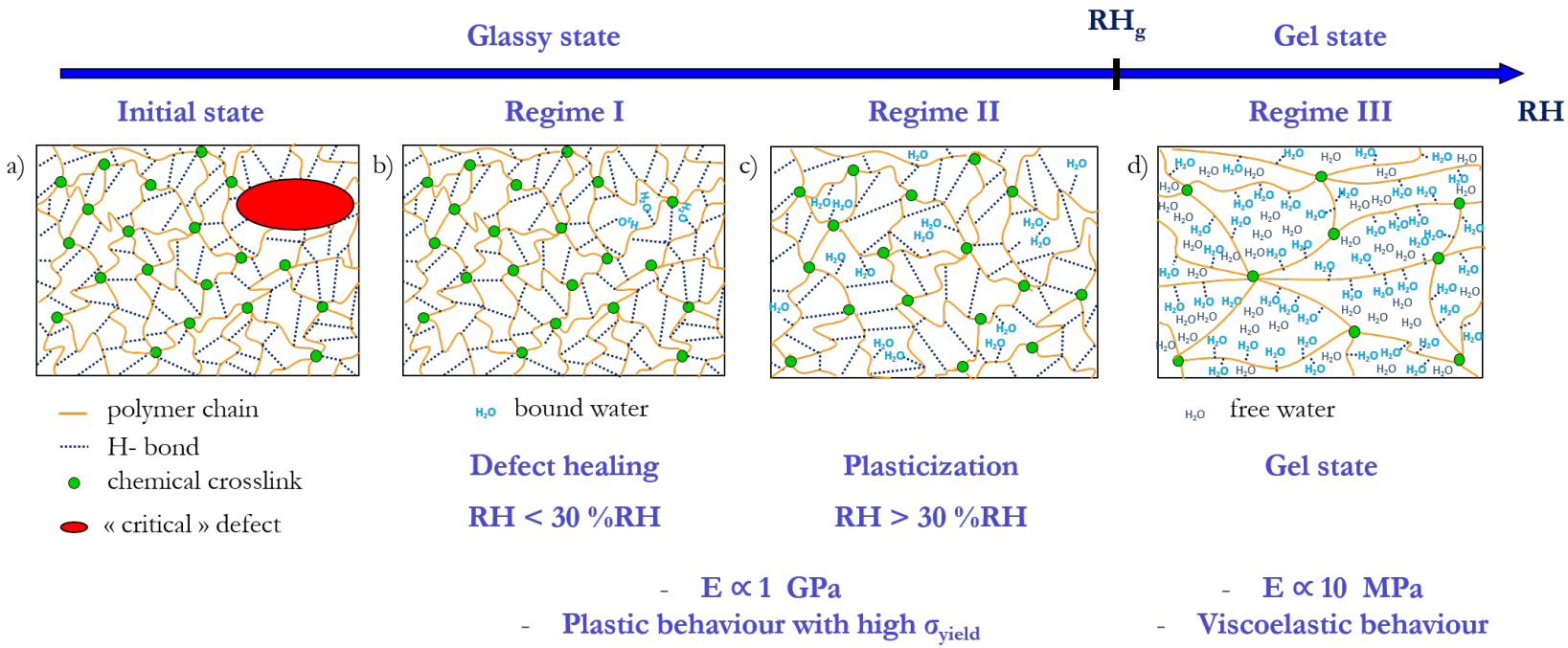

Figure 4.21 – Schematic summary of the molecular hydration process and related mechanical behaviour of the polyester resin.

Chapter 5

Influence of hygric history on polyester resin mechanics

5.1 Introduction

The properties of polyester resins are known to evolve over time upon exposure to humidity as a result of reversible or irreversible processes [4, 5, 6, 7]. In the previous chapter, preliminary results have already evidenced that despite the reversibility of the plasticization phenomenon, exposing pristine resin to multiple humidity cycles resulted in the presence of undesorbed water molecules in the polymeric network. This residual water led to an inherent reduction in yield stress between the first and subsequent humidity cycles when plotted as function of relative humidity. For humidities lower than the glass transition humidity, RH_g, additional processes could also take place due to the glassy behaviour of the polyester resin. Because of its non-equilibrium nature, a glassy state undergoes a slow microstructural evolution through a process known as physical ageing. Physical ageing affects the physical properties of the material, including its density and its mechanical properties [39, 40, 128]. Finally, upon hygrothermal ageing, polyester resins can also be subjected to irreversible damage such as hydrolysis of their ester bonds or micro-cracking as a result of swelling or osmotic stresses [84, 92, 96].

All these processes are of high interest for applications where the polyester resin will be exposed to cyclic weathering conditions during the entire life cycle of the industrial product.

As a consequence, the aim of this chapter is to provide a better understanding of the influence of hygric history on the polyester resin behaviour and macromolecular structure. To do so, pristine polyester resin will be exposed to multiple humidity cycles at ambient temperature and the ability of the polymer to recover its initial properties will be measured at each cycle. After a brief characterization of the influence of hygric history on the resin sorption/desorption properties by DVS, a more in-depth

investigation will be carried out by studying the development of internal stresses in a polyester thin film deposited on a silicon substrate. These internal stresses will be recorded on a home-made setup which allows long-term measurements under controlled humidity conditions. As suggested by Perera [128, 129, 130], the level of internal stresses will be considered as a signature of the extent of microstructural relaxation in organic coatings. Especially, we will look at the evolution of these stresses upon exposure to multiple humidity cycles with a view to shedding light on the molecular reorganization events occurring upon exposure to humidity. Altogether, these results will allow us decorrelating the reversible and irreversible processes taking place in the polyester resin under various hygrothermal ageing conditions.

5.2 Some preliminary evidence of the influence of hygric history - the polyester sorption properties

The sorption properties of the polyester resin are characterized upon exposure to multiple humidity cycles by DVS. To do so, pristine polyester micro fibers are exposed to two successive sorption/desorption cycles using the humidity cycling conditions "at equilibrium" described in Chapter 4. The sorption/desorption isotherms obtained are shown in Figure 5.1 (top) while Figure 5.1 (bottom) compares the temporal evolution of water uptake. Only the sorption cycles are displayed on this graph while the entire cycles can be found in Appendix A.3.

Clearly, the polyester sorption properties are influenced by the sample hygric history as evidenced both by the differences in the isotherms and the diffusion kinetics.

As already seen in Chapter 4 and recalled in Figure 5.1 (top), a large hysteresis exists between the first sorption and desorption cycles for humidities lower than 60 %RH while 2 %wt of residual water remains in the resin at the end of the first desorption cycle. The presence of residual water has been already reported in Chapter 4 where it resulted in an apparent reduction in yield stress for humidities lower than 60 %RH. There is also some hysteresis between the second sorption and desorption isotherms but in a much lower extent. Note finally the large discrepancy between the two sorption curves while the two desorption curves overlap. Interestingly, all the curves collapse for relative humidities larger than 60 %RH, humidity at which an increase in water uptake capacity is also observed.

The large hysteresis between the two sorption curves is also accompanied by a change in diffusion kinetics of water into the polymeric matrix as shown in Figure 5.1 (bottom). During the first sorption cycle, the water diffusion processes are initially very slow and no mass stabilization is reached by the end of the humidity step. The water diffusion kinetics suddenly increase above 60 %RH. On the contrary, a faster diffusion is observed during the second sorption cycle on the entire humidity range.

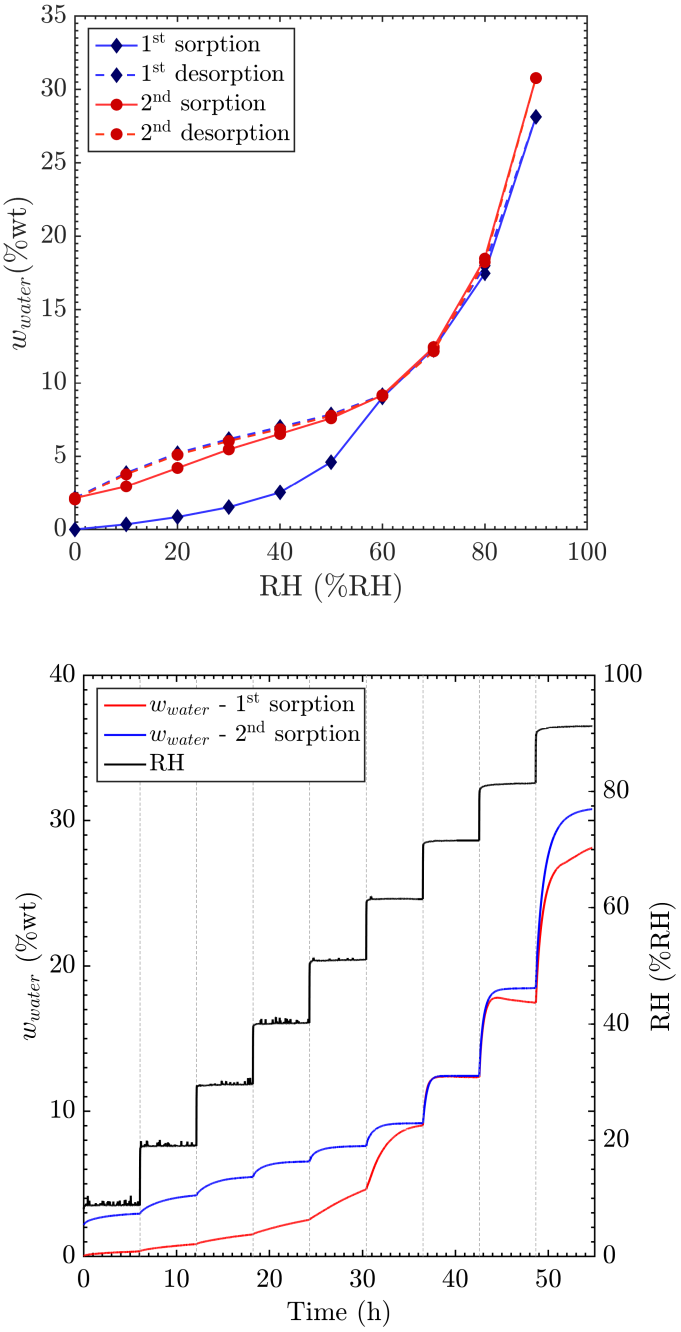

Figure 5.1 – Evolution of the sorption properties of pristine polyester resin subjected to two successive humidity cycles. Top: sorption/desorption isotherms. Bottom: temporal evolution of the weight fraction of water and relative humidity in the chamber. A faster diffusion of water is observed during the second sorption cycle.

These observations suggest that the polymer network undergoes an irreversible microstructural reorganization upon its first exposure to humidity as described by Bouvet [46] and Bao [70] who studied the evolution of sorption and diffusion properties of thermosetting resins exposed to successive sorption/desorption cycles. Briefly, the higher water uptake level and diffusivity during the re-absorption cycle were attributed to a water-induced relaxation of the glassy polymer. By acting as a plasticizer, water molecules increase the free volume of the polymer glass during the first sorption cycle which further facilitates water intake and makes polymer chains more accessible to water molecules during the subsequent cycles.

Although these phenomena clearly indicate the influence of hygric history on resin behaviour, all these preliminary observations remain qualitative. Moreover, the increase in polyester sorption properties could be associated to chemical ageing processes, including network hydrolysis or micro cracking [90, 96]. The effect of humidity cycles on polymer microstructure is thus further evaluated in the next section.

5.3 Internal stresses in polyester layers - a signature of the resin microstructural reorganization

In this study, the measurement of internal stresses in polyester thin film is used as a non-destructive method to indirectly follow the microstructural reorganization of the polymer as a function of time and relative humidity. This method is inspired from Perera [128, 129, 130] and Thurn [131] who demonstrated the influence of thermal history on the microstructural relaxation of glassy coatings through the evolution of internal stresses. After a brief description of the origin of internal stresses, we develop a home-made setup which allows long-term measurements of internal stresses in supported thin films under controlled humidity conditions. The characterization procedure is then presented and applied to a pristine polyester layer.

5.3.1 Origin of internal stresses

In-plane stresses develop in films adhering to a rigid substrate when a dimensional misfit exists between the two parts as sketched in Figure 5.2. These stresses are often referred to as internal stresses or residual stresses [8, 132, 133]. Stress itself is not an issue except when it induces damage in the coatings such as cracking when the stresses exceed the material strength or delamination in the case of weak coating/substrate interfaces.

In the case of polymer coatings, internal stresses are a consequence of various processes including preparation, environmental conditions and structural relaxation. Upon curing, most polymeric films shrink due to chemical reaction and solvent evaporation (see Figure 5.2.a). When the polymer is deposited on a rigid substrate, shrinkage

can occur only in the direction normal to the surface while material contraction is isotropic, resulting in constrained contraction in the directions parallel to the substrate. This frustration leads to the development of in-plane tensile stresses in the polymer layer. On the contrary, if the polymer layer expands with respect to the substrate, the frustration of volume expansion results in in-plane compressive stresses in the polymer coating. A macroscopic consequence of these internal stresses is the curvature of the substrate provided it is compliant (see Figure 5.2.b). The structure is concave in the case of tensile stresses and convex in the case of compressive stresses.

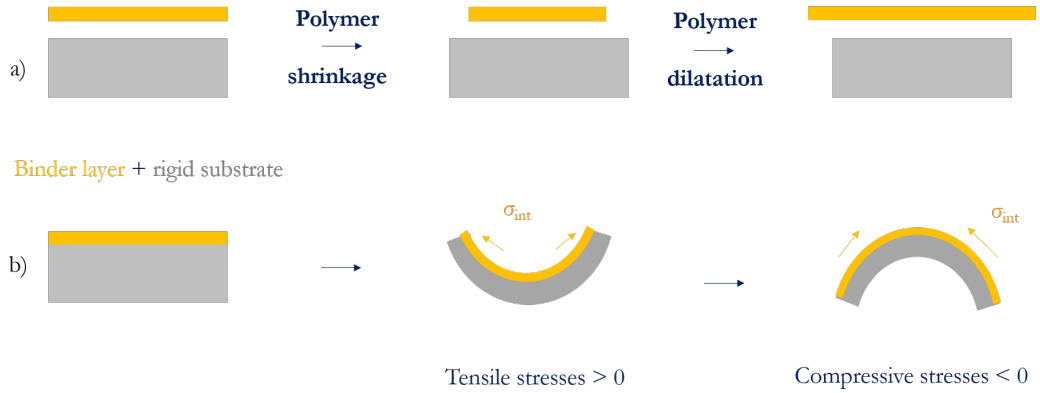

Figure 5.2 – a) Volume change in a polymer film and b) corresponding development of internal stresses when the polymer film is bonded to a rigid substrate. By convention, tensile stresses are positive while compressive stresses are negative.

Over time, these stresses in the polymer film may change as a result of environmental conditions. Most papers deal with thermal stresses, namely stresses arising from a temperature change because of the difference in thermal expansion coefficients between the polymer and the substrate [129, 131, 134]. Similarly, exposure to water also leads to a differential swelling between the polymer film and the substrate [134, 135, 136, 137, 138]. Upon water sorption, the polymer layer swells while being frustrated by its adhesion to the substrate. As a consequence, internal stresses build up and become more and more compressive as moisture is increasingly sorbed into the material. These stresses are sometimes referred to as hygroscopic stresses, σ_H. In the case of a elongategd strip [138], σ_H can be written using Equation 5.1:

$$\sigma_H = E_f \frac{\Delta V_{water}}{3V_0} \tag{5.1}$$

where E_f is the Young's modulus of the polymer film, respectively, V_0 is the dry volume of the film, ΔV_{water} is the change in film volume due to water uptake. Note that the right term in Equation 5.1 is equivalent to a biaxial water-induced strain. Assuming that the change in film volume is proportional to its weight variation due to water uptake, σ_H can be related to the water content in the polymer film, w_{water} (in g.g^{-1})

using Equation 5.2:

$$\sigma_H = \frac{E_f \rho v_{water}}{3} w_{water} \tag{5.2}$$

where ρ is the dry film density (in g.cm^{-3}) and v_{water} is the specific volume of water in polymer (in cm^3.g^{-1}). The linear dependence between hygroscopic stress and water content described in Equation 5.2 has been measured experimentally on glassy polymeric layers [136, 137, 138]. By analogy with thermally-induced stresses, the slope of the w_{water} - σ_H curve can be defined as a coefficient of moisture expansion. A deviation from this linear regime is sometimes reported [138] and may be attributed to the water-induced plasticization which decreases the yield strength and elastic modulus of the polymeric coating [139, 140].

Finally, the evolution of internal stresses has been used to indirectly follow the structural reorganization and relaxation processes induced by physical ageing [128, 129, 130] and by water diffusion [140, 141] in glassy polymeric films.

5.3.2 Description of the curvature measurement setup

Setup principle For a quantitative measurement of internal stresses, we measure the macroscopic change in curvature of a coated elastic substrate that arises as a consequence of internal stresses as illustrated in Figure 5.3. The average internal stress in a thin film coated on a narrow strip, σ_{int} can be deduced from the substrate curvature using Stoney's formula [142] in Equation 5.3:

$$\sigma_{int} = \frac{E_s t_s^2}{6 t_f (1 - \nu_s)} \left(\frac{1}{R} - \frac{1}{R_0} \right) \tag{5.3}$$

where E_s and ν_s are the Young's modulus and Poisson's ratio of the substrate, t_f is the film thickness, t_s is the substrate thickness, R is the radius of curvature of the coated substrate and R_0 is the radius of curvature of the substrate before film deposition. Assumptions made in this equation include a) the substrate deformation remains in the elastic limits of the film and substrate b) deflections are small relative to the substrate thickness c) the coating is significantly thinner than the substrate.

Note that in the literature, most papers considering narrow cantilevers for curvature measurements use an alternative equation for internal stresses estimation [139, 143, 140, 144]. Corcoran's equation is indeed more appropriate since the film is under a biaxial rather than a uniaxial stress configuration. However, since the film modulus and thickness are much smaller than those of the substrate, Corcoran's equation can be approximated to the Stoney's equation for our system.

A great advantage of the curvature-based method lies in the direct measurement of internal stresses. In other techniques such as the X-Ray diffraction-based method or hole drilling method [132, 133], internal stresses are indirectly determined from

the measurement of elastic strains and deduced using the generalized Hooke's law, which requires the knowledge of the film properties. For the curvature-based method, Equation 5.3 shows that the elastic bending of the substrate does not depend on the elastic modulus of the film which can be difficult to quantify as a function of ageing and environmental conditions.

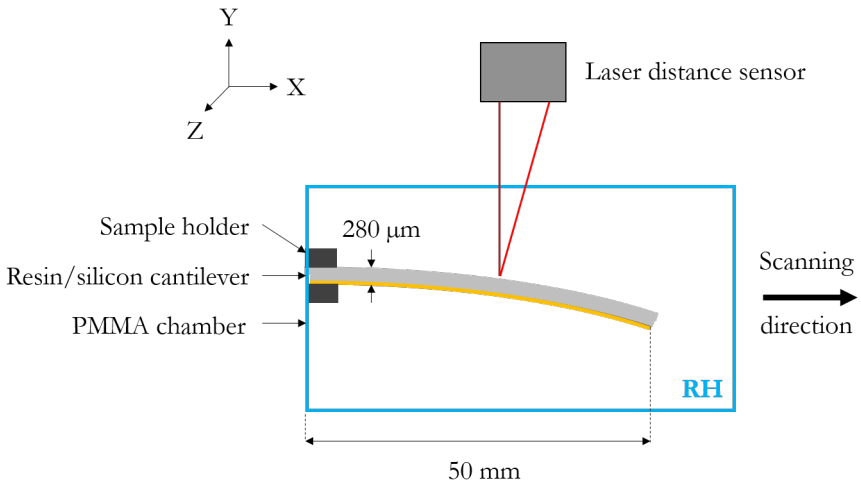

Figure 5.3 – Schematic of the curvature measurement setup (top view).

Description of the curvature-measurement setup Internal stresses are monitored with a home-made curvature measurement setup which allows measuring the evolution of stresses for several days at controlled relative humidity. A curvature measurement is preferred to a pointwise deflection measurement as the cantilever deflection may be impacted by sample clamping instability for long-term acquisition. After an unsuccessful attempt to measure the substrate 3D profile with the equal thickness fringes arising from the multiple reflections between the silicon strip and a reference surface, a setup based on laser deflection has been developed.

A schematic of the setup is shown in Figure 5.3. It consists of a laser distance sensor (OptoNCDT 1700 from Micro Epsilon), a 1D translational motor (M-403 Precision Translation Stage from Physik Instrumente), a sample holder to fix the cantilever beam and a controlled-humidity chamber made of transparent PMMA. The setup control and data readings are performed with a LabView code.

The sample for internal stresses measurements consists of a rectangular silicon cantilever coated with a polyester thin film. The silicon substrate has a length of about 50 mm, a width of about 5 mm and a thickness of 260 µm ± 10 µm. Resin thin films are prepared using a flat stamp in the micro molding process developed in Chapter 3. An adhesion primer (aminopropyltriethoxysilane from Sigma-Aldrich) is incorporated in the monomer solution to ensure a good polymer/silicon adhesion. At

the end of curing, we measure a final film thickness of 7 µm ± 0.5 µm using an optical profilometer (Fogale Nanotech).

The cantilever is mounted vertically to ensure that deflection due to weight variation is not a problem [143]. The sample holder is installed in the PMMA chamber in which the relative humidity can be controlled in order to investigate its effects on internal stress development. The relative humidity in the chamber is automatically adjusted using two automatic gas flow controllers. With this home made device, humidity cycles can be programmed with relative humidities ranging from 2 %RH to 95 %RH and a stability of 3 %RH. More details about the humidity control setup can be found in Appendix B. Tests are performed at room temperature which is not controlled (23 °C ± 2 °C).

The laser distance sensor measures the relative distance between the sensor and the cantilever. Distance measurement are made through the transparent PMMA window which does not affect acquisition. Surface curvature is monitored by scanning the cantilever along its length with the distance sensor. The scan duration is approximatively 80 s. The simultaneous acquisition of the relative sample-sensor distance and scanning motor position gives access to the 2D profile of the cantilever along its length. The radius of curvature R is estimated by interpolating the profile with a second order polynomial function. The curvature of the substrate before film deposition ${R_0}^{-1}$ has been found to be negligible for our experimental conditions.

Figure 5.4 shows a typical 2D profile for a polyester-coated cantilever stored at ambient atmosphere. Two successive scans are compared to assess the measurement reproducibility. There is a significant level of fluctuations. However, this is not noise since profiles superimpose for the two measurements. These repeatable variations are due to the imperfections of the translation stage. The resulting sensitivity, however, is acceptable for our case. A high quality translation stage would be required to reduce the amplitude of these fluctuations.

Considering the layers dimensions, these samples meet the limitation of Stoney's equation. The change in internal stresses is thus deduced using Equation 5.3. For the data shown in Figure 5.4, we obtain a value of -7.6 MPa ± 0.2 MPa by considering a biaxial modulus of 180 GPa for the silicon substrate [145].

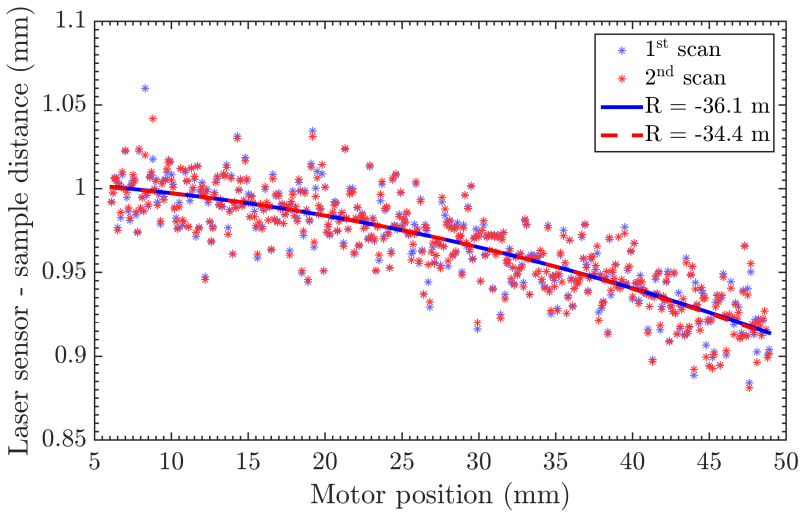

Figure 5.4 – 2D profiles of a polyester resin/silicon cantilever recorded with the curvature measurement setup. A good reproducibility is observed between the two successive measurements. Curvature is estimated by interpolation with a second order polynomial function (lines).

5.3.3 Measurement of internal stress isotherms

Protocole Just after film curing, samples are conditioned at a given relative humidity, RH_{cond}, for about 20 h. Internal stresses are simultaneously estimated by measuring the sample curvature every 20 min. Subsequently, the moisture-dependence of internal stresses is characterized by gradually increasing the relative humidity in discrete steps with a 270 min-interval between each change in humidity. One sorption cycle corresponds to an increase in relative humidity from 10 %RH up to 90 %RH with 10 %RH steps. The sample curvature is measured every 20 min. Because we have shown that the first humidity cycle produces irreversible structural changes in Section 5.2, up to three successive sorption cycles are applied. A characteristic time-relative humidity cycle is sketched in Figure 5.5.

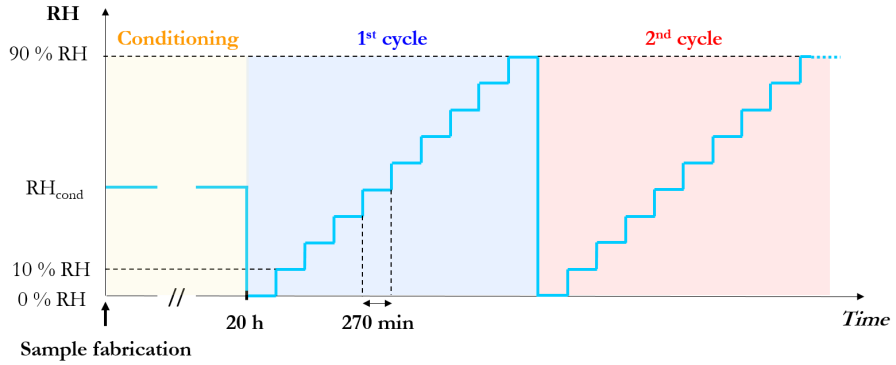

Figure 5.5 – Humidity cycling conditions for internal stresses measurement. After an initial 20 h-conditioning at a relative humidity of RH_{cond}, the sample is exposed to one or several sorption cycles.

We would like to draw the reader's attention on the fact that the coating thickness measured in the dry state just after preparation is used in all stress calculations. Thickness variation due to water sorption is not taken into consideration.

Internal stress isotherms As an illustration, the temporal evolution of the internal stresses for a supported resin film initially conditioned at ambient humidity (RH_{cond} = 40 %RH) is displayed in Figure 5.6.

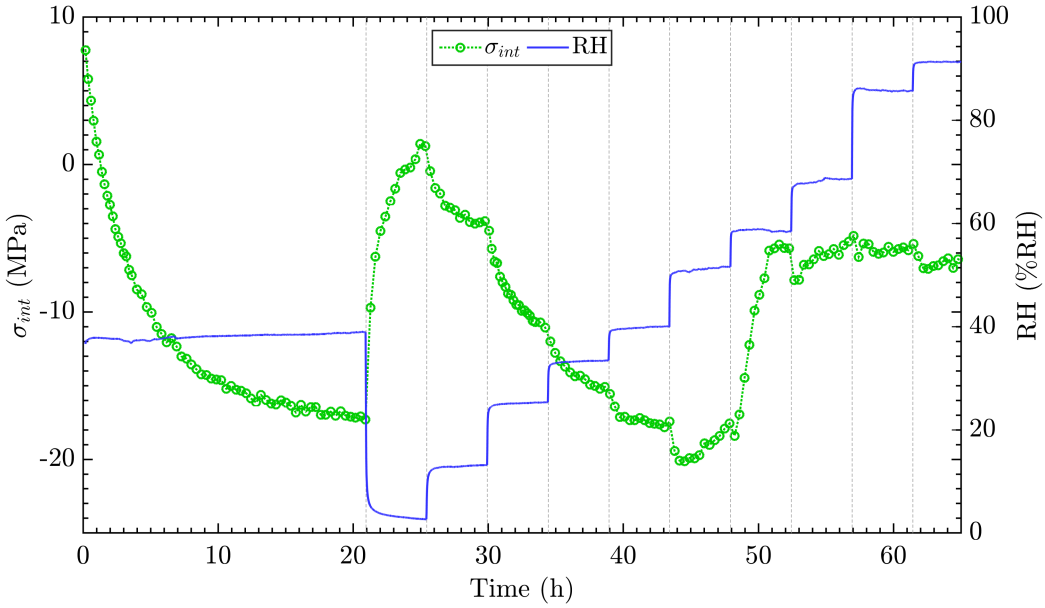

Figure 5.6 – Temporal evolution of relative humidity and internal stresses in a polyester film for an initial conditioning at ambient humidity (RH_{cond} = 40 %RH) followed by one sorption cycle.

During curing, tensile stresses in the polymer film develop because of film shrinkage upon crosslinking. At the beginning of the conditoning step, we find stresses of 8 MPa (tensile stress). During conditioning, they decrease toward a pseudo constant value of about -17 MPa (compressive stress). The transition toward a compressive state highlights the slow development of hygroscopic stresses in the polymeric layer when exposed to ambient moisture. This slow evolution could be related a) to the slow diffusion of water in the polymer matrix already evidenced by DVS in Section 5.2 and b) to the local molecular relaxation events taking place in glassy polymers. During the subsequent sorption cycle, a steady stress state is not systematically reached at each humidity step, which is consistent with the absence of mass stabilization observed in DVS in Section 5.2. Larger waiting times would be needed, but would preclude extensive measurements. As a result, our isotherms are only approximate.

The water content-internal stress isotherms are then constructed by plotting the internal stresses reached at the end of each humidity step as a function of water content. Water content is estimated by carrying out DVS tests under similar humidity

conditions and similar waiting times. The corresponding relative humidity-internal stress isotherms can be found in Appendix A.4. The water content-internal stress isotherm obtained for a pristine polyester film initially conditioned at ambient atmosphere (RH_{cond} = 40 %RH) is displayed in Figure 5.7.

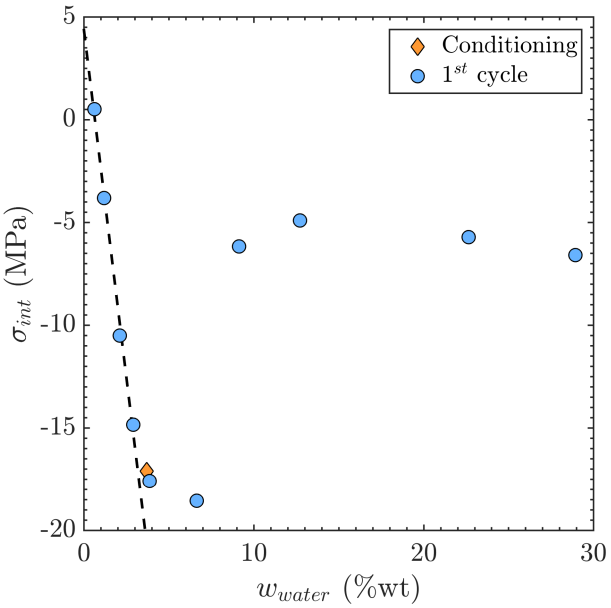

Figure 5.7 – Internal stress-water content isotherm obtained for a pristine polyester film initially conditioned at RH_{cond} = 40 %RH and exposed to one sorption cycle. The dashed line indicates the linear regression line for w_{water} lower than 3 %wt. A slope of -6.8 10^2 MPa is estimated (R^2 = 0.995).

At low water content, small tensile stresses develop in the polyester layer because of the initial polymer shrinkage upon curing. As relative humidity increases, swelling occurs and internal stresses decrease and then become more and more compressive. For water contents lower than 3 %wt, a linear relationship exists between the level of internal stresses and water content and reminds that observed in other polymeric coatings by Berry [136], Wong [137] and Langer [138]. Assuming a dry film density of about 1.1 $cm^3.g^{-1}$ [21] and a specific volume of water equal to that of bulk water (i.e., 1 $g.cm^{-3}$), we estimate an elastic modulus E_f of about 2.0 GPa for the polyester film using Equation 5.2. This rough estimation is of the same order of magnitude than the elastic modulus which has been deduced by tensile testing in Chapter 4, namely 4.5 GPa ± 0.4 GPa. The discrepancy between the two values could stem from the very different time scales considered in tensile testing (strain rate of 10^{-2} s^{-1}) and internal stress measurement (270 min-relaxation i.e., equivalent to a strain rate of 6 10^{-5} s^{-1}). Moreover, there are some uncertainties about the water content at equilibrium in the polyester film, the film density and the specific volume of sorbed water which has been reported to be lower than that of bulk water in polymers [138].

Around 8 %wt, a deviation from the linear regime is observed and internal stresses

relax toward a constant value of about -5 MPa. This non-zero value could be attributed to a plastic deformation in the polymer film [139]. Indeed, for increasing water contents, as the hygroscopic stress climbs and polymer yield stress is reduced due to plasticization, the polyester yield stress will eventually reach the internal stresses value, effectively setting an upper bound for the film stress.

The shape of the curve is reminiscent of the so-called "U-type shape" curve described by Perera who measured the evolution of thermal stresses in organic coatings [129, 130]. Perera attributed this deviation to the glass transition region of the coating which was followed at higher temperatures by the relaxation of stress in the rubbery region. This is consistent with the existence of a water-triggered glass transition in the polyester resin. Thurn [131] also showed that the temperature at which this deviation occurs correlated well with the glass transition temperature measured by differential scanning calorimetry under similar scanning conditions.

From our internal stress isotherms, the glass transition occurs at a threshold water content of about 10 %wt which corresponds to a glass transition relative humidity of about 60 %RH (see Appendix A.4). These values are much lower than the previous estimations of 20 %wt and 80 %RH measured by micro compression and micro tensile testing in Chapter 4. Similarly, the yield stress is evaluated as 5 MPa, a value which is much lower than the yield stress measured in the previous chapter in similar humidity conditions. These differences could stem from the different loading rates applied between the two sets of experiments. Because of its kinetic nature, the glass transition temperature is known to decrease for decreasing loading rate in polymers [34]. While the tensile and compressive properties have been measured at a strain rate of 10^{-2} s^{-1}, internal stresses are measured after a 270 min-relaxation i.e., an equivalent strain rate of 6 10^{-5} s^{-1}.

As a conclusion, the internal stress developing in a polyester layer can be seen as a combination of stress accumulation from constrained change in film volume with humidity and stress relief by structural relaxation. This relaxation is visible in Figure 5.6 during the 67 %RH humidity step where internal stresses quickly relax toward the plateau value after an initial build-up at - 7 MPa. The increase in chain mobility induced by water plasticization accelerates the relaxation rate as the resin gets closer to its glass transition. On the contrary, in the glassy state, relaxation rates are sufficiently slow to allow hygroscopic stresses to build-up upon water sorption.

5.4 Influence of hygric history on microstructural reorganization processes in the polyester resin

The evolution of the polymer microstructure is investigated as a function of hygric history using the internal stress isotherms methodology. Especially, the effect of multiple

humidity cycles on internal stresses development is studied. These results will allow us to infer a scenario for the hygric history dependence of the properties and structure of the polyester resin.

5.4.1 Evolution of internal stresses upon exposure to multiple humidity cycles

Figure 5.8 shows the internal stress isotherms for a polyester thin film initially conditioned at low humidity (RH_{cond} = 11 %RH) for 20 h and subsequently exposed to three successive sorption cycles.

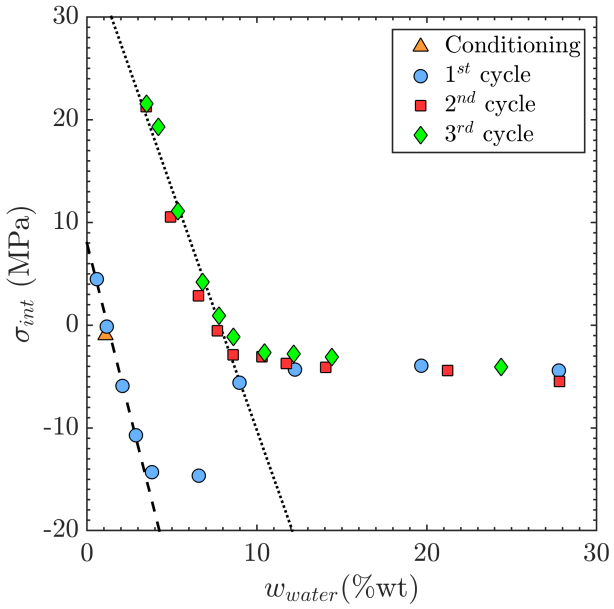

Figure 5.8 – Change in internal stresses plotted against water content for an unaged polyester resin film initially conditioned at RH_{cond} = 11 %RH and exposed to three sorption cycles. The dashed and dotted lines indicate the linear regression lines at low water contents for the first and subsequent humidity cycles, respectively. A slope of -6.8 10^2 MPa (R^2 = 0.995) and -4.6 10^2 MPa (R^2 = 0.92) are estimated, respectively.

While the first isotherm is similar to that observed in the previous section, a large stress hysteresis appears between the first and second sorption cycles. This hysteresis is absent during subsequent cycles as shown by the overlap of the second and third isotherms. The three isotherms all exhibit an initial build-up of hygroscopic stresses upon moist exposure followed by a relaxation of these stresses above 10 %wt. Internal stresses are however more tensile during the second and third sorption cycles. This hysteresis disappears above 10 %wt as internal stresses are relaxed in the layer. Interestingly, this behaviour bears close similarities with the hysteretic behaviour previously observed on sorption isotherms measured by DVS in Section 5.2. Note finally the slight decrease in the slope of the linear part after the first humidity cycle which

may be ascribed to a reduction in the polyester elastic modulus (see Equation 5.2).

These observations suggest that the polymer undergoes a microstructural reorganization after the first cycle which does not evolve during the subsequent cycles. Moreover, the stabilization of the properties after the second cycle implies that the material keeps a structural and chemical integrity and that water reacts only through hydrogen-bonding with the polyester resin. This is consistent with the reversibility of the plasticization phenomenon evidenced in Chapter 4.

5.4.2 A water-induced microstructural reorganization

Similarities with the influence of thermal history in glassy polymers The influence of hygric history on the polyester resin bears close similarities with the effect of thermal history on the development of internal stresses in glassy polymer coatings reported by Perera and Thurn [129, 130, 131]. In those studies, the coatings were initially conditioned at a temperature below their glass transition temperature and then exposed to successive temperature cycles which brought the materials through their glass transition. The differential thermal expansions between the two parts resulted in the development of thermal stresses whose dependence on temperature is schematically represented in Figure 5.9 for two successive cycles.

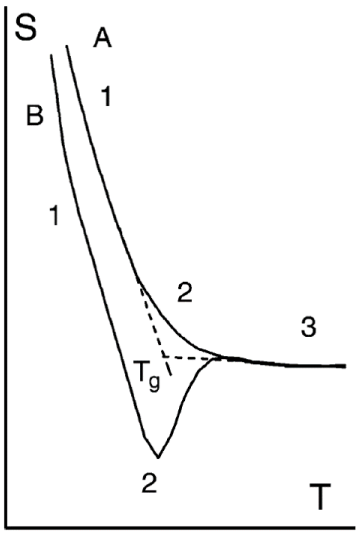

Figure 5.9 – Schematic representation of the evolution of the stress (S) with temperature (T) for a physically-aged glassy coating during the first (B) and second (A) thermal cycles. Curve segments 1, 2 and 3 represent the glassy region, the glass transition region and the rubbery region, respectively. Adapted from Perera [128].

While the change in the stress–temperature slope at T_g stems from the transition from a glassy to a rubbery state, the hysteretic behaviour in the glassy region arises from the non-equilibrium nature of glasses and especially from the extent of physical ageing. As mentioned in Section 2.2.2.2, physical ageing is the (typically slow) relax-

ation process which brings a glassy material toward a lower energy state through the existence of local motions. The "U-type" shape of curve B in Figure 5.9 is characteristic of all physically-aged coatings as discussed in detail by Perera [129]. The hysteresis between the curves A and B, especially the lower level of tensile stresses in sample B, can be attributed mainly to the stress relaxation (ie. to the physical ageing process) occurring during the initial conditioning step.

Contrary to chemical ageing which results in irreversible changes, physical ageing is a reversible process which can be erased by heating the material above T_g for sufficient time. This is what happens between the first (B) and second (A) cycles in Figure 5.9. During ageing, the tensile stresses imparted into the coating during the curing step are gradually relaxed. By heating the coating above its T_g, the material shifts to its equilibrium rubbery state, erasing the memory of the previous relaxed state. By quickly cooling the system from above to below its T_g, the polymer chains are not allowed to reorganize in the same configuration as in the physically-aged polymer. As a consequence, the coating is quenched in a rejuvenated microstructure with a lower degree of relaxation. In the rejuvenated sample, the specific volume is larger, which results in a larger tendency to contraction for the material. As a consequence, larger tensile stresses are observed during the second cycle.

A material model to account for the influence of hygric history on resin properties The similarities with Perera's and Thurn's papers [129, 130, 131] suggest that the effect of a humidity change on the polyester resin microstructure is similar to the effect of a temperature change on the structural recovery of physically-aged glassy polymers. This is consistent with the existence of a water-triggered glass transition in our system.

Altogether, our results allow us proposing a microscopic scenario to explain the evolution of the polyester sorption properties, internal stresses development and mechanical response observed upon exposure to multiple humidity cycles. Upon exposure to moisture, the polyester resin undergoes a microstructural reorganization which can be divided into the following steps as illustrated in Figure 5.14:

- Just after resin preparation, a dense polymeric microstructure initially free of water molecules is formed. Because of the resin shrinkage upon curing, tensile stresses develop in the polymer layer.
- During the conditioning step at a relative humidity RH_{cond} below RH_g, water molecules slowly penetrate the dense polymeric network. Physical ageing simultaneously occurs through local molecular motions. Both phenomena contribute to the gradual reduction of the internal stresses in the polyester film during the conditioning period.
- During the first sorption cycle and for humidities lower than RH_g, the polyester

resin behaves as a physically-aged polymer glass in which the relaxation rate is governed by the local mobility of the chains and thus, by the extent of plasticization. At low water content, the dense packing and reduced mobility of the polymer chains result in slow diffusion kinetics. Moreover, the polymer relaxation rate is initially too slow so that hygroscopic swelling stresses can build up upon water sorption for the time scale considered.

- As the material gets closer to its glass transition, chain mobility increases with increasing water content. Plasticization speeds up the chains relaxation rate which in turn accelerates the water diffusion kinetics and the development of internal stresses in the coating.
- At the end of the first sorption cycle, the polyester resin is in a gel state in which all polar sites are accessible to water molecules. The enhanced chain mobility of the polymer chains results in large water sorption and fast diffusion kinetics. Above RH_g, the stresses imparted into the coating during the curing and conditioning steps are fully relaxed, erasing the material memory.
- Upon desorption, the material undergoes a gel-to-glass transition. Because of the rapid humidity adjustement, the chain conformations in the glassy state differ from their initial arrangements and some residual water remains trapped in the polymer. The network structure is thus quenched in a rejuvenated state characterized by a lower extent of structural relaxation, a larger free volume and the development of higher tensile stresses upon drying. Moreover, the residual water "irreversibly" plasticizes the polyester and will contribute, for instance, to the apparent decrease in yield stress when plotted as a function of relative humidity during the subsequent cycles (see Chapter 4).
- The lower extent of structural relaxation in the rejuvenated state results in the development of larger tensile stresses during the second sorption cycle. This is also accompanied by a faster diffusion of water, a higher water uptake and a slight reduction in the polymer elastic modulus because of the larger free volume and the plasticizing effect of residual water. Similarly to the first cycle, internal stresses are relaxed when a sufficient extent of plasticization is reached.
- During the third sorption cycle, the polymer follows the same configurational path as in the second cycle. As the material no longer undergoes any irreversible structural change, the responses of the second and third cycles are identical.

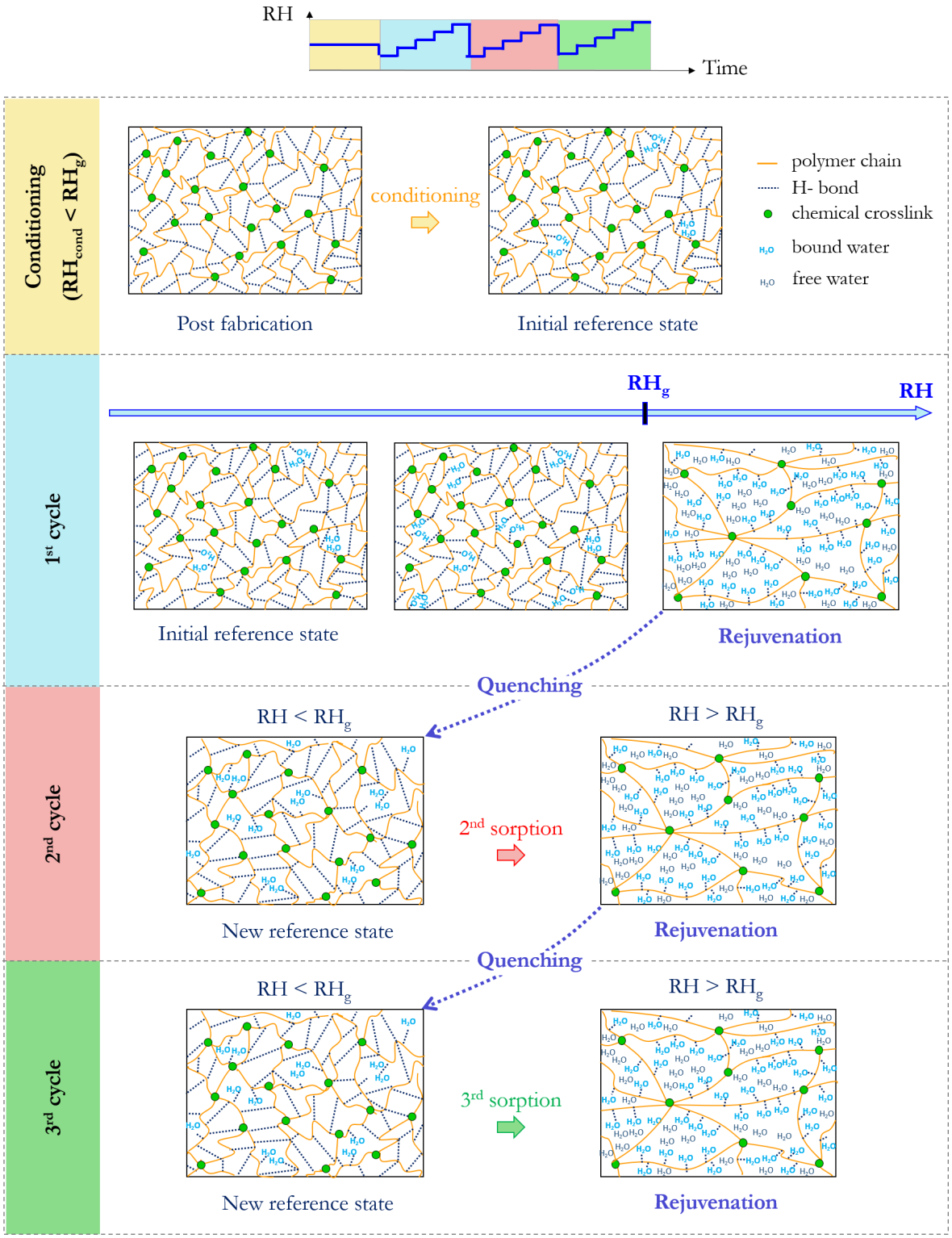

Figure 5.10 – Schematic illustration of the microstructural reorganization of an unaged polyester resin film initially conditioned at RH_{cond} below RH_g and subsequently exposed to three sorption cycles.

5.4.3 A methodology to compare polyester samples independently of hygric history

Because of its glassy nature below RH_g, we showed that the polyester response is not only defined by its water content but also by its hygric history. In this study, a rejuvenation-quenching protocole is applied with a view to decorrelating the effects of physical ageing and residual bound water from the effect of irreversible damage induced by chemical ageing.

The rejuvenation-quenching protocole The effect of physical ageing and hygric history are countered by applying a rejuvenation treatment. The material is exposed to a humidity larger than RH_g for an extended period of time in order to eliminate the effects imparted by physical ageing, moist exposure and preparation process (first cycle). The material is then quenched in a new reference state by abruptly decreasing humidity below RH_g. The resin characterization is then carried out on this new reference state (second cycle).

Illustration with the influence of the conditioning humidity on internal stress isotherms The validity of this protocole is illustrated by comparing three pristine polyester coatings initially conditioned at different relative humidities. Three conditioning humidities, RH_{cond}, are considered: 11 %RH and 40 %RH which are lower than RH_g and 85 %RH which is larger. After an initial 20 h-conditioning, the samples are exposed to two successive sorption cycles from which internal stress isotherms are deduced. The water content-internal stress isotherms are displayed in Figure 5.11. The associated relative humidity-internal stress isotherms can be found in Appendix A.4.

While the samples stored at humidities below RH_g display a hysteresis between the first and subsequent cycles, no hysteresis is observed for the sample initially conditioned above RH_g. All the isotherms collapse during the second cycles, namely for the rejuvenated samples, showing that the influence of the initial storage condition on the polyester response has been erased. The overlap of the first and second cycle responses for the sample stored above RH_g also confirms that no significant chemical ageing occurs at such time scales.

As a conclusion, a first humidity cycle through the glass transition must be initially performed in order to erase sample hygric history and physical ageing. The stabilization of the material properties after the second cycle confirms that the polyester resin does not undergo any significant chemical ageing for the environmental conditions considered.

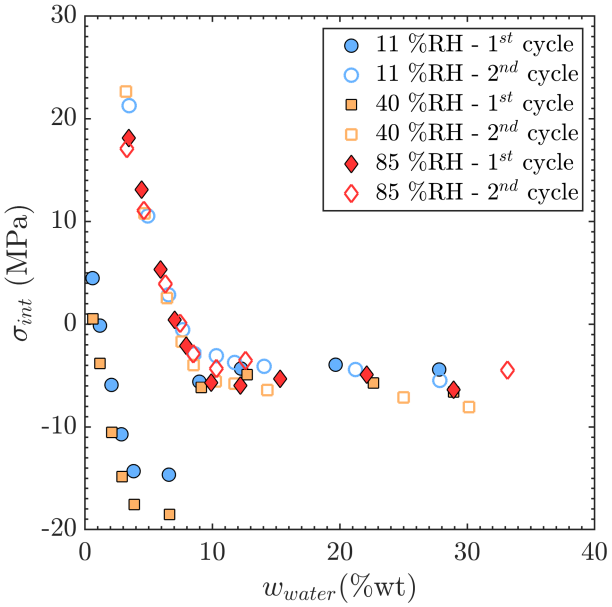

Figure 5.11 – Effect of the initial conditioning humidity, RH_{cond} on the internal stress isotherms of pristine polyester resin exposed to two successive sorption cycles after conditioning. Samples are conditioned for 20 h at three different relative humidities: 11 %RH, 40 %RH and 85 %RH.

5.5 A first insight into the effect of hygrothermal ageing on polyester mechanics

The impact of ageing under more elevated temperatures is investigated. Upon hygrothermal ageing, polyesters are known to undergo irreversible damage such as the hydrolysis of their ester bonds or the formation of cracks as a consequence of hygrothermal stresses [12, 96].

The effect of hygrothermal ageing on the polyester resin is investigated by storing polyester micro pillars at two relative humidities: a low humidity condition (11 %RH) and a high humidity condition (85 %RH). In contrast to the previous section, ageing of specimens is carried out for 1 month at 35 °C at each relative humidity. The mechanical response of the aged pillars is compared with that of an unaged material using micro pillar compression. Briefly, the compressive behaviour is recorded for two successive sorption cycles at ambient temperature with the same cycling conditions as those used in Chapter 4. With the first humidity cycle, the effects of hygrothermal history and physical ageing are erased. The sample mechanical responses are thus compared during the second sorption cycle. The associated true stress-strain curves are shown in Figure 5.12 while the relative humidity-yield stress curves can be found in Figure 5.13.

While the unaged and 11 %RH-aged samples display similar mechanical response, the sample aged at 85 %RH is significantly impacted by the ageing protocole. In Figure 5.12.c, the yield stress increases but the flow stress (plateau) decreases and less (no) strain hardening is observed. Moreover, in Figure 5.13, the specimen aged

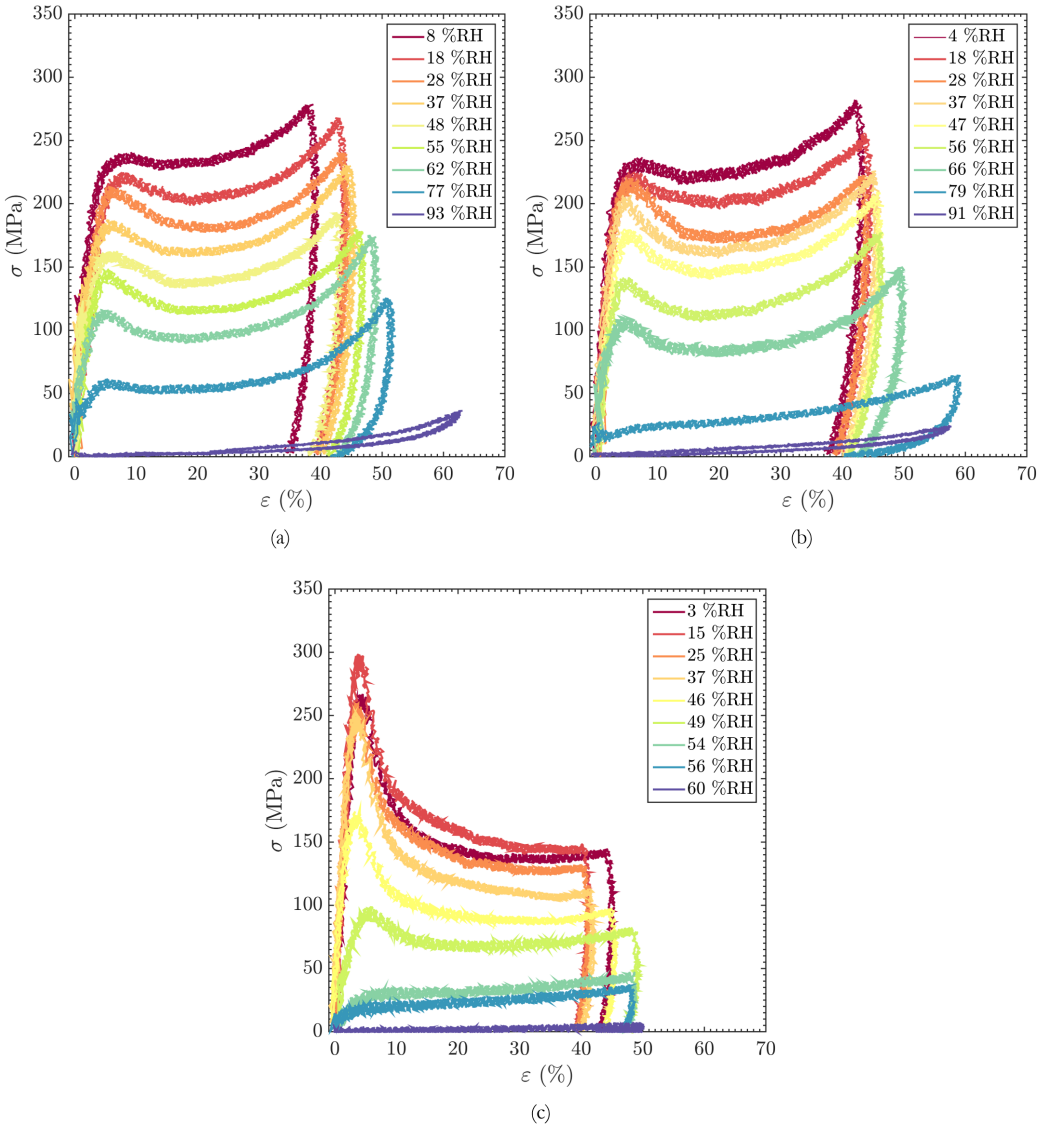

Figure 5.12 – Influence of hygrothermal ageing on the compressive response of polyester micro pillars. The mechanical response of (a) pristine polyester resin is compared to the responses of polyester samples aged (b) at 11 %RH and (c) at 85 %RH for 1 month at 35 °C. Only the curves measured during the second humidity cycle are displayed (i.e., after erasure of hygric history and physical ageing).

at 85 %RH exhibits a slight increase in its yield stress in the glassy regime coupled to a large decrease in its critical relative humidity RH_g. RH_g drops from 80 %RH to 60 %RH. These observations reveal a change in the polymer microstructure. While the suppression of strain hardening could be ascribed to the presence of shorter polymer chains, the reduction in RH_g highlights the existence of irreversible damage in the polyester resin. Both phenomena could be ascribed to hydrolysis [12, 87], especially to a reduction in the network crosslinking density [34]. This rearrangement of the polymer structure is obviously also slightly more resistant to shear, as evidenced by the increase in yield stress. It would be interesting to measure the Young's modulus in the glassy phase for a better assessment of the modifications of the polymer structure.

Additional investigations should be conducted to determine the nature of this degradation and the evolution of the macromolecular structure upon ageing. More specifically, the elastic modulus in the gel regime could indirectly reveal the evolution of the chemical crosslinking density upon ageing. However, the aged polyester micro fibers have been found to become too brittle to be tested using the tensile testing method.

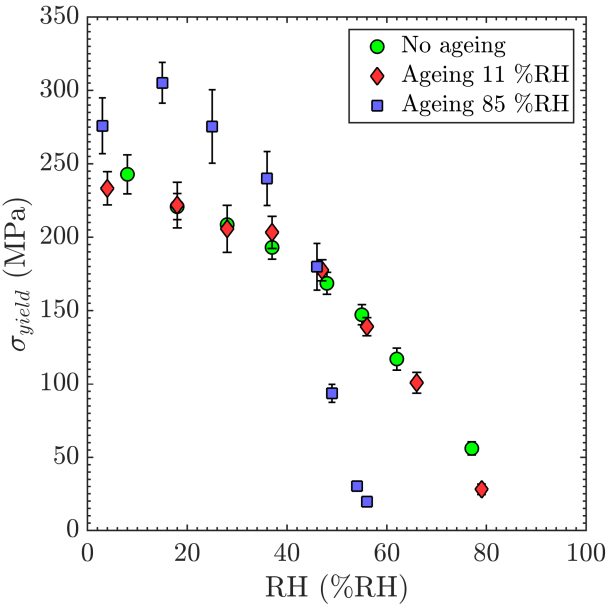

Figure 5.13 – Effect of hygrothermal ageing on the dependence of yield stress with relative humidity for the polyester resin. Three samples are compared: an unaged sample, a sample aged for 1 month at 11 %RH and 35 °C and a sample aged for 1 month at 85 %RH and 35 °C. The properties are compared during the second sorption cycle after the effect of hygric history and physical ageing have been erased.

5.6 Conclusion

In this chapter, we have demonstrated the influence of hygric history on the microstructure and properties of unaged polyester resin. When exposed to successive humidity cycles, an hysteresis appeared between the first and second sorption cycles but this hysteretic behaviour disappeared during the subsequent cycles. While the chemical ageing assumption was discarded due to the stabilization of material properties after the second cycle, the first cycle hysteresis was ascribed to the presence of residual bound water and to the microstructural reorganization of the glassy state.

The evolution of the polymer microstructure was first evidenced by the change in water diffusion kinetics and then confirmed by recording the development of internal stresses in the resin layer exposed to multiple humidity cycles. Internal stress isotherms were measured on a home-made setup which allowed long-term measurement at controlled relative humidities. In the glassy state, relaxation rates were sufficiently slow to allow hygroscopic stresses to build up upon water sorption. These stresses were relaxed above 60 %RH due to the gradual increase in chain mobility with plasticization and the transition of the polymer toward a gel state.

In the glassy region, the level of internal stresses was directly related to the extent of microstructural relaxation. During the first cycle, the dense polymer network obtained after fabrication and subsequent conditioning at low humidity behaved as physically-aged polymers. The rejuvenation of the resin above RH_g at the end of the first cycle followed by a rapid quenching below RH_g brought the system toward a new reference state characterized by a lower extent of relaxation and a larger free volume. As a consequence, larger internal tensile stresses developed in the glassy region during the second humidity cycle. By erasing the hygric history and physical ageing with this rejuvenation sequence, we could compare samples independently of the degree of structural relaxation and hygric history. Altogether, these results showed that the effect of a change of relative humidity in the polyester resin has an effect similar to that of a temperature change on physical ageing and structural recovery in standard glassy polymers.

While the previous phenomena observed did not alter the chemical structure of the polymer, irreversible damage were highlighted on polyester micro pillars subjected to long-term hygrothermal ageing (85 %RH - 35 °C - 1 month). This degradation resulted in a significant modification of the polymer structure, with reduced flow stress, a suppression of strain hardening and a reduction of the polyester glass transition relative humidity RH_g down to 60 %RH and in a slight increase in the yield stress in the glassy region. At the same time, a slight increase of the yield stress has been found, which results in significant strain softening right after yield. The exact nature of the polymer network rearrangement has not been established, but these results seem consistent with a reduction of chain length through hydrolysis.

Take-home messages

- The physical properties of the polyester resin, especially its mechanical, structural and sorption properties, are not only defined by its water content but also by its hygric history.
- Water content-internal stress isotherms are a simple way to study the microstructural reorganization and relaxation events taking place in the polyester resin when exposed to multiple humidity cycles.
- The effect of a change in humidity on the polyester microstructure is similar to the effect of a change in temperature on the microstructure of standard glassy polymers. Especially:
  - When exposed to humidities exceeding RH_g, the polyester resin is rejuvenated and sample memory erased
  - When dried abruptly below RH_g, the polyester microstructure is quenched with a lower extent of relaxation and higher free volume
- To decorrelate the reversible and irreversible effect of humidity, a rejuvenation sequence must be carried out before characterization in order to erase the sample hygric history.
- When subjected to long-term hygrothermal ageing under high humidity conditions (1 month - 85 %RH - 35 °C), the polyester resin undergoes an irreversible reduction in its RH_g which may shed light on the existence of chemical ageing.

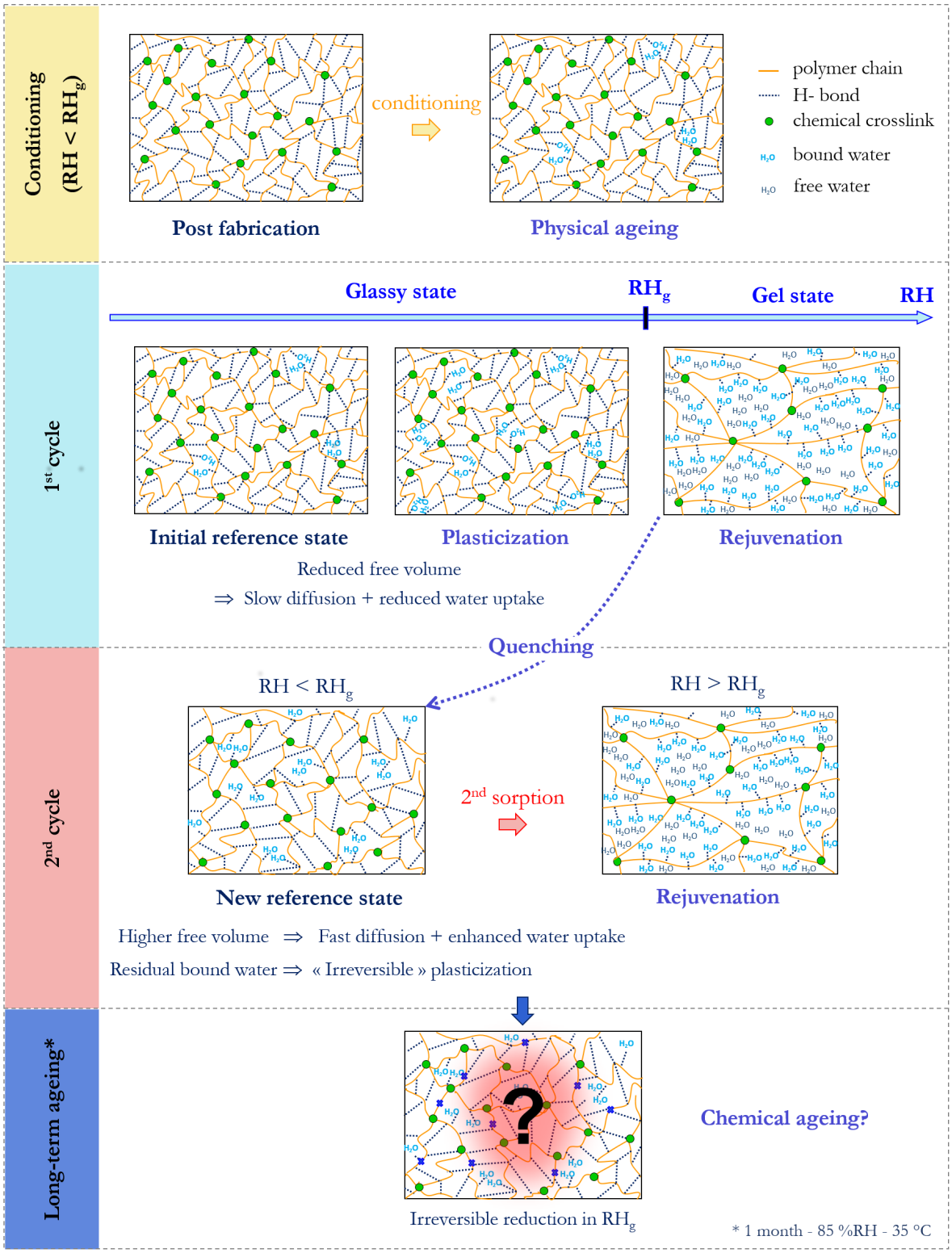

Figure 5.14 – Schematic summary of the influence of hygric history on the microstructure of an unaged polyester film initially conditioned below RH_g and subsequently exposed to two sorption cycles (short-term exposure) and hygrothermal ageing (long-term exposure).

Chapter 6

Conclusion and perspectives

The main purpose of this study was to understand how water affects the mechanical behaviour of model polyester thermosetting resins whose monomers are derived from renewable feedstock. Through experimental characterization, we studied in great detail the influence of humidity on the mechanical and structural properties of a model bio-based polyester resin and tried to identify the water-triggered mechanisms driving the variation in these properties.

Material characterization was mainly impeded by the resin foamability coupled to fast polymerization during processing which prevented the fabrication and characterization of macroscopic samples under technologically relevant conditions. We successfully developed an original micro molding process (Section 3.3) to prepare void-free polyester samples with micrometric sizes and in various controlled geometries (thin films, micro-patterned layers and free-standing specimens). The mechanical properties of these micro samples were then investigated using three micro mechanical characterization techniques: tensile testing of polymeric micro fibers (Section 3.5), micro compression of polymeric micro pillars (Section 3.4) and curvature measurement of supported thin films to evaluate the internal stress that had developed in the polymeric film (Section 5.3). Home-made setups were developed in order to perform mechanical testing at controlled relative humidities for durations ranging from 1 hour up to several days.

We first studied the influence of humidity on the mechanical response of pristine polyester (Chapter 4). Because of its large hydrophilicity which was attributed to the presence of unreacted polar groups (Section 4.2), the compressive and tensile mechanical properties of the polyester resin are highly sensitive to humidity (Section 4.3). Upon water sorption, the polymer undergoes a water-triggered glass transition between a glassy and a gel state at a threshold relative humidity, RH_g of approximatively 80 %RH. More precisely, we identified three mechanical regimes for the polyester resin as a function of humidity: a) below 30 %RH, a regime where the increase in fracture

strength may shed light on a water-induced healing of some critical defects (Section 4.4.2), b) between 30 %RH and 80 %RH, a plasticization regime where sorbed water reversibly screens the physical interactions between glassy polymer chains and gradually facilitates rearrangements, leading to a reduction in yield stress and fracture strength (Section 4.4.1) and c) above 80 %RH, a gel regime where the polymer behaves as a loosely crosslinked polymer (Section 4.4.3). We confirmed that after a first water-induced rejuvenation, all these processes are reversible and do not alter the chemical integrity of the network at the time scale considered (less than a day).

The sensitivity to humidity of the mechanical properties indirectly provided a better understanding of the macromolecular structure of the model resin. Especially, the polyester was found to be not as highly chemically crosslinked as standard thermosetting resins (Section 2.2). Below RH_g, its glassy behaviour is mainly driven by the large number of physical crosslinks (hydrogen bonds) formed between the residual polar groups. The comparison with a standard phenol formaldehyde resin with similar hygroscopy confirmed that the water-triggered glass transition of the polyester resin is an unusual behaviour in standard thermosetting resins (Section 4.5).

The behaviour of pristine polyester being more clearly understood, the next question was: how does the mechanical response evolve upon hygrothermal ageing, i.e., upon long-term exposure to humidity? We first investigated the influence of hygric history on the polyester microstructure by exposing pristine samples to multiple humidity cycles (Chapter 5). The extent of microstructural relaxation in resin thin films was indirectly studied using an original approach based on the internal stresses developing in thin polymer films upon water sorption (Section 5.4.1). We showed that the effect of a relative humidity change on the polyester microstructure is similar to that of a temperature change on the microstructure of physically-aged polymer glasses. The rejuvenation of the resin above RH_g followed by a rapid quenching below RH_g brings the system toward a new reference state characterized by a lower extent of relaxation and higher free volume without altering its chemical structure (Section 5.4.2). Moreover, since this rejuvenation-quenching sequence erases the hygric history, we can compare samples independently of the degree of structural relaxation and thus, decorrelating the reversible and irreversible effects of water on the resin properties (Section 5.4.3).

Finally, we considered the effect of long-term hygrothermal ageing on the durability of the polyester resin (Section 5.5). Ageing (1 month - 35 °C - 85 %RH) leads to an irreversible degradation of the resin mechanical properties, including a reduction of its glass transition relative humidity, RH_g down to 60 %RH. Although the reduction of RH_g could be ascribed to hydrolysis of chemical crosslinks, the nature of this damage has not been identified yet.

*
* *

Our work provides a fundamental picture of the influence of humidity on the polyester mechanical and structural properties and of the associated water-induced mechanisms. There are several results which are of practical interest to Saint-Gobain.

The preparation and characterization techniques developed in this study will help Saint-Gobain screen the mechanical behaviour of the new bio-based resins currently under development. As explained in the introduction, one crucial point is to forecast the performance of the resin component over the product's lifecycle under natural ageing conditions. As a consequence, the mechanical characterization under humidity-controlled conditions is of high interest to optimize the resin formulation for future industrial applications. The micrometric approach developed in this work is especially suitable since in micrometer-size samples homogeneous water diffusion is much faster than in standard macroscopic samples.

*
* *

To further understand the polyester resin behaviour, several points of our study could be investigated in future works.

First concerning the mechanical characterization of the polyester resin, additional loading conditions have been considered such as dynamic loading, stress relaxation and creep tests. Such loadings are of high interest since they are representative of the mechanical load encountered during the product's service life. However, these tests have not been implemented because of time limitations.

A preliminary work has shown that hygrothermal ageing may be detrimental for resin durability. It would be interesting, and certainly fruitful, to study more deeply the influence of hygrothermal ageing on the model polyester resin under various ageing conditions. This study should help understand the mechanisms responsible for the degradation of the mechanical properties with the goal to identifying sources of improvement (curing conditions, nature of the monomers, addition of hydrophobic additives...).

Finally, although indirect conclusions have been derived from the mechanical characterization, it is crucial to have a better knowledge of the polyester chemical structure, including the density of physical and chemical crosslinks, in order to fully understand the impact of water on the mechanical properties. The chemical structure of the polymer cannot be inferred from simple chemical reaction mechanism since the nature of the bio-based monomers is poorly characterized and that multiple side reactions occur in addition to esterification. In parallel with this study, the chemical reaction

pathways have been the subject of a PhD thesis [146] which confirmed the extreme complexity of the chemistry of the model bio-based resins. Further work is under way at Saint-Gobain.

Appendix A

Estimation of the water content in polymers

After a presentation of the DVS procedures carried out to estimate the water content in samples upon mechanical testing, this appendix gathers the following results: three successive sorption-desorption isotherms of pristine polyester micro pillars (Chapter 4), the evolution of the water diffusion kinetics in pristine polyester subjected to two successive sorption/desorption cycles (Chapter 5) and the internal stress isotherms plotted as a function of relative humidity (Chapter 5).

A.1 DVS protocol

DVS procedures are carried out in order to reproduce the humidity conditions under which the resin micro samples are mechanically characterized. This allows estimating the water content in polymer, w_{water} corresponding to a given relative humidity, RH. The following DVS procedures have been considered:

- **Protocol A:** three successive sorption cycles with a 75 min-stabilization at each humidity step are conducted on a micro-patterned resin film (about 6 mg) coated on glass substrate in order to relate the variation in compressive properties to the polymer water content.
- **Protocol B:** after an initial 20 h-conditioning at RH_{cond}, three successive sorption cycles with a 270 min-stabilization at each humidity step are conducted on a resin thin film (about 6 mg) coated on glass substrate in order to relate the variation in internal stresses to the polymer water content.

A.2 Sorption/desorption isotherms - Protocol A

The isotherms reproducing the humidity conditions used in Section 4.4.1 are displayed in Figure A.1.

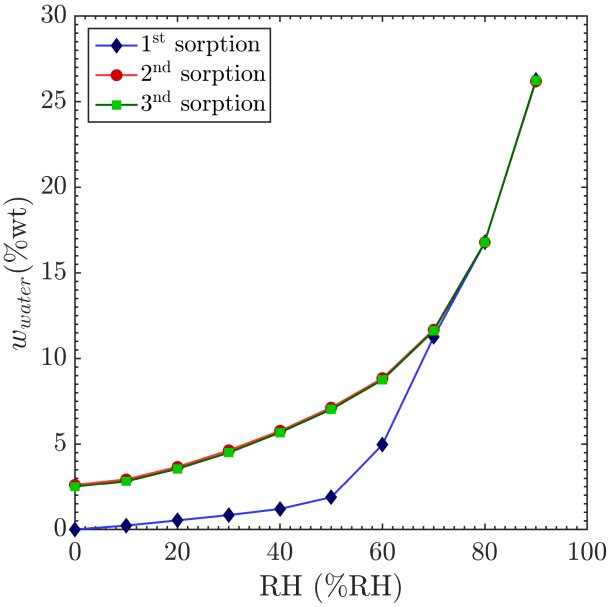

Figure A.1 – Sorption and desorption isotherms (protocol A) of a micro-patterned thin film made of pristine polyester subjected to three successive humidity cycles.

From the second cycle, residual water remains in the material and cannot be fully dried between two successive cycles with the drying conditions considered (75 min at 0 %RH). Interestingly, the sorption isotherms exhibit the same features as the relative humidity-yield stress curves shown in Chapter 4, namely a hysteresis between the first and subsequent cycles below 70 %RH and a stabilization for the subsequent cycles. The curves meet again above 70 %RH at which water contents equilibrate.

A.3 Water sorption/desorption kinetics in pristine polyester resin

Figure A.2 shows the temporal evolution of the water diffusion kinetics in pristine polyester micro fibers subjected to two successive sorption/desorption cycles using the humidity cycling conditions "at equilibrium". After the first sorption cycle, enhanced diffusion kinetics are observed due to the water-induced microstructural relaxation.

A.4 Sorption/desorption isotherms - Protocol B

The isotherms reproducing the humidity conditions used in Section 5.3.3, Section 5.4.1 and Section 5.4.3 are displayed in Figure A.3 while the relative humidity-internal stress isotherms are shown in Figure A.4.

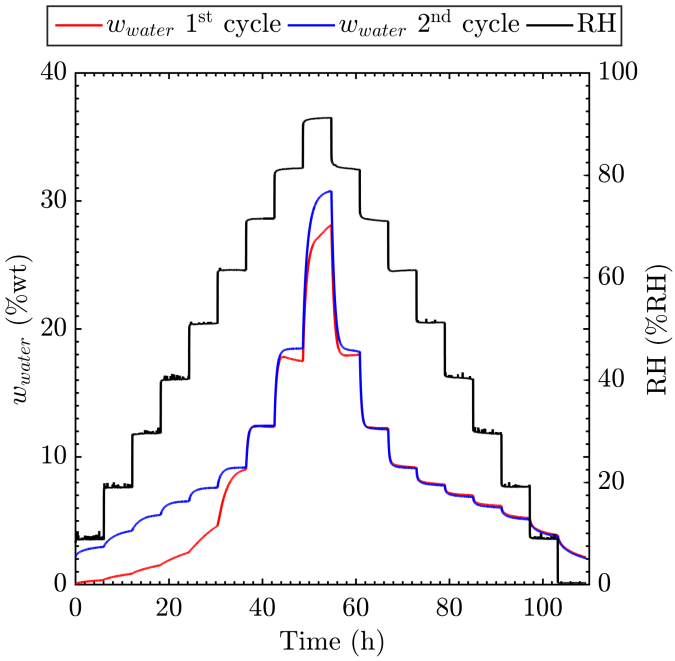

Figure A.2 – Temporal evolution of the weight fraction of water and relative humidity in the chamber for unaged polyester exposed to two successive sorption/desorption cycles. A faster diffusion of water is observed after the first sorption cycle.

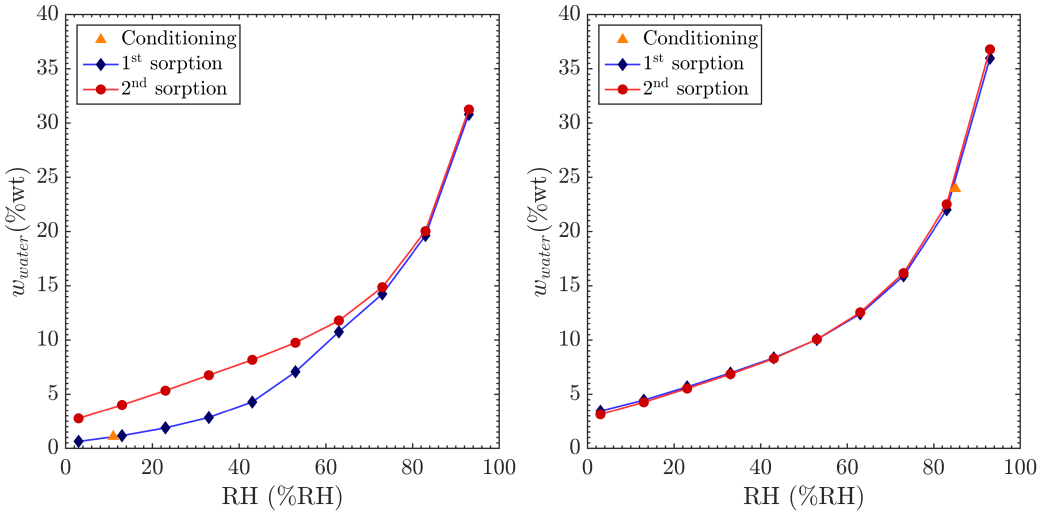

Figure A.3 – Sorption and desorption isotherms (protocol B) for thin films made of pristine polyester subjected to two successive humidity cycles after an initial 20 h-conditioning at RH_{cond}. Two values of RH_{cond} are considered: 11 %RH (left) and 85 %RH (right).

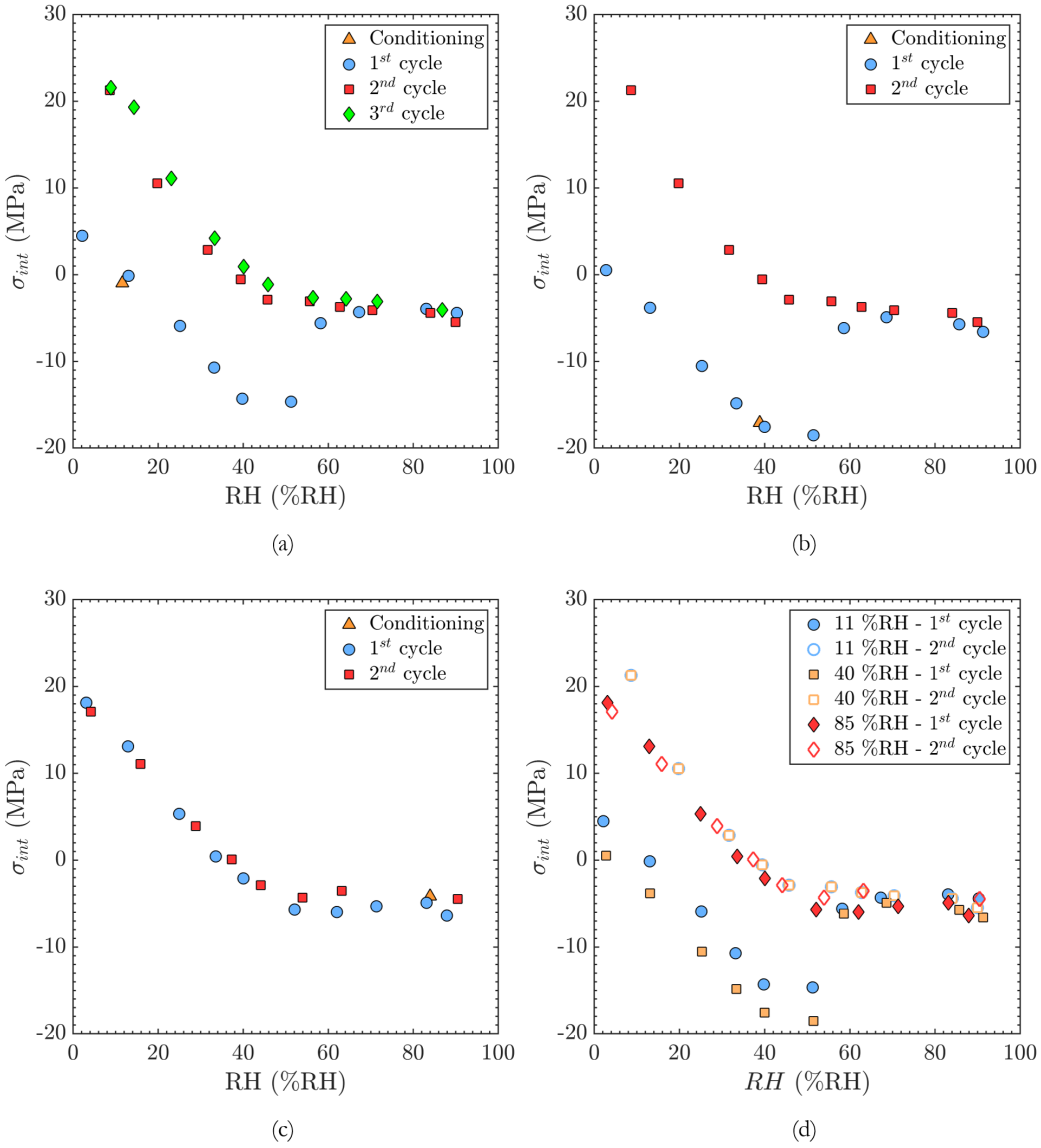

Figure A.4 – Relative humidity-internal stress isotherms of pristine polyester resin exposed to two successive sorption cycles after conditioning (three cycles for $RH_{cond} = 11$ %RH). Samples are conditioned for 20 h at three different relative humidities RH_{cond}: (a) 11 %RH, (b) 40 %RH and (c) 85 %RH. All curves are compared in Figure (d).

Appendix B

Humidity control setup description

Relative humidity in the mechanical testing chambers is controlled by mixing dry air (2 %RH) and water saturated air (95 %RH). A schematic of the setup is shown in Figure B.1. A pressurized ambient air flow is produced using an air pump. Dry flow is obtained by flowing ambient air through a column filled with dessicant salts (silica gel) while water vapour saturated flow is obtained by bubbling ambient air through deionized water. The relative humidity in the testing chamber is then controlled by mixing the two flows in varying amounts with two gas flow controllers. For compression and tensile testing, the flow rates are adjusted using manual mechanical flow valves (from KEY Instruments). For longer experiments such as internal stresses measurement, two automatic gas flow controllers (SLA5850 debimeter from Serv'Instrumentation) are used. In that case, gas flows are directly controlled with the software provided by the manufacturer. The relative humidity in the testing cell is simultaneously recorded with a humidity sensor (HC2-C04 humidity probe from Rotronic).

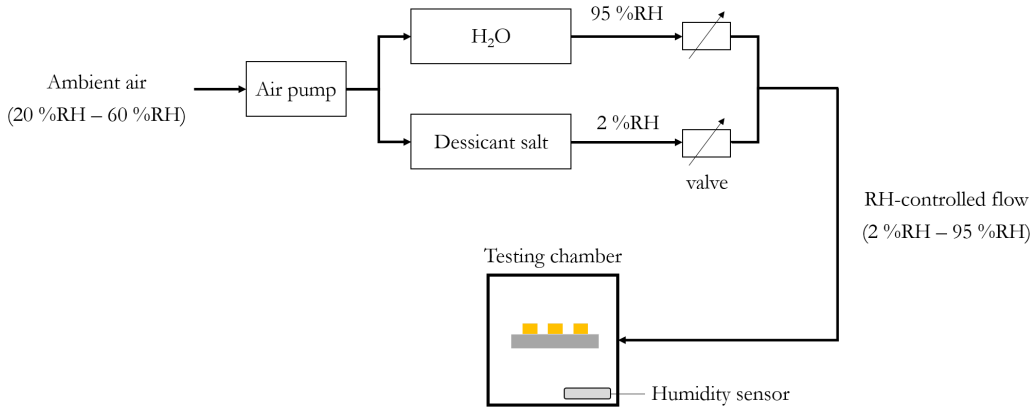

Figure B.1 – Schematic of the relative humidity control setup.

Bibliography

[1] Mark J Mendell. Indoor residential chemical emissions as risk factors for respiratory and allergic effects in children: a review. *Indoor air*, 17(4):259–277, 2007.

[2] Fernando Pacheco-Torgal, Said Jalali, and Aleksandra Fucic. *Toxicity of building materials*. Elsevier, 2012.

[3] Chuck Yu and Derrick Crump. A review of the emission of vocs from polymeric materials used in buildings. *Building and Environment*, 33(6):357–374, 1998.

[4] HP Abeysinghe, W Edwards, G Pritchard, and GJ Swampillai. Degradation of crosslinked resins in water and electrolyte solutions. *Polymer*, 23(12):1785–1790, 1982.

[5] A Apicella, C Migliaresi, L Nicolais, L Iaccarino, and S Roccotelli. The water ageing of unsaturated polyester-based composites: influence of resin chemical structure. *Composites*, 14(4):387–392, 1983.

[6] M Bakar and F Djaider. Effect of plasticizers content on the mechanical properties of unsaturated polyester resin. *Journal of Thermoplastic Composite Materials*, 20(1):53–64, 2007.

[7] Hideto Tsuji. Hydrolytic degradation. *Poly (Lactic Acid) Synthesis, Structures, Properties, Processing, and Applications*, pages 343–381, 2010.

[8] William D Nix. Mechanical properties of thin films. *Metallurgical transactions A*, 20(11):2217, 1989.

[9] MA Haque and MTA Saif. A review of mems-based microscale and nanoscale tensile and bending testing. *Experimental mechanics*, 43(3):248–255, 2003.

[10] VT Srikar and SM Spearing. A critical review of microscale mechanical testing methods used in the design of microelectromechanical systems. *Experimental mechanics*, 43(3):238–247, 2003.

[11] Maria F Pantano, Horacio D Espinosa, and Leonardo Pagnotta. Mechanical characterization of materials at small length scales. *Journal of Mechanical Science and technology*, 26(2):545–561, 2012.

[12] X Colin and J Verdu. Humid ageing of organic matrix composites. In *Durability of composites in a marine environment*, pages 47–114. Springer, 2014.

[13] Jean-Pierre Pascault, Henry Sautereau, Jacques Verdu, and Roberto JJ Williams. *Thermosetting polymers*, volume 477. Marcel Dekker New York, 2002.

[14] MJ Mullins, D Liu, and H-J Sue. Mechanical properties of thermosets. In *Thermosets*, pages 28–61. Elsevier, 2012.

[15] Michel Biron. *Thermosets and composites: material selection, applications, manufacturing and cost analysis*. Elsevier, 2013.

[16] Robert Nobbs Haward. *The physics of glassy polymers*. Springer Science & Business Media, 2012.

[17] Xavier Morelle. *Mechanical characterization and physics-based modeling of highly-crosslinked epoxy resin*. PhD thesis, UCL-Université Catholique de Louvain, 2015.

[18] Anthony James Kinloch. *Fracture behaviour of polymers*. Springer Science & Business Media, 2013.

[19] RD Maksimov, EZ Plume, and JO Jansons. Comparative studies on the mechanical properties of a thermoset polymer in tension and compression. *Mechanics of Composite Materials*, 41(5):425–436, 2005.

[20] Robert S Hoy. Why is understanding glassy polymer mechanics so difficult? *Journal of Polymer Science Part B: Polymer Physics*, 49(14):979–984, 2011.

[21] James E Mark et al. *Physical properties of polymers handbook*, volume 1076. Springer, 2007.

[22] Wayne D Cook, Anthony E Mayr, and Graham H Edward. Yielding behaviour in model epoxy thermosets—ii. temperature dependence. *Polymer*, 39(16):3725–3733, 1998.

[23] J Richeton, S Ahzi, KS Vecchio, FC Jiang, and RR Adharapurapu. Influence of temperature and strain rate on the mechanical behavior of three amorphous polymers: characterization and modeling of the compressive yield stress. *International journal of solids and structures*, 43(7-8):2318–2335, 2006.

[24] AD Mulliken and MC Boyce. Mechanics of the rate-dependent elastic–plastic deformation of glassy polymers from low to high strain rates. *International journal of solids and structures*, 43(5):1331–1356, 2006.

[25] Pierre-Yves Le Gac, Mael Arhant, Maelenn Le Gall, and Peter Davies. Yield stress changes induced by water in polyamide 6: Characterization and modeling. *Polymer Degradation and Stability*, 137:272–280, 2017.

[26] Henry Eyring. Viscosity, plasticity, and diffusion as examples of absolute reaction rates. *The Journal of chemical physics*, 4(4):283–291, 1936.

[27] Richard E Robertson. Theory for the plasticity of glassy polymers. *The Journal of Chemical Physics*, 44(10):3950–3956, 1966.

[28] AS Argon. A theory for the low-temperature plastic deformation of glassy polymers. *Philosophical Magazine*, 28(4):839–865, 1973.

[29] HGH Van Melick, LE Govaert, and HEH Meijer. On the origin of strain hardening in glassy polymers. *Polymer*, 44(8):2493–2502, 2003.

[30] Robert S Hoy and Mark O Robbins. Strain hardening of polymer glasses: effect of entanglement density, temperature, and rate. *Journal of Polymer Science Part B: Polymer Physics*, 44(24):3487–3500, 2006.

[31] DJA Senden, JAW Van Dommelen, and LE Govaert. Strain hardening and its relation to bauschinger effects in oriented polymers. *Journal of Polymer Science Part B: Polymer Physics*, 48(13):1483–1494, 2010.

[32] Robert S Hoy and Mark O Robbins. Strain hardening in polymer glasses: limitations of network models. *Physical review letters*, 99(11):117801, 2007.

[33] Thomas Hobbiebrunken, Bodo Fiedler, Masaki Hojo, and Mototsugu Tanaka. Experimental determination of the true epoxy resin strength using micro-scaled specimens. *Composites Part A: Applied Science and Manufacturing*, 38(3):814–818, 2007.

[34] Jean Louis Halary, Françoise Lauprêtre, and Lucien Monnerie. *Polymer materials: macroscopic properties and molecular interpretations*. John Wiley & Sons, 2011.

[35] Lawrence E Nielsen. Cross-linking–effect on physical properties of polymers. *Journal of Macromolecular Science, Part C*, 3(1):69–103, 1969.

[36] Ananyo Bandyopadhyay, Pavan K Valavala, Thomas C Clancy, Kristopher E Wise, and Gregory M Odegard. Molecular modeling of crosslinked epoxy polymers: The effect of crosslink density on thermomechanical properties. *Polymer*, 52(11):2445–2452, 2011.

[37] Paul J Flory and John Rehner Jr. Statistical mechanics of cross-linked polymer networks i. rubberlike elasticity. *The journal of chemical physics*, 11(11):512–520, 1943.

[38] Masatsugu Ogata, Noriyuki Kinjo, and Tatsuo Kawata. Effects of crosslinking on physical properties of phenol–formaldehyde novolac cured epoxy resins. *Journal of applied polymer science*, 48(4):583–601, 1993.

[39] LCE Struik. *Physical aging in amorphous polymers and other materials*. PhD thesis, TU Delft, Delft University of Technology, 1977.

[40] John M Hutchinson. Physical aging of polymers. *Progress in Polymer Science*, 20(4):703–760, 1995.

[41] Angela V Cugini and Alan J Lesser. Aspects of physical aging, mechanical rejuvenation, and thermal annealing in a new copolyester. *Polymer Engineering & Science*, 55(8):1941–1950, 2015.

[42] HGH Van Melick, LE Govaert, B Raas, WJ Nauta, and HEH Meijer. Kinetics of ageing and re-embrittlement of mechanically rejuvenated polystyrene. *Polymer*, 44(4):1171–1179, 2003.

[43] George Wypych. *Handbook of plasticizers*. ChemTec Publishing, 2004.

[44] E Lee McKague Jr, Jack D Reynolds, and John E Halkias. Swelling and glass transition relations for epoxy matrix material in humid environments. *Journal of Applied Polymer Science*, 22(6):1643–1654, 1978.

[45] S Masoumi and H Valipour. Effects of moisture exposure on the crosslinked epoxy system: an atomistic study. *Modelling and Simulation in Materials Science and Engineering*, 24(3):035011, 2016.

[46] G Bouvet, S Cohendoz, X Feaugas, S Touzain, and S Mallarino. Microstructural reorganization in model epoxy network during cyclic hygrothermal ageing. *Polymer*, 122:1–11, 2017.

[47] Jiming Zhou and James P Lucas. Hygrothermal effects of epoxy resin. part i: the nature of water in epoxy. *Polymer*, 40(20):5505–5512, 1999.

[48] Maëva Bocqué, Coline Voirin, Vincent Lapinte, Sylvain Caillol, and Jean-Jacques Robin. Petro-based and bio-based plasticizers: Chemical structures to plasticizing properties. *Journal of Polymer Science Part A: Polymer Chemistry*, 54(1):11–33, 2016.

[49] Tizazu Mekonnen, Paolo Mussone, Hamdy Khalil, and David Bressler. Progress in bio-based plastics and plasticizing modifications. *Journal of Materials Chemistry A*, 1(43):13379–13398, 2013.

[50] G Dlubek, F Redmann, and R Krause-Rehberg. Humidity-induced plasticization and antiplasticization of polyamide 6: A positron lifetime study of the local free volume. *Journal of Applied Polymer Science*, 84(2):244–255, 2002.

[51] Emanuele Parodi, Gerrit WM Peters, and Leon E Govaert. Prediction of plasticity-controlled failure in polyamide 6: Influence of temperature and relative humidity. *Journal of Applied Polymer Science*, 135(11):45942, 2018.

[52] RM Hodge, TJ Bastow, GH Edward, GP Simon, and AJ Hill. Free volume and the mechanism of plasticization in water-swollen poly (vinyl alcohol). *Macromolecules*, 29(25):8137–8143, 1996.

[53] MV Konidari, KG Papadokostaki, and M Sanopoulou. Moisture-induced effects on the tensile mechanical properties and glass-transition temperature of poly (vinyl alcohol) films. *Journal of applied polymer science*, 120(6):3381–3386, 2011.

[54] Jiming Zhou and James P Lucas. Hygrothermal effects of epoxy resin. part ii: variations of glass transition temperature. *Polymer*, 40(20):5513–5522, 1999.

[55] A Apicella, R Tessieri, and C De Cataldis. Sorption modes of water in glassy epoxies. *Journal of Membrane Science*, 18:211–225, 1984.

[56] ZH Ping, QT Nguyen, SM Chen, JQ Zhou, and YD Ding. States of water in different hydrophilic polymers—dsc and ftir studies. *Polymer*, 42(20):8461–8467, 2001.

[57] Yurina Sekine and Tomoko Ikeda-Fukazawa. Structural changes of water in a hydrogel during dehydration. *The Journal of chemical physics*, 130(3):034501, 2009.

[58] S Cotugno, D Larobina, G Mensitieri, P Musto, and G Ragosta. A novel spectroscopic approach to investigate transport processes in polymers: the case of water–epoxy system. *Polymer*, 42(15):6431–6438, 2001.

[59] Susana Mali, Lyssasetsuko S Sakanaka, Fabio Yamashita, and MVE Grossmann. Water sorption and mechanical properties of cassava starch films and their relation to plasticizing effect. *Carbohydrate Polymers*, 60(3):283–289, 2005.

[60] YP Chang, PB Cheah, and CC Seow. Plasticizing—antiplasticizing effects of water on physical properties of tapioca starch films in the glassy state. *Journal of Food Science*, 65(3):445–451, 2000.

[61] Shuichi Ito, Masanori Hashimoto, Bakul Wadgaonkar, Nadia Svizero, Ricardo M Carvalho, Cynthia Yiu, Frederick A Rueggeberg, Stephen Foulger, Takashi Saito, Yoshihiro Nishitani, et al. Effects of resin hydrophilicity on water sorption and changes in modulus of elasticity. *Biomaterials*, 26(33):6449–6459, 2005.

[62] P Nogueira, C Ramirez, A Torres, MJ Abad, J Cano, J Lopez, I López-Bueno, and L Barral. Effect of water sorption on the structure and mechanical properties of an epoxy resin system. *Journal of Applied Polymer Science*, 80(1):71–80, 2001.

[63] Hongjiu Hu, Xiaolong Zhang, Yaolong He, Zhan-sheng Guo, Junqian Zhang, and Yicheng Song. Combined effect of relative humidity and temperature on dynamic viscoelastic properties and glass transition of poly (vinyl alcohol). *Journal of Applied Polymer Science*, 130(5):3161–3167, 2013.

[64] Masahiko Annaka, Toyoaki Matsuura, Shinji Maruoka, and Nahoko Ogata. Dehydration and vitrification of corneal gel. *Soft Matter*, 8(31):8157–8163, 2012.

[65] Muhammad Ilyas, Md Anamul Haque, Youfeng Yue, Takayuki Kurokawa, Tasuku Nakajima, Takayuki Nonoyama, and Jian Ping Gong. Water-triggered ductile–brittle transition of anisotropic lamellar hydrogels and effect of confinement on polymer dynamics. *Macromolecules*, 50(20):8169–8177, 2017.

[66] Louise Slade and Harry Levine. Glass transitions and water-food structure interactions. In *Advances in food and nutrition research*, volume 38, pages 103–269. Elsevier, 1995.

[67] Bruno C Hancock and George Zografi. The relationship between the glass transition temperature and the water content of amorphous pharmaceutical solids. *Pharmaceutical research*, 11(4):471–477, 1994.

[68] Ye Liu, Ying Li, Guang Yang, Xiaotong Zheng, and Shaobing Zhou. Multi-stimulus-responsive shape-memory polymer nanocomposite network cross-linked by cellulose nanocrystals. *ACS applied materials & interfaces*, 7(7):4118–4126, 2015.

[69] WM Huang, B Yang, Y Zhao, and Z Ding. Thermo-moisture responsive polyurethane shape-memory polymer and composites: a review. *Journal of materials chemistry*, 20(17):3367–3381, 2010.

[70] Li-Rong Bao, Albert F Yee, and Charles Y-C Lee. Moisture absorption and hygrothermal aging in a bismaleimide resin. *polymer*, 42(17):7327–7333, 2001.

[71] Dominique Champion, Camille Loupiac, Denise Simatos, Peter Lillford, and Philippe Cayot. Structural relaxation during drying and rehydration of food ma-

terials—the water effect and the origin of hysteresis. *Food biophysics*, 6(1):160–169, 2011.

[72] TC Wong and LJ Broutman. Moisture diffusion in epoxy resins part i. non-fickian sorption processes. *Polymer Engineering & Science*, 25(9):521–528, 1985.

[73] Eric M Davis, Matteo Minelli, Marco Giacinti Baschetti, and Yossef A Elabd. Non-fickian diffusion of water in polylactide. *Industrial & Engineering Chemistry Research*, 52(26):8664–8673, 2012.

[74] T Cui, P Verberne, and SA Meguid. Characterization and atomistic modeling of the effect of water absorption on the mechanical properties of thermoset polymers. *Acta Mechanica*, 229(2):745–761, 2018.

[75] YP Chang, A Abd Karim, and CC Seow. Interactive plasticizing–antiplasticizing effects of water and glycerol on the tensile properties of tapioca starch films. *Food Hydrocolloids*, 20(1):1–8, 2006.

[76] CC Seow, PB Cheah, and YP Chang. Antiplasticization by water in reduced-moisture food systems. *Journal of food science*, 64(4):576–581, 1999.

[77] Paola Pittia and Giampiero Sacchetti. Antiplasticization effect of water in amorphous foods. a review. *Food Chemistry*, 106(4):1417–1427, 2008.

[78] WJ Jackson Jr and JR Caldwell. Antiplasticization. ii. characteristics of antiplasticizers. *Journal of Applied Polymer Science*, 11(2):211–226, 1967.

[79] D Lourdin, H Bizot, and P Colonna. "antiplasticization" in starch-glycerol films? *Journal of Applied Polymer Science*, 63(8):1047–1053, 1997.

[80] Yachuan Zhang and JH Han. Crystallization of high-amylose starch by the addition of plasticizers at low and intermediate concentrations. *Journal of food science*, 75(1):N8–N16, 2010.

[81] Kevin J Calzia, Anne Forcum, and Alan J Lesser. Comparing reinforcement strategies for epoxy networks using reactive and non-reactive fortifiers. *Journal of applied polymer science*, 102(5):4606–4615, 2006.

[82] JS Vrentas, JL Duda, and HC Ling. Antiplasticization and volumetric behavior in glassy polymers. *Macromolecules*, 21(5):1470–1475, 1988.

[83] Mina Roussenova, Mathieu Murith, Ashraf Alam, and Job Ubbink. Plasticization, antiplasticization, and molecular packing in amorphous carbohydrate-glycerol matrices. *Biomacromolecules*, 11(12):3237–3247, 2010.

[84] I Ghorbel and D Valentin. Hydrothermal effects on the physico-chemical properties of pure and glass fiber reinforced polyester and vinylester resins. *Polymer Composites*, 14(4):324–334, 1993.

[85] Maria Partini and Roberto Pantani. Ftir analysis of hydrolysis in aliphatic polyesters. *Polymer degradation and stability*, 92(8):1491–1497, 2007.

[86] Pierre-Yves Le Gac and Bruno Fayolle. Impact of fillers (short glass fibers and rubber) on the hydrolysis-induced embrittlement of polyamide 6.6. *Composites Part B: Engineering*, 153:256–263, 2018.

[87] GZ Xiao and MER Shanahan. Irreversible effects of hygrothermal aging on dgeba/dda epoxy resin. *Journal of applied polymer science*, 69(2):363–369, 1998.

[88] Dieter Kockott. Natural and artificial weathering of polymers. *Polymer Degradation and Stability*, 25(2-4):181–208, 1989.

[89] Spiros Zervos and *Σπυρίδων Γ* Ζερβός. Natural and accelerated ageing of cellulose and paper. 2015.

[90] Jacques Verdu. *Action de l'eau sur les plastiques.* Ed. Techniques Ingénieur, 2000.

[91] Hee-Soo Kim and Hyun-Joong Kim. Enhanced hydrolysis resistance of biodegradable polymers and bio-composites. *Polymer Degradation and Stability*, 93(8):1544–1553, 2008.

[92] E Kollia, Th Loutas, E Fiamegkou, A Vavouliotis, and V Kostopoulos. Degradation behavior of glass fiber reinforced cyanate ester composites under hydrothermal ageing. *Polymer Degradation and Stability*, 121:200–207, 2015.

[93] Timothy P Ferguson and Jianmin Qu. Elastic modulus variation due to moisture absorption and permanent changes upon redrying in an epoxy based underfill. *IEEE Transactions on Components and Packaging Technologies*, 29(1):105–111, 2006.

[94] A Boubakri, K Elleuch, N Guermazi, and HF Ayedi. Investigations on hygrothermal aging of thermoplastic polyurethane material. *Materials & Design*, 30(10):3958–3965, 2009.

[95] KHG Ashbee, Frederick Charles Frank, and RC Wyatt. Water damage in polyester resins. *Proceedings of the Royal Society of London. Series A. Mathematical and Physical Sciences*, 300(1463):415–419, 1967.

[96] L Gautier, B Mortaigne, V Bellenger, and J Verdu. Osmotic cracking nucleation in hydrothermal-aged polyester matrix. *Polymer*, 41(7):2481–2490, 2000.

[97] MH Shirangi and B Michel. Mechanism of moisture diffusion, hygroscopic swelling, and adhesion degradation in epoxy molding compounds. In *Moisture sensitivity of plastic packages of IC Devices*, pages 29–69. Springer, 2010.

[98] Friederike von Burkersroda, Luise Schedl, and Achim Göpferich. Why degradable polymers undergo surface erosion or bulk erosion. *Biomaterials*, 23(21):4221–4231, 2002.

[99] M Anders, J Lo, T Centea, and SR Nutt. Eliminating volatile-induced surface porosity during resin transfer molding of a benzoxazine/epoxy blend. *Composites Part A: Applied Science and Manufacturing*, 84:442–454, 2016.

[100] J Lo, M Anders, T Centea, and SR Nutt. The effect of process parameters on volatile release for a benzoxazine–epoxy rtm resin. *Composites Part A: Applied Science and Manufacturing*, 84:326–335, 2016.

[101] Cédric Pupin, Annie Ross, Charles Dubois, Jean-Christophe Rietsch, Nicolas Vernet, and Edu Ruiz. Formation and suppression of volatile-induced porosities in an rtm epoxy resin. *Composites Part A: Applied Science and Manufacturing*, 94:146–157, 2017.

[102] Technical report sgr/pcrs – ms/sr – n°0239/13. Technical report, Saint-Gobain Recherche.

[103] Morten Bo Mikkelsen, Alban A Letailleur, Elin Søndergård, Etienne Barthel, Jérémie Teisseire, Rodolphe Marie, and Anders Kristensen. All-silica nanofluidic devices for dna-analysis fabricated by imprint of sol–gel silica with silicon stamp. *Lab on a Chip*, 12(2):262–267, 2012.

[104] Younan Xia and George M Whitesides. Soft lithography. *Angewandte Chemie International Edition*, 37(5):550–575, 1998.

[105] J Cooper McDonald, David C Duffy, Janelle R Anderson, Daniel T Chiu, Hongkai Wu, Olivier JA Schueller, and George M Whitesides. Fabrication of microfluidic systems in poly (dimethylsiloxane). *ELECTROPHORESIS: An International Journal*, 21(1):27–40, 2000.

[106] TC Merkel, VI Bondar, K Nagai, BD Freeman, and I Pinnau. Gas sorption, diffusion, and permeation in poly (dimethylsiloxane). *Journal of Polymer Science Part B: Polymer Physics*, 38(3):415–434, 2000.

[107] Aránzazu del Campo and Christian Greiner. Su-8: a photoresist for high-aspect-ratio and 3d submicron lithography. *Journal of micromechanics and microengineering*, 17(6):R81, 2007.

[108] Paul Elzière. *Laminated glass: dynamic rupture of adhesion.* PhD thesis, Université Pierre et Marie Curie-Paris VI, 2016.

[109] Hyunsik Yoon, Hyemin Lee, and Won Bo Lee. Toward residual-layer-free nanoimprint lithography in large-area fabrication. *Korea-Australia Rheology Journal*, 26(1):39–48, 2014.

[110] Michael D Uchic and Dennis M Dimiduk. A methodology to investigate size scale effects in crystalline plasticity using uniaxial compression testing. *Materials Science and Engineering: A*, 400:268–278, 2005.

[111] Hongbin Bei, Sanghoon Shim, Easo P George, Michael K Miller, EG Herbert, and George Mathews Pharr. Compressive strengths of molybdenum alloy micropillars prepared using a new technique. *Scripta Materialia*, 57(5):397–400, 2007.

[112] Rémi Lacroix, Vincent Chomienne, Guillaume Kermouche, Jérémie Teisseire, Etienne Barthel, and Samuel Queste. Micropillar testing of amorphous silica. *International Journal of Applied Glass Science*, 3(1):36–43, 2012.

[113] G Kermouche, G Guillonneau, J Michler, J Teisseire, and E Barthel. Perfectly plastic flow in silica glass. *Acta Materialia*, 114:146–153, 2016.

[114] S Wang, Y Yang, LM Zhou, and Y-W Mai. Size effect in microcompression of epoxy micropillars. *Journal of materials science*, 47(16):6047–6055, 2012.

[115] Sandipan Chattaraj, Prita Pant, Dnyanesh N Pawaskar, and Hemant Nanavati. How many network chains of a densely crosslinked glassy thermoset deform cooperatively at yield? *Polymer*, 82:305–318, 2016.

[116] Tingge Xu, Jun Hyeon Yoo, Sachin Babu, Samit Roy, Jeong-Bong Lee, and Hongbing Lu. Characterization of the mechanical behavior of su-8 at microscale by viscoelastic analysis. *Journal of Micromechanics and Microengineering*, 26(10):105001, 2016.

[117] Thimmappa Shetty Guruprasad, Shantanu Bhattacharya, and Sumit Basu. Size effect in microcompression of polystyrene micropillars. *Polymer*, 98:118–128, 2016.

[118] Anthony E Mayr, Wayne D Cook, and Graham H Edward. Yielding behaviour in model epoxy thermosets—i. effect of strain rate and composition. *Polymer*, 39(16):3719–3724, 1998.

[119] Ph Colomban, JM Herrera Ramirez, Raphaël Paquin, Alba Marcellan, and A Bunsell. Micro-raman study of the fatigue and fracture behaviour of single pa66 fibres: Comparison with single pet and pp fibres. *Engineering fracture mechanics*, 73(16):2463–2475, 2006.

[120] EPS Tan, SY Ng, and CT Lim. Tensile testing of a single ultrafine polymeric fiber. *Biomaterials*, 26(13):1453–1456, 2005.

[121] Christophe Malhaire, Cédric Seguineau, Michel Ignat, Charles Josserond, Laurent Debove, Sebastiano Brida, Jean-Michel Desmarres, and Xavier Lafontan. Experimental setup and realization of thin film specimens for microtensile tests. *Review of Scientific Instruments*, 80(2):023901, 2009.

[122] Y Yang, JC Ye, J Lu, FX Liu, and PK Liaw. Effects of specimen geometry and base material on the mechanical behavior of focused-ion-beam-fabricated metallic-glass micropillars. *Acta Materialia*, 57(5):1613–1623, 2009.

[123] F Doumenc, H Bodiguel, and B Guerrier. Physical aging of glassy pmma/toluene films: Influence of drying/swelling history. *The European Physical Journal E*, 27(1):3–11, 2008.

[124] Mingyang Chen, Benoit Coasne, Robert Guyer, Dominique Derome, and Jan Carmeliet. Role of hydrogen bonding in hysteresis observed in sorption-induced swelling of soft nanoporous polymers. *Nature communications*, 9(1):3507, 2018.

[125] B Yang, WM Huang, C Li, CM Lee, and L Li. On the effects of moisture in a polyurethane shape memory polymer. *Smart materials and structures*, 13(1):191, 2003.

[126] C Bauwens-Crowet, J-C Bauwens, and Georges Homes. The temperature dependence of yield of polycarbonate in uniaxial compression and tensile tests. *Journal of Materials Science*, 7(2):176–183, 1972.

[127] Paul J Flory. Network structure and the elastic properties of vulcanized rubber. *Chemical reviews*, 35(1):51–75, 1944.

[128] Dan Y Perera. Physical ageing of organic coatings. *Progress in organic coatings*, 47(1):61–76, 2003.

[129] Dan Y Perera and Patrick Schutyser. Effect of physical aging on thermal stress development in powder coatings. *Progress in organic coatings*, 24(1-4):299–307, 1994.

[130] Dan Y Perera. Effect of thermal and hygroscopic history on physical ageing of organic coatings. *Progress in Organic Coatings*, 44(1):55–62, 2002.

[131] Jeremy Thurn and Theresa Hermel-Davidock. Thermal stress hysteresis and stress relaxation in an epoxy film. *Journal of materials science*, 42(14):5686–5691, 2007.

[132] FA Kandil, JD Lord, AT Fry, and PV Grant. A review of residual stress measurement methods. *A Guide to Technique Selection, NPL, Report MATC (A)*, 4, 2001.

[133] Grégory Abadias, Eric Chason, Jozef Keckes, Marco Sebastiani, Gregory B Thompson, Etienne Barthel, Gary L Doll, Conal E Murray, Chris H Stoessel, and Ludvik Martinu. Stress in thin films and coatings: Current status, challenges, and prospects. *Journal of Vacuum Science & Technology A: Vacuum, Surfaces, and Films*, 36(2):020801, 2018.

[134] AF Abdelkader and JR White. Curing characteristics and internal stresses in epoxy coatings: effect of crosslinking agent. *Journal of materials science*, 40(8):1843–1854, 2005.

[135] Srikanth Singamaneni, Michael E McConney, Melburne C LeMieux, Hao Jiang, Jesse O Enlow, Timothy J Bunning, Rajesh R Naik, and Vladimir V Tsukruk. Polymer–silicon flexible structures for fast chemical vapor detection. *Advanced materials*, 19(23):4248–4255, 2007.

[136] Brian S Berry and Walter C Pritchet. Bending-cantilever method for the study of moisture swelling in polymers. *IBM journal of research and development*, 28(6):662–667, 1984.

[137] EH Wong, R Rajoo, SW Koh, and TB Lim. The mechanics and impact of hygroscopic swelling of polymeric materials in electronic packaging. *Journal of Electronic Packaging*, 124(2):122–126, 2002.

[138] James L Langer, James Economy, and David G Cahill. Absorption of water and mechanical stress in immobilized poly (vinylbenzyltrialkylammonium chloride) thin films. *Macromolecules*, 45(7):3205–3212, 2012.

[139] H Lei, JA Payne, AV McCormick, LF Francis, WW Gerberich, and LE Scriven. Stress development in drying coatings. *Journal of Applied Polymer Science*, 81(4):1000–1013, 2001.

[140] LF Francis, AV McCormick, DM Vaessen, and JA Payne. Development and measurement of stress in polymer coatings. *Journal of Materials Science*, 37(22):4717–4731, 2002.

[141] HM Tong and KL Saenger. Bending-beam study of water sorption by thin poly (methyl methacrylate) films. *Journal of applied polymer science*, 38(5):937–950, 1989.

[142] George Gerald Stoney. The tension of metallic films deposited by electrolysis. *Proc. R. Soc. Lond. A*, 82(553):172–175, 1909.

[143] Jason A Payne, Alon V McCormick, and Lorraine F Francis. In situ stress measurement apparatus for liquid applied coatings. *Review of scientific instruments*, 68(12):4564–4568, 1997.

[144] Katherine R Thomas and Ullrich Steiner. Direct stress measurements in thin polymer films. *Soft Matter*, 7(17):7839–7842, 2011.

[145] JJ Wortman and RA Evans. Young's modulus, shear modulus, and poisson's ratio in silicon and germanium. *Journal of applied physics*, 36(1):153–156, 1965.

[146] Jocelyn Clenet. *Confidential*. PhD thesis, Institut National des Sciences Appliquées de Lyon, 2018.

RÉSUMÉ

Dans un contexte de transition énergétique induite par la raréfaction des ressources énergétiques fossiles et le changement climatique, les polymères traditionnels dérivés de ressources pétrochimiques tendent à être remplacés par des chimies bio-sourcées. Cette thèse a pour objet de nouvelles résines polymères thermodurcissables de type polyester élaborées à partir de matières premières renouvelables. L'optimisation de leur formulation nécessite une meilleure connaissance de leur comportement mécanique en vue de leur application dans un contexte industriel. La caractérisation mécanique de ces matériaux est cependant limitée par l'impossibilité de réaliser des échantillons massifs dans des conditions représentatives des procédés industriels. Pour surmonter ces difficultés, nous préparons des échantillons d'une taille caractéristique de l'ordre d'une dizaine de microns et de géométrie contrôlée à partir d'un polyester bio-sourcé modèle. Nous étudions ensuite expérimentalement le comportement mécanique de ces échantillons grâce à des outils de caractérisation micro-mécanique adaptés. En raison de son hydrophilie élevée, le comportement mécanique du polymère se révèle fortement dépendant de l'humidité. Dans le cas d'échantillons non vieillis, cette dépendance se traduit par une transition du polymère d'un état vitreux vers un état gel que nous attribuons à un phénomène réversible de plastification par l'eau. Nous montrons dans un second temps que l'histoire thermohydrique agit sur les propriétés mécaniques, diffusives et microstructurales du matériau de manière similaire à l'impact de l'histoire thermomécanique sur les polymères vitreux. Enfin, le vieillissement thermohydrique prolongé du polymère entraine une dégradation irréversible de ses propriétés mécaniques qui pourrait révéler un phénomène d'hydrolyse.

MOTS CLÉS

polyester, biosourcé, micro mécanique, humidité, plastification, vieillissement

ABSTRACT

In order to meet growing environmental concerns, there has been a considerable interest in generating bio-based polymers with a view to replacing the traditional oil-based chemistries. This thesis focuses on polyester thermosetting resins derived from renewable feedstock. Product optimization is however currently impeded by the limited knowledge about the mechanical properties of these new polymers. Indeed, the material foamability coupled to fast polymerization during processing prevents the fabrication and characterization of macroscopic polymer samples under technologically relevant conditions. To overcome this limitation, we prepare samples with micrometric sizes (typically in the 10 µm range) and controlled geometries from a model bio-based polyester resin. The mechanical behaviour of these micro samples is investigated experimentally using various micro mechanical characterization techniques. Because of its large hydrophilicity, the model polymer exhibits a large change in its mechanical properties upon exposure to humidity. For increasing humidity, pristine specimens undergo a water-triggered glass transition from a glassy to a water-swollen gel state which is attributed to the dramatic plasticization of the material by water. We also evidence the influence of hygric history on the mechanical, structural and sorption properties of the polymer and show that this dependence bears close similarities with the effect of thermo-mechanical physical ageing on polymer glasses. Finally, when subjected to long-term hygrothermal ageing conditions, the polymer exhibits an irreversible degradation of its mechanical properties which may be ascribed to the existence of hydrolysis process.

KEYWORDS

polyester, bio-based, micro mechanics, humidity, plasticization, ageing